Review Article

Murni Handayani*, Hendrik, Aumber Abbas, Isa Anshori*, Rahmat Mulyawan, Ardianto Satriawan, Wervyan Shalannanda, Casi Setianingsih*, Charline Tiara Rehuellah Pingak, Qurriyatus Zahro, Ayu Candra Sekar Rurisa, Iwan Setiawan, Khusnul Khotimah, Gagus Ketut Sunnardianto, and Yosephin Dewiani Rahmayanti*

Development of graphene and graphene quantum dots toward biomedical engineering applications: A review

https://doi.org/10.1515/ntrev-2023-0168 received March 19, 2023; accepted November 19, 2023

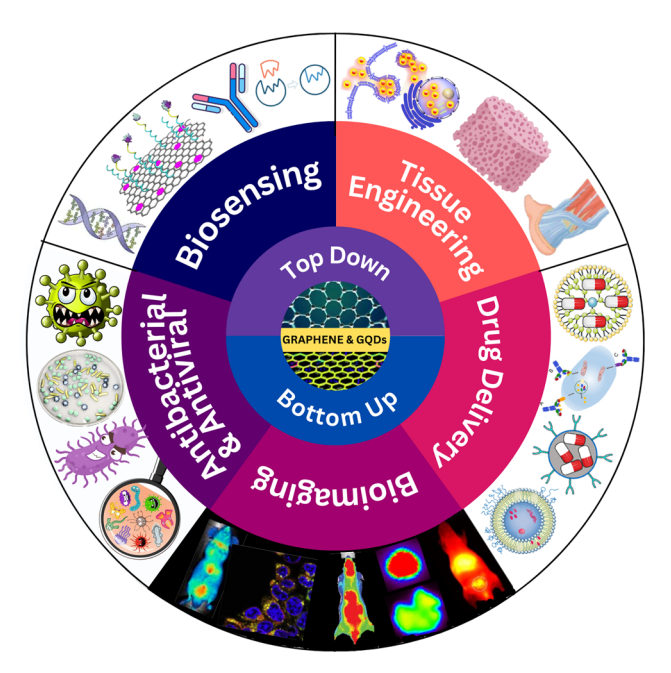
Abstract: Research on the application of graphene (G) and graphene quantum dots (GQDs) for biomedical engineering has attracted much attention over the last decade. Graphene and its derivatives have shown great biocompatibility, solubility,

- * Corresponding author: Murni Handayani, Research Centre for Advanced Material, National Research and Innovation Agency (BRIN), Tangerang Selatan, 15314, Indonesia, e-mail: murn003@brin.go.id
- * Corresponding author: Isa Anshori, School of Electrical Engineering and Informatics, Bandung Institute of Technology, Bandung, 40132, Indonesia, e-mail: isaa@staff.stei.itb.ac.id
- * Corresponding author: Casi Setianingsih, Department of Computer Engineering, School of Electrical Engineering, Telkom University, Bandung, Indonesia, e-mail: setiacasie@telkomuniversity.ac.id
- * Corresponding author: Yosephin Dewiani Rahmayanti, Research Centre for Advanced Material, National Research and Innovation Agency (BRIN), Tangerang Selatan, 15314, Indonesia, e-mail: yose008@brin.go.id Hendrik: Research Centre for Metallurgy, National Research and Innovation Agency (BRIN), Tangerang Selatan, 15314, Indonesia, e-mail: hend028@brin.go.id

Aumber Abbas: School of Engineering, Newcastle University, Newcastle Upon Tyne, NE1 7RU, United Kingdom, e-mail: a.abbas2@newcastle.ac.uk Rahmat Mulyawan: School of Electrical Engineering and Informatics, Bandung Institute of Technology, Bandung, 40132, Indonesia Ardianto Satriawan: School of Electrical Engineering and Informatics, Bandung Institute of Technology, Bandung, 40132, Indonesia, e-mail: asatriawan@staff.stei.itb.ac.id

Wervyan Shalannanda: School of Electrical Engineering and Informatics, Bandung Institute of Technology, Bandung, 40132, Indonesia, e-mail: wervyan@telecom.stei.itb.ac.id

Charline Tiara Rehuellah Pingak Mechanical Engineering Department, Faculty of Engineering and Technology, Sampoerna University, Jakarta, 12780, Indonesia, e-mail: charline.pingak@my.sampoernauniversity.ac.id Qurriyatus Zahro: Mechanical Engineering Department, Faculty of Engineering and Technology, Sampoerna University, Jakarta, 12780, Indonesia, e-mail: qurriyatus.zahro@my.sampoernauniversity.ac.id Ayu Candra Sekar Rurisa: Mechanical Engineering Department, Faculty of Engineering and Technology, Sampoerna University, Jakarta, 12780, Indonesia, e-mail: ayu.rurisa@my.sampoernauniversity.ac.id



Graphical abstract

selectivity, large surface area, high purity, biofunctionalization, high drug loading capacity, and cell membrane penetration capability potential to be applied in biomedical engineering areas. The unique physical and chemical properties of GQDs, including small size, chemical inertness, high photolumines-

Iwan Setiawan: Mechanical Engineering Department, Faculty of Engineering and Technology, Sampoerna University, Jakarta, 12780, Indonesia, e-mail: iwan.setiawan@sampoernauniversity.ac.id **Khusnul Khotimah:** Research Centre for Advanced Material, National Research and Innovation Agency (BRIN), Tangerang Selatan, 15314, Indonesia, e-mail: khus002@brin.go.id

Gagus Ketut Sunnardianto: School of Materials Science and Engineering, Nanyang Technological University, 50 Nanyang Avenue, Singapore, 639798, Singapore; Research Center for Quantum Physics, National Research and Innovation Agency (BRIN), Tangerang Selatan, Indonesia; Research Collaboration Center for Quantum Technology 2.0, Bandung, 40132, Indonesia, e-mail: gagusketut.s@ntu.edu.sg, gagu001@brin.go.id

cence stability, low cytotoxicity, and good biocompatibility, made them a promising candidate for biomedical engineering applications. The recent progress related to the development of G and GQDs toward biomedical engineering applications is presented in this work. This study reviews and discusses the development of G and GQDs, both top-down and bottom-up synthesis methods, for biomedical engineering applications, such as biosensing, tissue engineering, drug delivery, bioimaging, antibacterial, and antiviral.

Keywords: graphene, graphene quantum dots, synthesis, biomedical engineering

1 Introduction

Graphene (G) and graphene quantum dots (GQDs) are two intriguing nanomaterials that have garnered significant interest in the field of biomedical engineering [1]. Graphene is an extremely thin layer composed of carbon atoms, with a thickness of just one atom. Graphene exhibits exceptional mechanical strength, flexibility, high thermal and electrical conductivity, a large surface area, high resistance to corrosion, and excellent biocompatibility [2]. These properties make G suitable for a wide range of biomedical applications. On the other hand, GQDs are nanoscale particles made from G [3]. GQDs possess distinct structural and electronic properties. Due to their incredibly small size, they exhibit unique optical properties and the capability to selectively release electrons. This makes GQDs highly promising for biomedical applications. The distinct characteristics of both materials make them highly promising candidates for applications in the biomedical field [4]. As a result, an upsurge of research based on G and nanocomposite materials has accelerated, especially after the discovery of singlelayer G by Novoselov et al. in 2004 [5].

Generally, researchers observed that G possesses dual properties that make new fields of its properties go beyond G and depend on the material the G is composited. For example, intrinsic G has a zero band-gap semiconductor in which electron mobility (200,000 cm 2 V $^{-1}$ s $^{-1}$) is very promising for sensor applications because its conduction and valence bands meet at Dirac points [6]. Furthermore, its transport characteristics and thermal conductivity (5,000 W m $^{-1}$ K $^{-1}$) can be tuned by electrostatic or magnetostatic gating *via* chemical doping.

Besides the electronic properties, G has excellent mechanical properties: elastic modulus (elastic to a maximum of 20%), substantially lighter than paper, and a high surface area (2,630 m² g⁻¹) that exceeds known steel but is difficult to cut into a precise dimension [7]. One of the most

popular approaches that may provide hugely positive environmental impacts is using the flash Joule heating process to turn almost any carbon-based rubbish – from banana skins to car tires – into G flakes due to lower production costs. Graphene can be produced by heating waste products up to 3,000 K (2,727°C) that breaks the carbon bonds inside the target material and is reconstructed as G in 10 ms [8], similar to the process that researchers used previously in forming metal nanoparticles. In contrast, the G generated is inexpensive and can be used in more places, for instance, as reinforcement in concrete that can reduce greenhouses gases that waste food would have emitted in landfills [9]. It also applies to other renewable precursors and may open a new avenue for the low-cost synthesis of G films [10].

More recently, some researchers have attempted different classes of material that can be placed on G. Some examples of G metal nanocomposite include Mg [11], Boron Nitride [12], Si/Cu [13], and ion metals [14], such as lithium and noble metals [15]. The metal oxide-based nanocomposite, including a semiconducting metal oxide, could be strengthened by G [16-20]. Polymer-based nanocomposite could also be reinforced by G [21]. These nanocomposites have properties distinct from 2-Dimensional (2D) and conventional 3-Dimensional (3D) materials, leading to the development of large-scale practical applications, such as electric cars and mobile devices. Coupled graphene oxide (GO) possesses beneficial properties for biomedical applications, particularly when used in conjunction with hybrid metallic nanoparticles as electrochemical biosensors for the precise detection of ascorbic acid in blood [22]. In addition, integrating G with Au nanostars, represents a significant advancement toward the direct detection of IgG antibodies of SARS-CoV-2 in blood [23].

2D G has opened new perspectives in studying some basic quantum relativistic phenomena compared to zerodimensional (0D) fullerenes and one-dimensional carbon nanotubes (CNTs). It has a large surface area, high intrinsic carrier mobility, excellent mechanical properties, and superior flexibility [24–27]. Recently, GQDs have emerged as a new type of 0D G material [28]. It is defined as graphene sheets (GSs) with a plane size of less than 100 nm and a thickness of fewer than ten layers. The GQDs emerge as superior and universal fluorophores because of their unique physical and chemical properties, including small size, chemical inertness, high photoluminescence stability, low cytotoxicity, and good biocompatibility [28]. Owing to their unique size-dependent optical and physicochemical properties, GQDs find promising biomedical applications in the selective and sensitive sensing of various analytes. Doping plays a pivotal role in enhancing the properties of GQDs. For example, sulfur-doped GQDs (S-GQDs) exhibit excellent water solubility and display stronger fluorescence

compared to undoped GQDs. Additionally, they possess a significantly higher quantum yield (QY) of 57.44%, making them promising candidates for a wide range of applications, including biomedical uses [29]. In addition, boronsulfur GQDs have demonstrated exceptional efficiency in the detection of dopamine, showcasing their potential for highly sensitive and accurate biomedical sensing applications [30].

This review discusses the recent G and GQDs development for biomedical engineering applications. We provide an overview of G derivatives, synthesis methods of G and GQDs, and their applications in the field of biomedicine. Specifically, we demonstrate five representative types of biomedical applications based on G and GQDs for biosensing, tissue engineering, drug delivery, bioimaging, and antibacterial and antiviral. This review provides essential insights for researchers and practitioners in the field, enabling them to explore the potential of G-based materials for advancing biomedical engineering applications. It also addresses the challenges and proposes solutions to optimize the use of G and GQDs in biomedical applications.

2 G and its derivatives

2.1 Pristine G

Graphene is a monolayer of carbon atoms arranged in a 2D honeycomb lattice with sp2 hybridization with a C–C bond length of 0.142 nm (Figure 1). It possesses remarkable properties, including a large surface area (2,630 m²), high thermal conductivity (5,000 W m $^{-1}$ K $^{-1}$), high electrical conductivity (10 6 S cm $^{-1}$), high mechanical strength (~40 N m $^{-1}$), great optical transmittance (~97.7%), high modulus of elasticity (1 TPa), and high electron intrinsic mobility (250,000 cm 2 V 1 s $^{-1}$) [31]. These

extraordinary characteristics have attracted significant attention from researchers, opening up new avenues for advanced materials research. Graphene has gained popularity in both academic and industrial domains due to its exceptional properties, driving its demand in research and the market [32]. Initially, the mechanical exfoliation technique was employed for making pristine G, pioneered by Nobel Prize winners Geim and Novoselov [33]. This method involves the peeling off of layers from highly oriented pyrolytic graphite (HOPG) sheets using scotch tape. Pure G holds significant potential for biomedical applications, such as the development of a G-based femtogramlevel sensitive molecularly imprinted polymer of SARS-CoV-2 [34]. Furthermore, in the field of energy storage, computational studies have explored the interaction between G and hydrogen for hydrogen storage, offering valuable insights into G's potential as a medium for hydrogen storage [35]. Furthermore, when G is employed in the form of nanographene, it exhibits additional fascinating properties arising from quantum confinement effects, making it even more promising for various applications [36].

2.2 GO

One derivative of G materials is GO, which is the oxidized form of G containing oxygen-functional groups such as epoxides, hydroxyls on the basal plane, and carboxyl groups at the edges (Figure 1) [38]. Recently, GO has acquired increasing interest due to its excellent attributes. The abundance of oxygen-containing groups, including –OH and –COOH, makes GO exhibit strong hydrophilic properties [39]. Therefore, it can be dispersed in water or other solvents to form a stable suspension owing to the oxygen-functional groups. Furthermore, GO offers the advantage of facile combination with other molecules through covalent or noncovalent interactions.

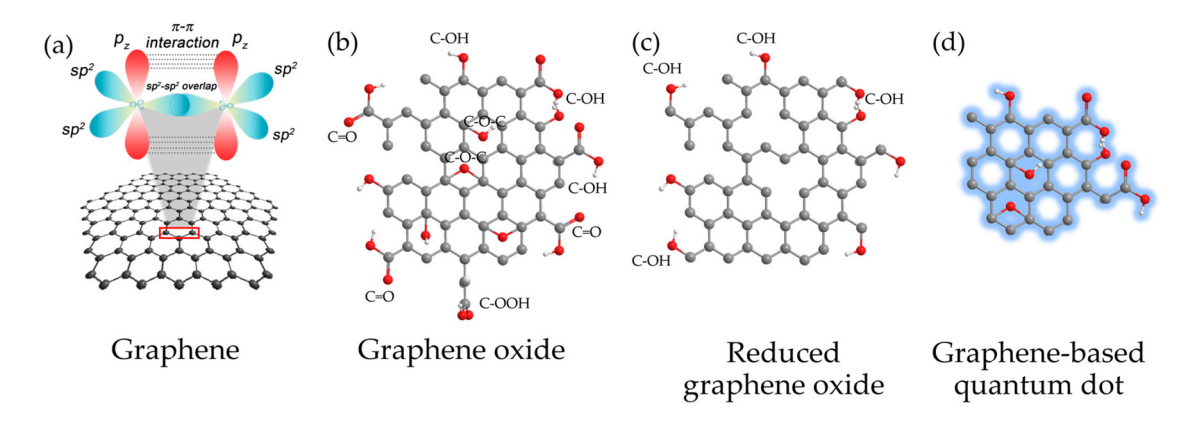


Figure 1: The structure of G and its derivative. (a) G, (b) GO, (c) reduced graphene oxide (rGO), and (d) GQD. Reproduced from [37].

The commonly used method for producing GO is the Hummers' method [40,41]. In the synthesis process of GO, graphite oxide is first prepared from graphite by forming hydroxyl or carboxyl groups, covalently bound to a graphite planar carbon network. The material is then treated with oxidizing agents, such as sulfuric acid, nitric acid, and potassium permanganate. The resulting layers of GO are thicker than pristine GSs due to the displacement of sp3 hybridizations. The ability of GO to form stable suspensions in water has positioned it as a prominent product segment in the G market. GO exhibits great potential for biomedical applications, and its utility can be enhanced by compositing it with other materials, as demonstrated by Hashemi et al. They successfully developed an ultrasensitive biomolecule-less nanosensor by decorating GO with β-Cyclodextrin/Quinoline, enabling prompt and distinguishable detection of corona and influenza viruses [42].

2.3 rGO

rGO is a form of GO that is produced using thermal, chemical, and other techniques to reduce the content of oxygen functional groups in GO (Figure 1). rGO sheets exhibit higher conductivity compared to GO due to the restoration of the conjugated network within the sheets. rGO possesses oxygen-containing functional groups, which contribute to its exceptionally high specific surface area, superior electronic conductivity, and excellent mechanical behavior [43]. The chemical reduction of GO sheets can be achieved using various reducing agents such as hydrazine, sodium borohydride, and ascorbic acid [44]. Coupling GO with hybrid metallic nanoparticles shows promising potential for biomedical applications, as demonstrated by Hashemi et al. They reported the utilization of coupled GO with hybrid metallic nanoparticles as electrochemical biosensors for precise detection of ascorbic acid in blood [22]. Another application is in the field of energy storage systems, where the development of composite materials, such as rGO/chitosan/zinc oxide, has shown remarkable potential. These composites exhibit superior performance as supercapacitor electrodes, offering enhanced electrochemical properties [45].

2.4 GQDs

GQDs belong to a class of nanomaterials that possess unique and fascinating properties attributed to their size and G-like structure (Figure 1). GQDs typically exhibit a nanoscale size, ranging from a few nanometers to a few hundred nanometers. They consist of sp2-hybridized carbon atoms arranged in a two-dimensional lattice, similar to G. However, GQDs differ in that they possess finite dimensions and often have irregular edges or a non-hexagonal structure, resulting in quantum confinement effects [46]. Significant progress has been made in synthesizing and controlling the size and structure of GQDs [47]. Various methods, such as chemical oxidation, laser ablation, and hydrothermal/solvothermal processes, have been developed to precisely control the dimensions of GQDs. Techniques like size-selective precipitation, size sorting, and template-assisted synthesis have facilitated the production of GQDs with uniform size distributions and customized structures [48].

GQDs exhibit fascinating optical properties, making them highly appealing for a wide range of applications [49]. They have size-dependent optical absorption and emission phenomena, commonly known as quantum confinement. As the size of GQDs decreases, their bandgap increases, allowing for tunable absorption and emission wavelengths across the ultraviolet (UV), visible, and nearinfrared (NIR) regions [50]. This tunability proves advantageous for optoelectronic applications such as photodetection, imaging, and sensing [51]. Extensive research has been conducted on the tunable optical properties of GQDs. Researchers have demonstrated the size-dependent absorption and emission spectra of GQDs across various wavelengths. By precisely controlling synthesis parameters, such as reaction temperature and time, it becomes possible to obtain GQDs with desired absorption and emission characteristics [52]. Furthermore, surface functionalization and doping techniques have been employed to further customize the optical properties of GQDs [53].

GQDs exhibit strong and stable photoluminescence, which refers to the emission of light upon excitation by a light source. The fluorescence emission of GQDs can be adjusted by modifying their size, surface functionalization, or surrounding environment [54]. Numerous efforts have been dedicated to enhancing the fluorescence properties of GQDs. Surface passivation, chemical modification, and ligand exchange techniques have been explored to improve the QY, photostability, and emission color of GQDs [55]. Moreover, doped-GQDs can be integrated into materials to achieve tunable photoluminescence. For instance, a recent study conducted by Kumar et al. demonstrated the incorporation of sulfur-doped GQDs for achieving tunable photoluminescence in quasi-2D CH₃NH₃PbBr₃ [56]. Furthermore, strategies such as bandgap engineering and energy transfer mechanisms have been employed to enhance the emission efficiency of GQDs, enabling their applications in bioimaging and optoelectronics [57,58].

GQDs possess unique electronic properties due to the quantum confinement effects. As the size of GQDs decreases, the energy levels become discrete due to the confinement of the charge carriers. This leads to a size-dependent bandgap, and GQDs can exhibit either direct or indirect bandgap characteristics. The tunable bandgap of GQDs makes them suitable for electronic devices, including field-effect transistors, light-emitting diodes, and solar cells [59,60]. Extensive research has been conducted on the electronic properties of GQDs. The size-dependent bandgap of GQDs has been characterized using various spectroscopic and electrochemical techniques. Techniques such as doping and edge functionalization have been employed to modify the electronic structure of GQDs, allowing for control over their conductivity, carrier mobility, and band alignment. GQDs have been successfully integrated into electronic devices, demonstrating their potential for advanced electronic applications [61-64].

The surface of GQDs can be easily functionalized by introducing various functional groups or doping them with heteroatoms [65]. Functionalization enhances the dispersibility, stability, and compatibility of GQDs in different solvents or matrices. It also provides a means to tailor the properties and interactions of GQDs with other materials, facilitating their integration into composite structures and enabling applications in energy storage, catalysis, and biomedicine [58]. Surface functionalization plays a crucial role in improving the dispersibility, stability, and compatibility of GQDs in diverse environments. Various functionalization methods, including covalent functionalization, noncovalent interactions, and surface modification with polymers or biomolecules, have been developed. These approaches have enabled the introduction of desired functional groups, tailoring the surface charge, and enhancement of interactions with target materials, thus expanding the application potential of GODs [66,67].

GQDs exhibit excellent biocompatibility, low cytotoxicity, and minimal long-term toxicity, making them highly suitable for biomedical applications [68]. Extensive research has been conducted on their use in bioimaging, drug delivery, biosensing, and photothermal therapy, leveraging their unique optical properties and biocompatibility. GQDs can be functionalized with targeting ligands or encapsulated within biocompatible matrices, enabling selective targeting and controlled release of therapeutics [69]. GQDs have demonstrated good biocompatibility and have been extensively studied for biomedical applications, as reported by Kalkal et al. By integrating the quantum confinement and edge effects of carbon dots with the G structure, GQDs have emerged as a remarkable material with remarkable biocompatibility [70]. Research efforts have focused on optimizing synthesis methods to produce biocompatible GQDs with low

cytotoxicity. Surface functionalization with biocompatible polymers or targeting ligands has enabled selective targeting, cellular uptake, and controlled release of GQDs for drug delivery applications. Moreover, GQDs have found applications in bioimaging, biosensing, and photothermal therapy, showcasing their potential in various biomedical fields [71,72].

GQDs exhibit high electrical conductivity, thermal conductivity, and charge carrier mobility, making them promising candidates for electronic and thermal management applications [73]. Their exceptional electrical conductivity arises from the intrinsic G-like structure and the high crystallinity of GQDs. Additionally, GQDs can be integrated into polymer composites or used as conductive ink for printed electronics, enabling the development of flexible and wearable electronic devices [49]. Techniques such as chemical doping, surface functionalization, and heteroatom incorporation have been employed to enhance the electrical conductivity of GQDs for improved biomedical applications. In a study conducted by Chatterjee et al., they demonstrated the use of fluorescent Boron and Sulfur codoped GQDs for efficient dopamine detection, thus opening up the possibility of designing a low-cost biosensor [30]. Integration of GQDs into conductive matrices, such as polymers or G-based materials, has facilitated their utilization in flexible and printable electronics. Moreover, GQDs have shown promise as fillers in composite materials to enhance thermal conductivity and mechanical strength [74].

GQDs possess remarkable mechanical properties, including high strength and flexibility. These properties stem from their sp2 carbon framework and the absence of defects or impurities. However, research progress specifically focused on their mechanical properties is relatively limited compared to other aspects. Nonetheless, GQDs can be integrated into composite materials to enhance their mechanical strength or used as reinforcing agents in polymers [75]. For instance, the incorporation of GQDs into polymers or carbon-based matrices has demonstrated improved mechanical properties, opening opportunities for applications in flexible electronics and structural materials. Additionally, GQDs have been explored for use in energy storage devices, such as supercapacitors, due to their mechanical robustness [76,77].

Finally, GQDs exhibit a diverse range of properties, including size-dependent optical and electronic characteristics, excellent photoluminescence, biocompatibility, high electrical and thermal conductivity, and remarkable mechanical strength. These properties make GQDs as promising candidates for various applications, including optoelectronics, biomedicine, energy storage, and electronics [78].

6 — Murni Handayani et al. DE GRUYTER

3 Synthesis methods

Synthesis of G is referred to as any procedure for producing or extracting graphene based on the required size, purity, and efflorescence of the result [79]. Various synthesis processes can yield G materials with varying surface area sizes and number of layers, as well as introduce defects that impact the chemical and physical properties of graphene. These factors ultimately influence the suitability of G for applications in the biomedical field [80-83]. Furthermore, the impact of functionalizing G [84] and GQDs [85], as well as doping them with other materials [86], is significant in terms of influencing the characteristics of these materials. Another synthesis approach of G provides variable numbers of wrinkles in the G surface, which are correlated with the chemical flexibility of G materials [87,88]. The increased chemical flexibility exhibited by G enables a broader spectrum of analyte components to be efficiently attached onto its surface. Furthermore, the increased surface area of G material increases its susceptibility to chemical and biological agents, making it an important component in the use of biosensors. Thus, it is critical to understand G and GQDs synthesis because it will provide insight into its applicability in biomedical disciplines.

Various techniques have been exploited to synthesize G and GQDs resulting in top-down and bottom-up routes. The top-down approach focuses on separating G precursor (graphite) layers or exfoliating the bulk graphite material to produce G. Whereas the bottom-up approach focuses on implementing carbon molecules from alternative sources as building blocks, also it is described as small molecular growth from carbon precursors. On that note, synthesis methods for G and GQDs could be categorized as shown in Figures 2 and 3. These synthesis methods mentioned in the figures will be discussed in this section.

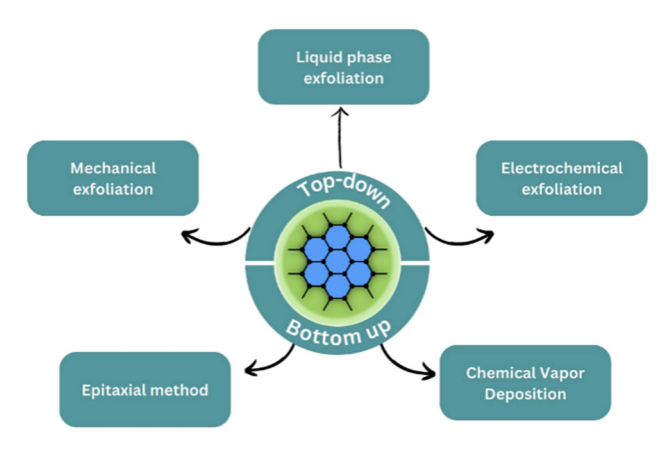


Figure 2: Graphene-based nanocomposites synthesis flowchart.

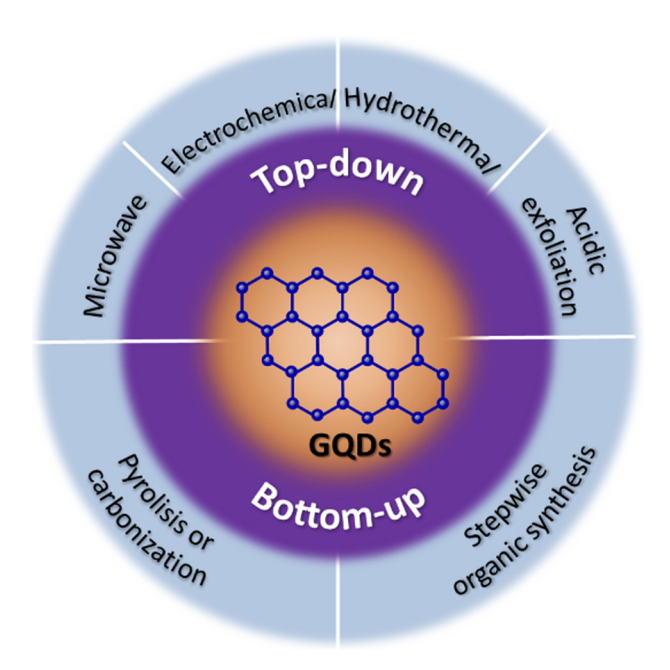


Figure 3: GQDs-based nanocomposites synthesis.

3.1 Synthesis methods of G

Numerous chemical synthesis routes have been developed by researchers to synthesize G. Chemical vapor deposition (CVD) is one example of chemical synthesis methods involving precise control over synthesis parameters: temperature, pressure, deposition time, and precursor type. Despite its complexity, it remains an appealing method for producing high-quality G. Other methods based on physical routes, such as mechanical exfoliation, pyrolysis, drop-casting, and high-current arc evaporation, are also developed a lot. The approach to synthesizing G and GO through chemical and physical synthesis has shown great prospects depending on the availability of simple industrial-scale synthesis. These considerations make the approaches on using the green synthesis of graphene and GO an interesting topic due to its continuous development in environmental applications. For G and G-based materials to have specific properties, their synthesis must be carefully controlled. As is well known, G can be synthesized in two ways, which are bottom-up and top-down. Bottom-up methods involve the synthesis of G from alternative carbon sources, whereas top-down methods involve separating stacked graphite layers to produce single GSs.

3.1.1 Top-down synthesis

3.1.1.1 Mechanical exfoliation

In 2004, a team of scientists, headed by Geim and Novoselov, published a study detailing a mechanical exfoliation method

for the synthesis of single-layer G [89]. Graphene layers were produced through the process of mechanical exfoliation of HOPG with adhesive tape. The initial step involved the preparation of graphite on particles through the utilization of dry etching in an oxygen plasma environment. Subsequently, the prepared graphite was pressed onto a layer of photoresist that had been applied onto a glass substrate. The graphite mesas become affixed to the photoresist layer upon the application of heat. The adhesive tape was attached onto the graphite surface and subsequently removed, therefore causing the separation of the G flakes from the mesas. Following that, the G flakes were dissolved in acetone and then transferred onto a clean SiO₂/Si substrate, resulting in the generation of flakes exhibiting diverse dimensions in terms of both size and thickness [90]. This technique is commonly known as the Scotch tape or peel-off technique. Despite the ability of this approach to generate G monolayers of highquality efficiently and affordably, its reproducible results and yield are significantly low. Furthermore, the size of G exhibits non-uniformity. Ball milling is another method employed for the mechanical exfoliation of G layers from bulk graphite. The milling process involves the participation of both normal and lateral forces in the exfoliation of GSs. However, the crystalline structure of GSs may be compromised during the milling process [91].

3.1.1.2 Liquid-phase exfoliation

Another commonly used method for producing G is liquid phase exfoliation, which involves three steps: dispersion in a solvent or surfactant, exfoliation, and purification to separate the exfoliated material from the non-exfoliated and, if supplied as a powder, completely remove any solvent traces [92]. Sonication duration is critical since longer sonication times can generate greater G concentrations at the trade-off of increased energy consumption. Following the sonication process, the material comprises thicker flakes that should then be extracted by ultracentrifugation. Higher centrifugation rates produce thinner flakes with tiny lateral sizes, which are unsuitable for applications such as composites. For G dispersion, a range of liquids, including aqueous surfactants, can be utilized. The yield of single-layer G percentage, defined as the ratio of the number of single-layer flakes to the total number of graphitic flakes in the dispersion, estimates this technique's output [93].

Paton et al. demonstrated that large shear forces, rather than ultrasonic cavitation, may be utilized to exfoliate G on a 100 L scale. The essential shear rate for G exfoliation was discovered to be 10⁴ s⁻¹, which is achievable even with

standard kitchen blenders. Following centrifugation, the average number of layers was fewer than 10, with typical lateral diameters of the nanosheets ranging from 300 to 800 nm. However, it should be emphasized that the yield obtained was rather low, and the choice of starting material and rotor optimization might significantly impact exfoliation efficiency [94]. Furthermore, Dimiev et al. prepared graphene nanoplatelets (GNPs) at room temperature for 3-4 h, and the conversion yield from graphite to GNPs was nearly 100%. Due to current industry expertise and equipment, liquid exfoliation may be the most practical approach for upscaling G synthesis [95].

3.1.1.3 Electrochemical exfoliation

The specific technique involves employing a liquid solution (electrolyte) and an electrical current to consume a graphite electrode. The graphite-based electrode undergoes anodic oxidation or cathodic reaction during this procedure. Cathodic reaction techniques are better suited for producing high-quality, few-layer conductive G for energy and optical applications [96]. Furthermore, anodic oxidation has received greater attention in the scientific literature. In contrast to pure monolayer G, the resultant anodic substance is composed of many G layers, has a limited yield, and mimics GO in an oxidation state [97]. Figure 4 shows a schematic illustration of (a) the electrochemical exfoliation of graphite and (b) the mechanism of electrochemical exfoliation. Figure 4a shows natural graphite flakes and platinum wires partially immersed in H₂SO₄ while the other end is connected to a 10 V voltage source. The bias voltage applied results in water oxidation and produces hydroxyl (OH') and oxygen radicals (O'), which trigger oxidation or hydroxylation of the graphite electrode (step 1), as shown in Figure 4b. The graphite electrode defective sites caused by oxidation facilitate intercalation by anionic SO_4^{2-} (step 2). This process causes the release of SO₂ gas and depolarization of the anion, thus expanding the distance between the graphite layers.

The benefit of electrochemical exfoliation over other methods is that it occurs in a single step, making it easier to run, and it occurs within minutes/hours, as opposed to most procedures, which need longer timeframes for preparation and stability of the final material. The lateral size of the flakes produced in nanocomposites is an essential characteristic that depends on the graphite supply and the intercalation-exfoliation process parameters. Intercalation products with nonoxidative salts can have lateral dimensions of 50 µm and a layer thickness of 2-3 layers [99].

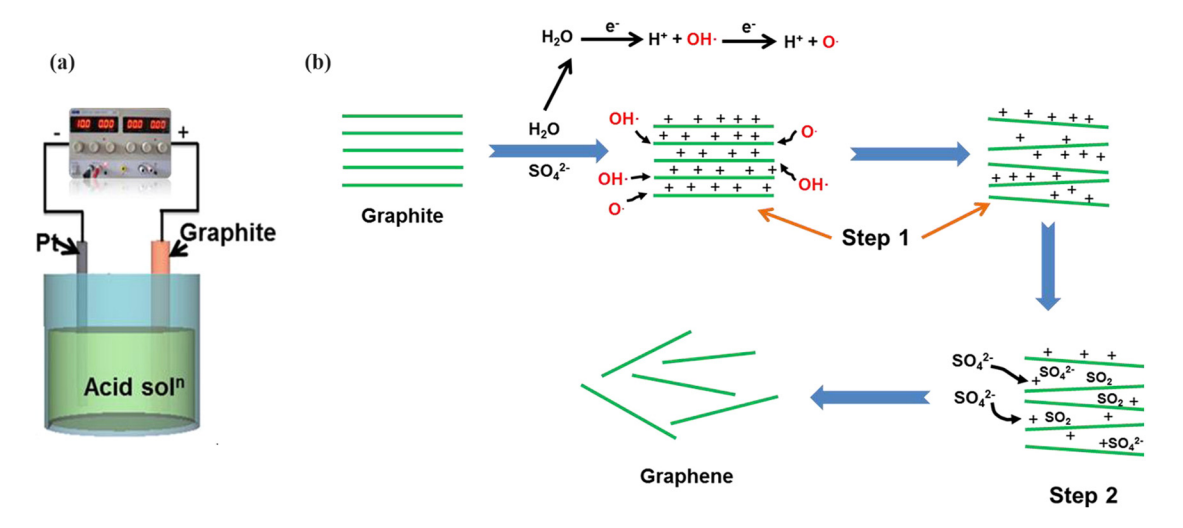


Figure 4: Schematic illustration of (a) electrochemical exfoliation of graphite and (b) mechanism of electrochemical exfoliation. Reproduced with permission from Ref. [98].

3.1.2 Bottom-up synthesis

3.1.2.1 Epitaxial method

The epitaxial method yields epitaxial G, and the size of G flakes is determined by the size of wafers, *e.g.*, SiC. According to studies, the surface of SiC influences the thickness, mobility, and carrier density of G generated in this system [100]. Unlike exfoliated G, G generated by this procedure has mild anti-localization. SiC-epitaxial G, on the other hand, has extremely large, temperature-independent mobility, similar to G generated by drawing or peeling off, but not as high as exfoliated G. Graphene may be epitaxially grown on SiC substrates, making it excellent for usage in transistors and circuits due to the thin GSs obtained (>50 m). Graphene is produced using this approach by heating a silicon carbide (SiC) to 1,100°C [101].

The weak van der Waals forces responsible for multilayer cohesion in multi-layered epitaxial G do not always affect the electrical characteristics of individual sheets within a stack. This effect is connected to interlayer interaction symmetry [102]. In other circumstances, such as bulk graphite, this behavior does not occur, and electrical characteristics are altered. A 2 in SiC wafer may provide cut-off frequencies of up to 100 GHz [103]. This technique produces high-quality G at a high cost due to the high cost of the SiC substrate and the limited yield produced. As a result, this approach is unsuitable for industrial manufacturing.

3.1.2.2 CVD

CVD is the chemical process of depositing material as a thin layer onto surfaces from vapor species, a popular bottomup method for producing multi-layer and single-layer G

films. Many complicated elements influence the process and types of chemical reactions in a CVD reactor, including system setup, reactor layout, gas feedstock, gas ratios, reactor and partial gas pressures, reaction temperature, growth time, and temperature. A schematic diagram of the CVD reaction for G from methane and hydrogen is shown in Figure 5 [104]. The CVD reaction begins with the reactants' convective transport in a gas stream (step 1), followed by their thermal activation (step 2). The reactants are then transported by gaseous diffusion from the main gas stream through the stationary boundary layer (step 3). The reactants are adsorbed on the substrate surface (step 4) and diffused into the substrate bulk (step 5), depending on the carbon's solubility and the substrate's physical properties. Reactive species catalytic decomposition occurs in addition to surface migration to the attachment site and other heterogeneous reactions (step 6). After the film growth, by-products are desorbed from the substrate (step 7). The by-products are subsequently diffused through the boundary layer into the main gas stream (step 8) to be carried by convection forces to the exhaust system (step 9).

Thermal CVD on metals (such as Ru, Ir, Pt, Co, Pd, and Re) was initially used to create highly crystalline graphite films on Nickel (Ni) substrates in 1966 [104]. Ni and copper (Cu) are less expensive, have greater control over G layers, and are easier to transfer G. As a result, they are commonly employed as CVD substrates. The CVD development of G was accomplished using cold-wall and hot-wall reaction chambers [97]. The development of G in this approach is quick, has excellent quality, and requires little power. There is also an improvement in charge carrier mobility. (Table 1).

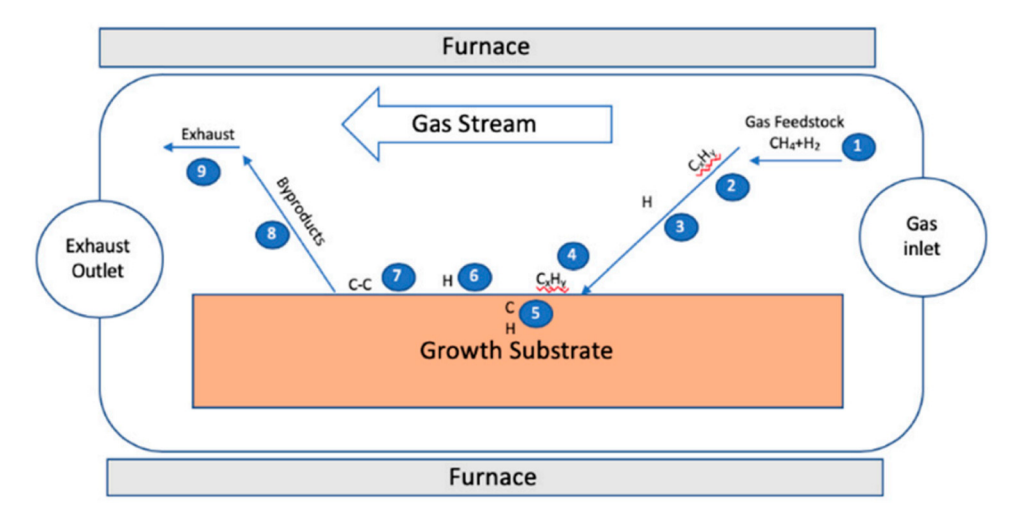


Figure 5: Schematic diagram of the CVD reaction for G from methane and hydrogen. Reproduced with permission from Ref. [104].

3.2 Synthesis method of GQDs

GQDs can be synthesized top-down or bottom-up, with varying structures and characteristics. The top-down approach is obtained by cutting the carbons into small-sized GQDs using chemical or physical procedures such as oxidative cleavage, hydrothermal methods, electrochemical oxidation, acidic exfoliation and oxidation, and microwave-assisted processes that use carbon materials, including fullerenes, GO, carbon fibers, carbon black, or graphite into small-sized GQDs [108,109]. Alternatively, GQDs could be synthesized from small organic compounds using pyrolysis, carbonization, stepwise organic synthesis, and cage-opening of C60. Various approaches are shown to analyze their properties and effects on the GOD [110].

3.2.1 Top-down synthesis

3.2.1.1 Hydrothermal method

Hydrothermal synthesis is a widely utilized and facile technique for synthesizing GQDs. Additionally, it also affects the structure and particle size distribution of GQDs. There are several techniques used in the synthesis process. In 2010, Pan *et al.* published the first report on a hydrothermal method for cutting GSs into surface-functionalized GQDs [28]. The GSs were first oxidized in concentrated H₂SO₄ and HNO₃. However, treating GO with acidic oxidizing agents (*e.g.*, H₂SO₄ and HNO₃) introduced numerous strong oxidizing acids in a comprehensive operation and was time-consuming, requiring 10–24 h [111]. In addition, it is challenging for rGO oxidation while making GQDs with specified optical properties. Because of this, Yang *et al.* described an easier and more efficient way to make GQDs from rGO

utilizing an ozonation pre-oxide technique [112]. Ozone system pH can be modified to influence GQD fluorescence. Ozone exposure changed the emission peaks of the GQDs. Comparatively, ozonation processing is easy to manage, efficient, and low-cost [112]. Another technique reported by Tetsuka *et al.* is an amino-hydrothermal method to synthesize amino-functionalized GQDs with distinct molecular weights and edges [113]. The amino-hydrothermal method [111] allows tuning the PL of GQDs by altering the hydrothermal treatment temperature and initial ammonia percentage.

Figure 6 shows the process of crystalline GQDs from paddy straw waste using hydrothermal method. The process started by grinding the paddy straw into powder. The powder was then cleaned with 0.15 M HCl and heated at 50°C for 3 h. 100 mg cleaned powder was then dissolved in 25 mL of water and kept in an autoclave hydrothermal at a temperature of 160°C for 6 h. After the hydrothermal finished, the solution was then filtered and centrifugated to obtain GQDs [114].

3.2.1.2 Acidic exfoliation and oxidation

Acid exfoliation and oxidation of carbon sources were early GQD preparation processes. These researchers improved the previous method by adding fluorescence to the reduction of the graphite oxide (hydrazine hydrate) [116]. In the previous experiment, GO was oxidized by HNO₃ for 24 h to cut into small GO sheets [110]. However, the large tracts of GO had to be removed, which required an ultrasonic cell crusher. Moreover, GO is commonly generated by oxidizing bulk graphite particles over several days using a large number of chemical reagents. In another case, a facile one-step method uses three different types of coal: anthracite, bituminous coal, and coke to synthesize GQDs. According to Dong

10 — Murni Handayani et al. DE GRUYTER

Fable 1: Synthesis methods of graphene

Type of synthesis Method	Method	Process	Advantage	Ref.
Top-down	Liquid phase exfoliation	The method consists of three steps: dispersion in a solvent or surfactant, exfoliation, and Scalable process; suitable for large-scale purification.	Scalable process; suitable for large-scale production.	[92,105]
	Electrochemical exfoliation The method emplo The graphite electro	The method employs an electrolyte and an electric current to consume graphite electrodes. Straightforward process (only takes one step [96,106] The graphite electrode undergoes anodic oxidation or cathodic reaction during the process. of synthesis).	Straightforward process (only takes one step of synthesis).	[96,106]
Bottom-up	Epitaxial method	Graphene is grown epitaxially on a silicon carbide (SiC) substrate, by heating (thermal decomposition).	Produce high quality G; suitable for electronic [103,107] application.	[103,107
	CVD	The CVD technique involves exposing the substrate to a volatile precursor, then chemically Produce high quality of G layers; potential to [104] reacting and decomposing the precursor on the surface of the substrate to form G coatings. be upscaled.	Produce high quality of G layers; potential to be upscaled.	[104]

et al., an efficient and less expensive method for producing GQDs uses a new facile method by chemically oxidizing a commonly used carbon source, CX-72 carbon black [117].

3.2.1.3 Microwave-assisted synthesis

The utilization of microwave-assisted technologies to produce G materials is gaining prominence. Nguyen et al. announced complete breakthroughs in refining the production procedure of GQDs and nitrogen-doped GQDs (N-GQDs) from citric acid (CA) and urea [118]. Microwaves speed up GOD production. It was discovered using Raman scattering spectra of the typical C-C G vibration mode (G-peak), and GQD defects detected these GQDs (D-peak) [118]. Other reports use highly acidic or alkaline conditions, sonication, or thermal reactions to create GQD. However, these operations take a long time to complete [111]. Luo et al. reported a simple microwave-assisted two-color GQD synthesis technique using a two-step hydrothermal technique in acidic conditions [119]. Surprisingly, they created white-light-emitting graphene quantum dots (WGQDs) by exfoliating oxidized graphite with ultrasonication and microwave irradiation. The collected WGODs had a consistent size of 2-5 nm and a 1.25-2.75 nm thickness during microwave irradiation. As a result, the microwave-assisted approach may minimize reaction time and boost product yield, but it requires specialized equipment.

Figure 7 shows the procedures to synthesis GQDs from spent tea using a microwave-assisted technique. The process started with pyrolysis of the spent tea to produce carbonrich precursor. The carbon-rich precursor was then converted into GQDs *via* microwave-assisted technique. The study was carried out at a microwave power range of 100–900 W with 15–180 min duration. It is found from the experiment, the optimum condition of power and duration for the synthesis of high quality GQDs with excellent optical properties derived from spent tea is 500 W and 120 min [118].

3.2.1.4 Electrochemical oxidation

The electrochemical method may be worth considering for sizing GQDs. It is possible to obtain GQDs by electrochemical selective oxidation and reduction. Shinde and Pillai synthesized GQDs electrochemically from MWCNTs [120]. However, because of the high temperature and prolonged oxidation duration, the overall reaction time is relatively long [120,121]. Electrochemical synthesis at room temperature for a short time may be a viable alternative by using big electrodes for facilitating bulk synthesis. Figure 8a shows hydroxyl and oxygen radicals attacking graphite

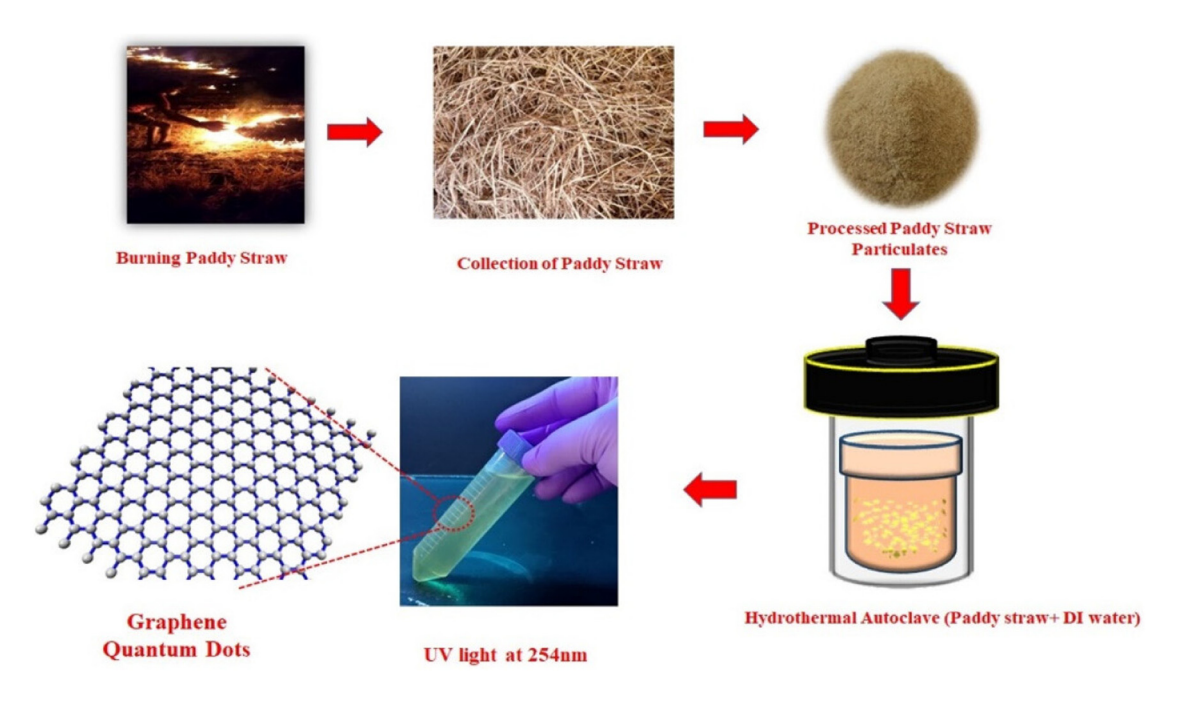


Figure 6: Synthesis process of crystalline GQDs from paddy straw waste using hydrothermal method. Reproduced with permission from Ref. [115].

edge planes during exfoliation [122]. Li *et al.* used an electrochemical approach to create functional GQDs with green fluorescence that are stable in water for months [111]. Zhang *et al.* demonstrated a simple electrochemical

approach for manufacturing GQDs with a 14% QY [123]. As illustrated in Figure 8b, Ananthanarayanan *et al.* reported a simple electrochemical approach to exfoliate GQDs from 3D G [124].

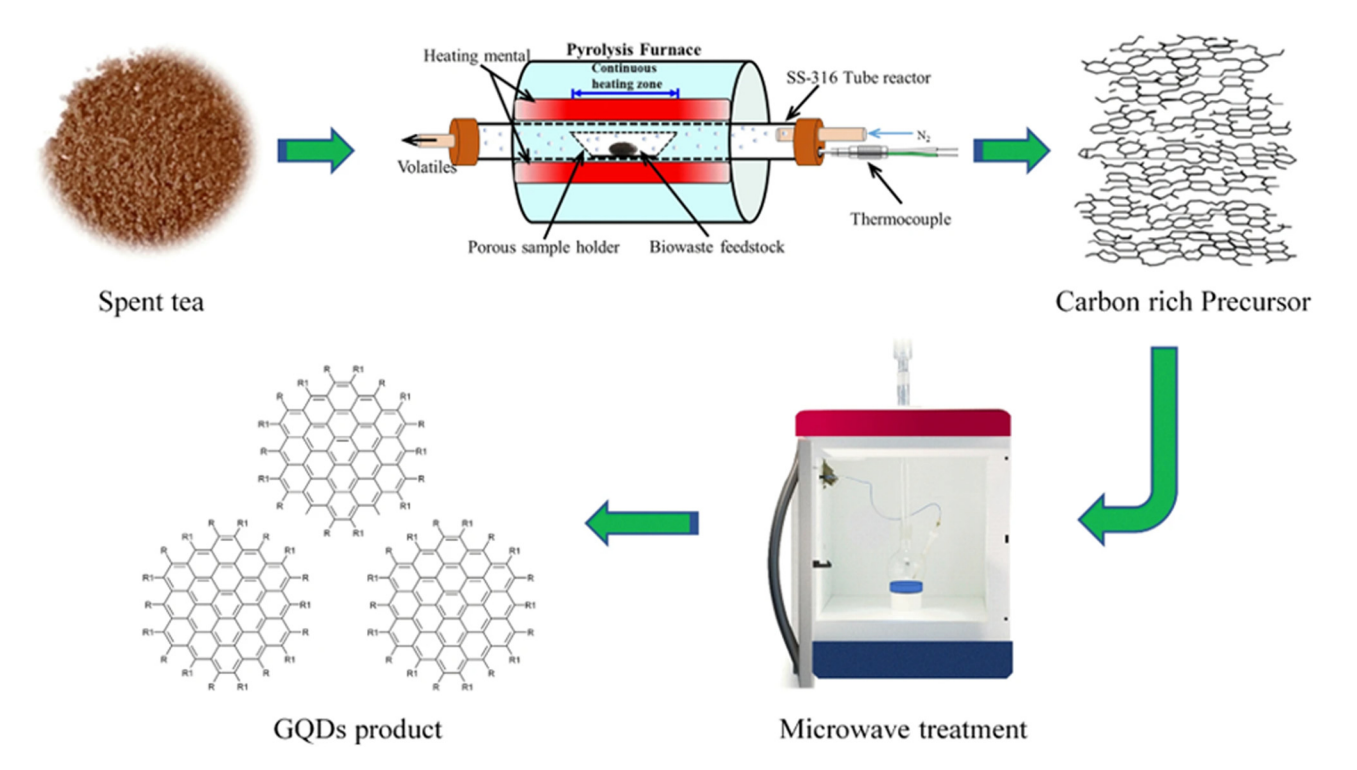


Figure 7: Illustration of the synthesis procedure for GQDs derived from spent tea using microwave assisted treatment. Reproduced with permission from Ref. [118].

3.2.2 Bottom-up methods

3.2.2.1 Pyrolysis or carbonization

The bottom-up approaches involve complex reaction processes, and specialized organic ingredients make optimizing it challenging. GQDs can be produced by pyrolysis or the carbonization of organic precursors. Precursors used in pyrolysis or carbonization include CA, L-glutamic acid, 1,3,5-triamino-2,4,6-trinitrobenzene, and glucose [125]. To overcome this, Dong *et al.* produced blue fluorescent GQDs and GO from CA, carbonized to varying degrees [126]. The GQDs were made by pyrolyzing CA. Figure 9a shows that Li *et al.* used TATB as the only precursor that underwent a single-layered intermolecular carbonization process [127]. Figure 9b depicts a bottom-up synthesis of massive GQDs with 132 carbon atoms from 3-iodo-4-bromoaniline [128].

3.2.3 Electron beam irradiation (EBI) method

The EBI approach is not frequently utilized since it needs expensive expert equipment and exposes users to radiation [129]. Wang *et al.* reported that single-crystal fluorescent GQDs were produced at ambient temperature [130].

1,3,6-trinitropyrene was dissolved in a solution of hydrazine hydrate to produce the desired results. The mixture was sealed in a plastic bag after being stirred and exposed to ionizing radiation through a titanium window in a dynamitron electron accelerator. To get GQDs with 32% QY, the sample was dialyzed for 2 days using a 0.22 mm microporous membrane filter and a dialysis bag. Precursors for GQD synthesis include 1-Nitropyrene, urea, and CA [129]. Possible reaction formation mechanism pathway of GQDs in hydrazine hydrate solution from 1,3,6-trinitropyrene molecules is shown in Figure 10. (Table 2).

4 Applications of G and GQDs

4.1 Graphene for biomedical applications

4.1.1 Biosensing application

Sensors comprise a receptor and a transducer (Figure 11). The receptor is the organic or inorganic substance that specifically interacts with the target molecule. Organic, inorganic, or even complete cells might be used as the target molecule. The transducer is the sensor component

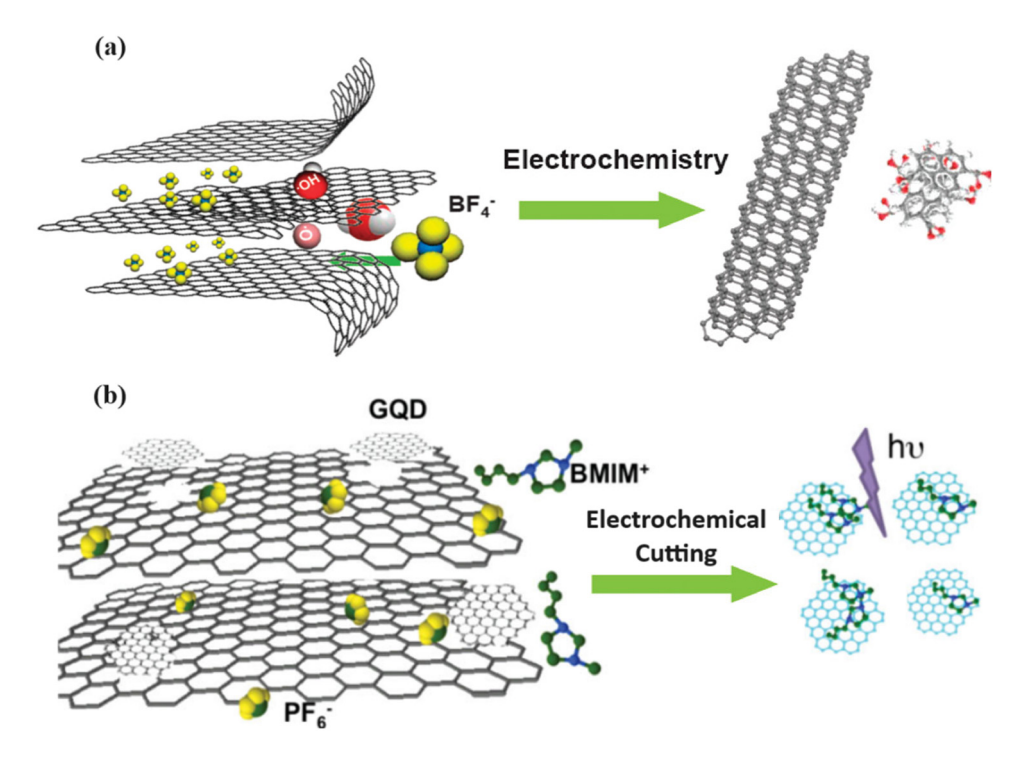


Figure 8: Schematic representation of the preparation route for green-luminescent GQDs and blue-luminescent GQDs. (a) Exfoliation process showing the attack on the graphite edge planes by hydroxyl and oxygen radicals, and intercalation of BF₄ anion [122]. (b) Schematic illustration of GQD synthesis from 3D G [124]. Adapted with permission from Refs [122 and 124].

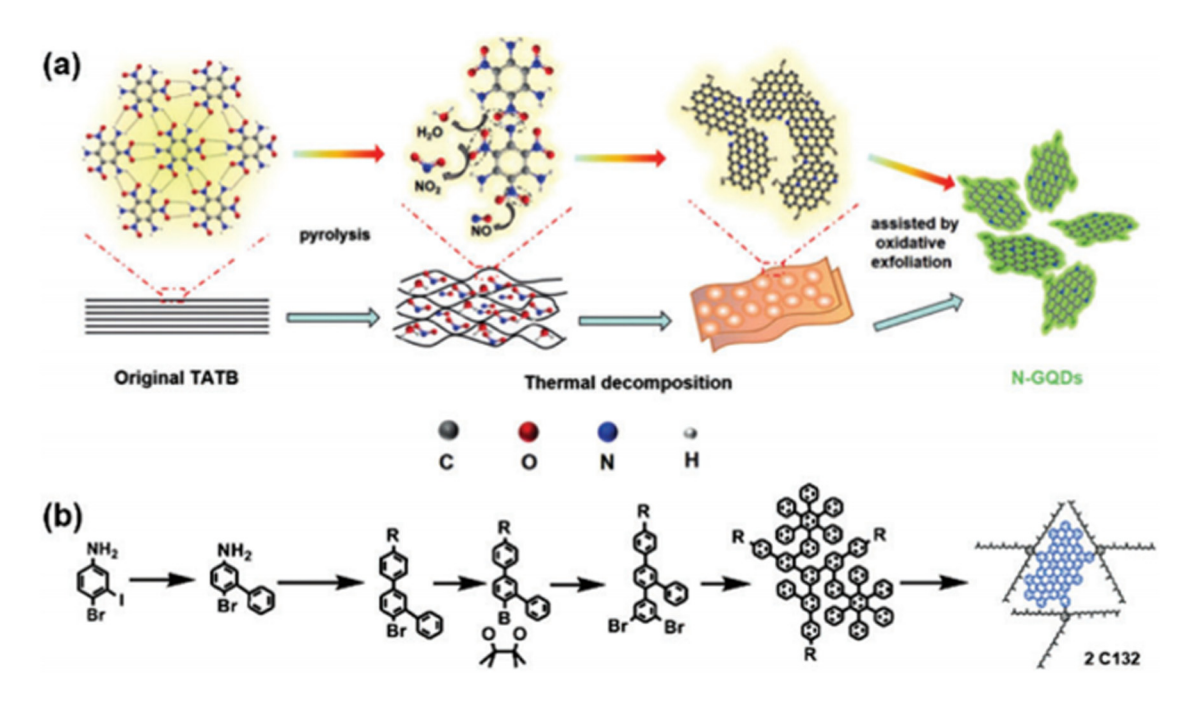


Figure 9: (a) Illustration of the proposed formation mechanism of N-GQDs from single-layered TATB intermolecular condensation (reproduced with permission from Ref. [51], Copyright 2016, Springer) [127]. (b) Bottom-up synthesis of large GQDs containing 132 carbon atoms from 3-iodo-4-bromoaniline *via* stepwise organic chemistry [128].

that turns chemical information into a quantifiable signal. Graphene-based nanomaterials (GBNs) are excellent biosensor transducers, translating the interactions between the receptor and the target molecules into observable readings [136].

The bioreceptor (molecules such as antibodies, ssDNA, and enzymes) must be linked to the transducer surface for this to happen. EDC/NHS/1-pyrenebutyric acid *N*-hydroxysuccinimide ester (PBASE) chemistry is the most often used attachment approach for antibodies and ssDNA

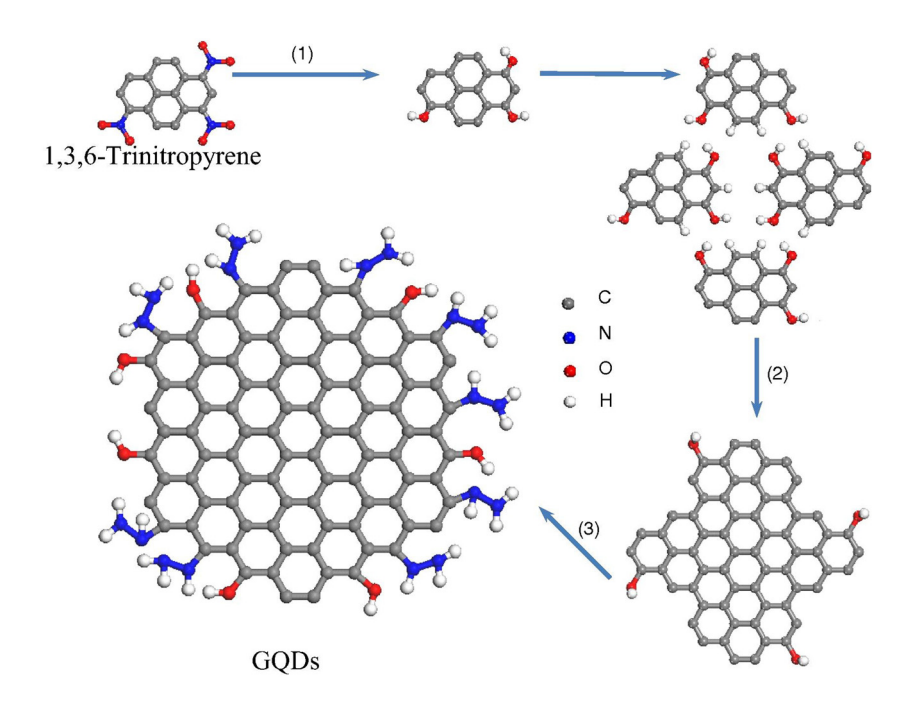


Figure 10: Formation mechanism of GQDs (reproduced with permission from Ref. [130]).

Type of synthesis Method	Method	Process	Advantage	Ref.
Top-down	Hydrothermal	This approach employs an aqueous solution as the reaction system in a closed reaction Simple and inexpensive vessel, such as a Teflon-lined autoclave	Simple and inexpensive	[111,131]
1	Acid exfoliation and oxidation	Acid exfoliation and oxidation Strong acid such as HNO ₃ is used for this method to exfoliate GQDs from carbon-based Suitable for large scale production materials	Suitable for large scale production	[111,132]
I	Microwave-assisted synthesis	Microwave-assisted synthesis – This method uses microwave irradiation to escalate the reaction	Short reaction time; uniform GQDs size distribution	[118,133]
1	Electrochemical oxidation	An electric potential is given to the precursor to push charged ions to the graphitic layers of carbon material and break carbon–carbon bonds to form GQDs	Produce uniform sized GQDs; tunable properties of GQDs	[122,134]
Bottom-up	Pyrolysis or carbonization	The carbon-containing materials is carbonized under high temperature and often under non-oxidizing atmosphere	Inexpensive; short reaction time; high yield; suitable for large production	[127,135]
ı	EBI method	This method uses high-energy electrons to break the carbon–carbon bond in the graphitic layers in the carbon materials	Produce uniform sized GQDs	[136]

immobilization onto G and its derivatives (GO, rGO). In contrast, physisorption is the most regularly used method for enzyme immobilization. Seo *et al.* succeeded in developing a COVID-19 field effect transistor (FET) sensor based on integration of SARS-CoV-2 spike antibody with G [137]. The developed platforms use PBASE for immobilization of the SARS-CoV-2 spike antibody and have a limit of detection (LOD) SARS-CoV-2 antigen protein of 1 fg/mL (Figure 12).

Because of its huge surface area, electrical conductivity, rapid electron transfer rate, and ability to immobilize diverse compounds, G has been used in the creation of several biosensors of various transduction modalities [138]. In addition, G's connected structure can enhance electron flow between the bioreceptor and transducer, resulting in high signal sensitivity for electrochemical sensors [139]. Additionally, GBNs can operate as a quencher in the transducer to produce fluorescent biosensors. G, GO, and rGO have been shown in studies to have very high efficiency in fluorescent quenching [140].

Li et al. developed a dual-channel biosensor based on fluorescence and surface-enhanced Raman spectroscopy [141]. Upconversion G was combined with Au and Ag nanoparticles resulting in Au@Ag-G upconversion. These nanohybrids were then conjugated to complementary DNA and immobilized into polymethacrylic acid magnetite-magnetic colloidal nanocrystal clusters which were previously conjugated with aptamers. The fluorescence of the sample solution was quenched if no Hg²⁺ was detected. The detection limit of this dual sensor is also sufficient to be used as a qualified sensor which is 0.33 and 1 ppb [141]. Wong et al. functionalized rGO with folic acid through covalent interaction [142]. This FA-rGO is then mixed with bovine serum albumin-templated AuNCs (BSA/AuNCs) so that it can be used as a fluorescence biosensor for glutathione. Fluorescence quenching was generated by the strong connection between glutathione and FA-rGO-BSA/AuNCs, which was primarily mediated by van der Waals interaction and hydrogen bonding. Glutathione also has a tendency to bind with Au nuclei and BSA/AuNCs ligands. These interactions can cause Au cluster aggregation and alterations in electron transport, resulting in fluorescence interference. This is where FA-rGO comes in to assist in the stabilization of BSA/AuNCs [142]. In addition to glutathione sensors, rGO has been claimed to have the potential to be employed as a virus sensor for Ebola [143], SARS-CoV-2 [143], and Hepatitis C [144].

4.1.2 Tissue engineering (implant)

Due to its ability to react with other biomolecules such as DNA, enzymes, proteins, and peptides for regenerative

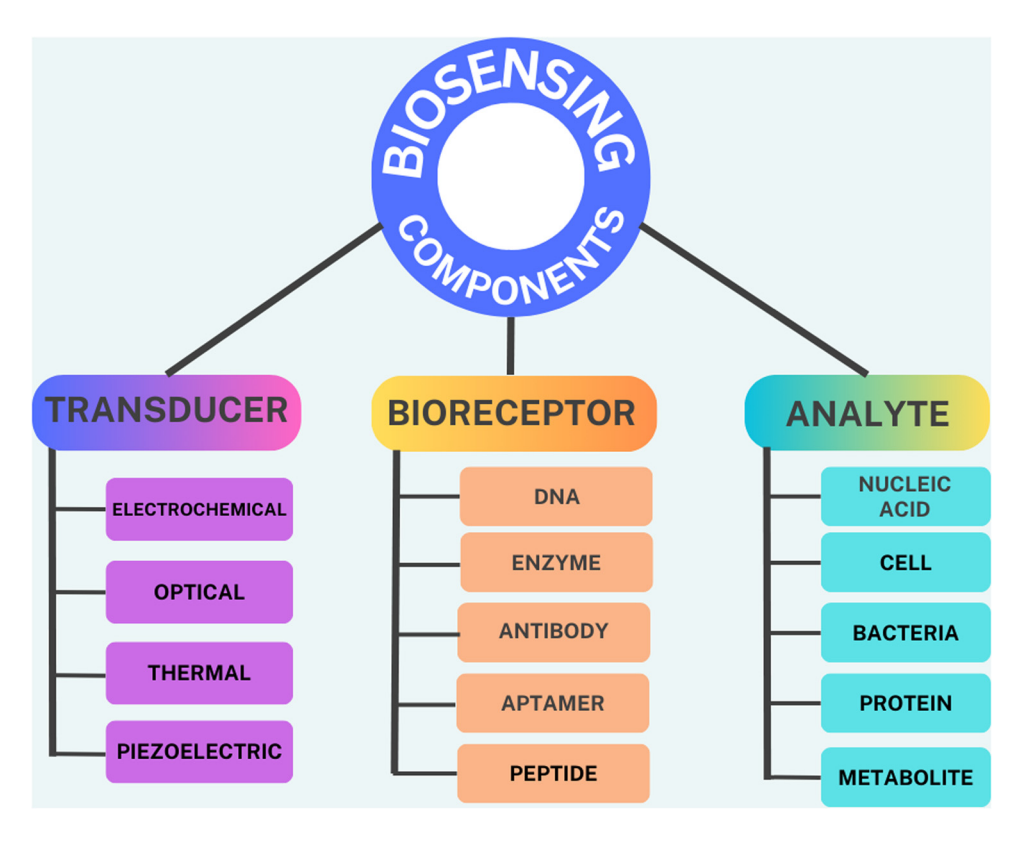


Figure 11: Biosensors and components on a biosensing platform.

medicine, G nanomaterial is now widely used in the medical and tissue engineering fields. Graphene and its by-products have recently gained new interest in the development and application of biocompatible systems. Nayak *et al.* investigated the effect of G on stem cell growth and discovered

that G-based films do not inhibit the proliferation of human mesenchymal stem cells (hMSCs). Instead, it controls their specific differentiation into bone cells by using growth factors and osteogenic inducers, implying the potential use of stem cells for proliferation and

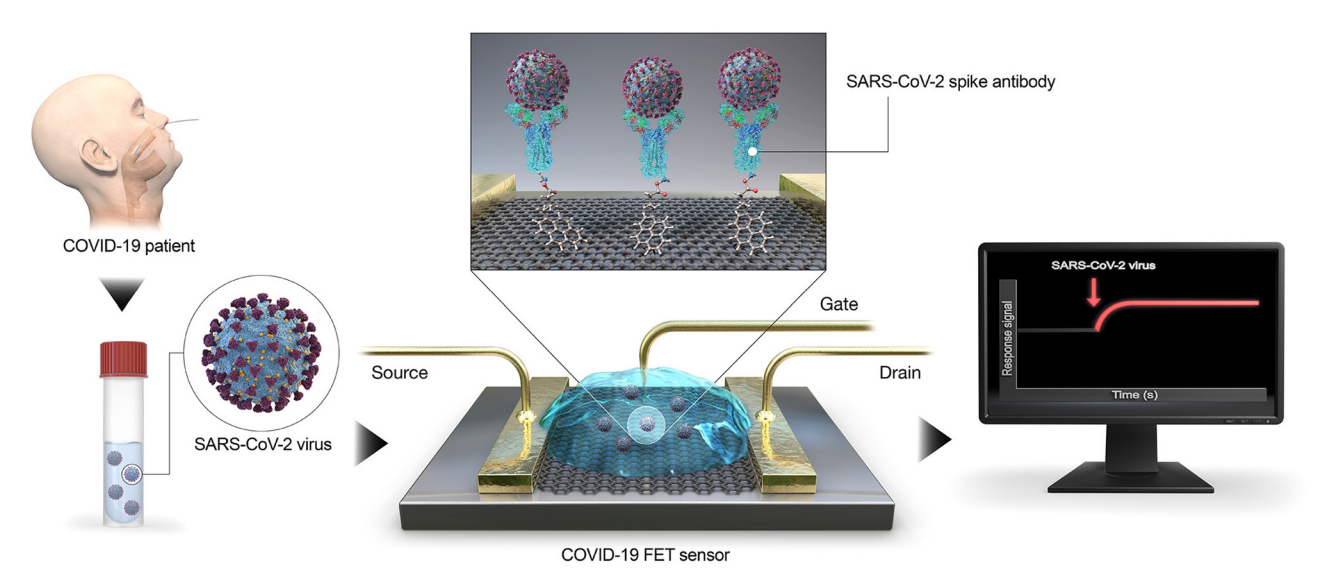


Figure 12: Schematic diagram of COVID-19 FET sensor operation procedure based on integration of SARS-CoV-2 spike antibody with G. Reprinted with permission from [137].

transplantation and their specific differentiation into muscles, bones, and cartilage for bone regeneration therapy [154]. A further recent study discovered that G could improve the biological characteristics used in bone regeneration therapy. They concluded that G nanocomposites could pave the way to construct scaffolds for specific organ/tissue targets [155].

Mohammadi et al. used the electrospinning method and successfully fabricated uniform and bead-free GO-reinforced polycaprolactone (GO-PCL) fibrous scaffolds [156]. The total porosity of the samples was greater than 95% during the porosity measurement test, which appears to be the ideal solution for tissue regeneration and fibers that adsorb more protein while incorporating GO. Cell-surface attachment and cell spreading patterns were also evaluated, and it shows that cells cultivated on GO-PCL fibrous scaffolds reached higher confluency and spread out over larger areas, indicating that GO-PCL provides excellent cell attachment. Furthermore, low-magnification micrographs revealed that GO-PCL (2%) had the highest cell viability and proliferation rate, implying that GO nanosheets (GONS) in fibers may enhance cell attachment and growth. It concluded that adding GONS to MG-63 cells significantly improved the adhesion and proliferation. Compared to bulk PCL, GO-PCL biocomposites increased physicomechanical properties and significantly enhanced biological features in bone tissue engineering *via* electrospun fibers [157].

Also, regarding in vitro cell study, Kalbacova et al. found that G substrate created by CVD is biocompatible with human osteoblasts and hMSCs, with higher cell proliferation than SiO2 substrate and stimulates cell growth and differentiation [158]. In a further study by Li et al., CVD-grown G film was examined as a substrate for neurites, the essential structures for neural functions during development in a mouse hippocampal culture model. The average length of neurites was substantially increased on G film than on tissue culture polystyrene (TCPS) during the first 2–7 days following cell seeding. GAP-43 expression was also much higher in the G group compared to the TCPS group, most likely due to an increase in neurite sprouting and outgrowth, suggesting that pristine G could be used as a novel material for neural interfacing [159]. In another study, Ahmed et al. reported that GO was applied to nanofiber scaffolds made of cellulose acetate and polyvinyl alcohol (PVA) that had been modified with Fe₃O₄ nanoparticles for use in wound healing. The result showed that the incorporation of GO induced a significant variation in cell growth, where cells seem to spread over the GO surfaces. In addition, GO also contributed to the mechanical stability of nanofiber [160].

4.1.3 Drug delivery

Nanomaterial-based drug delivery systems (DDS) have been widely researched for cancer treatment during the last decade, aiming to improve therapeutic efficacy while reducing hazardous side effects. Many organizations have begun to investigate G-based medication delivery methods since 2008. The surface area of G (2,600 m² g⁻¹) is higher, which makes researchers to explore them for drug delivery [168]. A G monolayer, in essence, offers an extreme scenario in which every atom is exposed on the surface, allowing for a substantially larger drug-loading capacity. Chemical modification by electrostatic contact and binding to the aromatic molecule via p-p stacking interaction are the two most prevalent alterations described in the literature for drug delivery utilizing GBNs. Another advantage of drug delivery through GBNs is adjusting the release rate for long-term medication release [169].

Figure 13 shows the schematic design of the cellular protease-mediated G-based co-delivery system. The main component of the nanocomposites is composed of DOXloaded GO, polyethylene glycol (PEG) linker, and TRAIL-conjugated furin-cleavable peptide as can be seen in Figure 13a. The delivery process of TRAIL/DOX-fGO, from vessel administration to drug release in the cell nucleus is shown in Figure 13b. (i) The process started by intravenous administration of GO, (ii) accumulation of GO at the tumor site through passive and active targeting effects, (iii) TRAIL binding on the death receptor and degradation of peptide linker by furin on the cell membrane, (iv) activation of caspase-mediated apoptosis, (v) induction of cell death, (vi) endocytosis of GO by the tumor cells, (vii) acid-promoted DOX release in endosome, (viii) accumulation of released DOX into nucleus, and (ix) induction of DNA damagemediated apoptosis and cytotoxicity.

4.1.4 Bioimaging

In bioimaging, GO is used in many ways, such as optical imaging. Non-invasive optical imaging combines visible light and the unique characteristics of photons to provide comprehensive pictures of organs and tissues, as well as tiny objects such as cells and molecules [179]. It offers several benefits over other imaging modalities, including low cost, high sensitivity (10⁹–10¹² mol/L), nonionizing radiation, real-time imaging, a rapid acquisition time, and multiplexing capacity. This modality, however, has low tissue penetration (0–2 cm), substantial photon scattering in the visible light area (395–600 nm), and considerable background

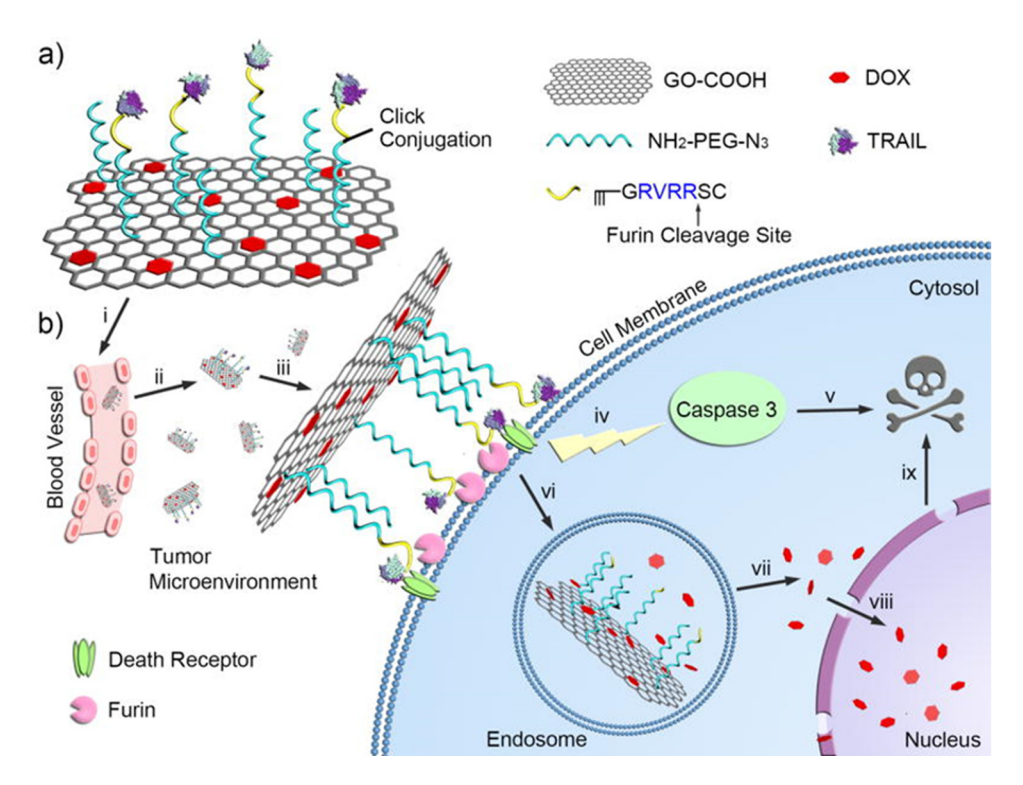


Figure 13: Schematic design of the cellular protease-mediated G-based co-delivery system. (a) Main components of TRAIL/DOX-fGO, (b) site-specific delivery of TRAIL to cell membrane and DOX to nuclei for enhanced synergistic cancer treatment. Reproduced with permission from Ref. [153].

due to tissue autofluorescence and light absorption by proteins (257-280 nm), heme groups (absorbance maximum at 560 nm), and even water (above 900 nm). To address these challenges, NIR window (NIR, 650-900 nm) and second NIR window (NIR-II, 1,000-1,700 nm) imaging modalities with reduced autofluorescence, lower tissue scattering, and better depth of penetration for in vivo imaging have been investigated [180]. The bioimaging application of nanocomposite consisting of GO was reported by Nunez et al. They covalently attached mono-iodinated boron-cluster derivatives into GO. In vitro cytotoxicity experiments with HeLa cells for up to 48 h revealed negligible cytotoxicity of the nanocomposite, as shown by cell mortality of less than 10%. Furthermore, in vivo testing indicates a similar outcome to in vitro tests, in which Caenorhabditis elegans was used to prove that nanocomposite could be ingested by the worms, with no substantial harm and very low toxicity [181].

4.1.5 Antibacterial and antiviral property

Graphene and its by-products were found to be a superior antibacterial agent against various bacteria because of their sharp edges and induction of oxidative stress. Akhavan and Ghaderi discovered that using GO and G to treat *Escherichia coli* and *Staphylococcus aureus* results in bacterial RNA

efflux. The result shows that the bacterial cell membrane is harshly pierced by the direct sinking of sharp ends of nanosheets into the bacterial cell membrane. According to their study, some GO sheets are almost perpendicular to the surface of bacterial cells. These perpendicular sheets have incredibly sharp edges that damage bacterial cell membranes and cause RNA efflux into the solution [190].

The study by Liu *et al.* found that the antibacterial activities of GO and rGO are time and concentration dependent. A significant bacterial inactivation occurs during the first hour of incubation, and the cell death rate constantly increases as material concentration increases. The increase in GO concentration from 5 to 80 g/mL resulted in the loss of *E. coli* viability from 10.5 \pm 6.6% at the GO concentration of 5 µg/mL to 91.6 \pm 3.2% at the GO concentration of 80 µg/mL. Furthermore, the result also shows that the loss of *E. coli* viability increases consistently as the GO treatment's incubation time increases. They also discovered that rGO has a similar effect as GO on *E. coli* viability loss [191].

Liu *et al.* examined wound recovery and infection control using GO quaternary ammonium nanocomposites (GO-QAS). The GO-QAS nanocomposite demonstrates outstanding biocompatibility and synergistic antibacterial efficacy against multi-drug bacteria resistance to mechanical membrane disruption and oxidative stress induction. Specifically, GO-QAS has the potential effectiveness of re-epithelialization and

18 — Murni Handayani et al. DE GRUYTER

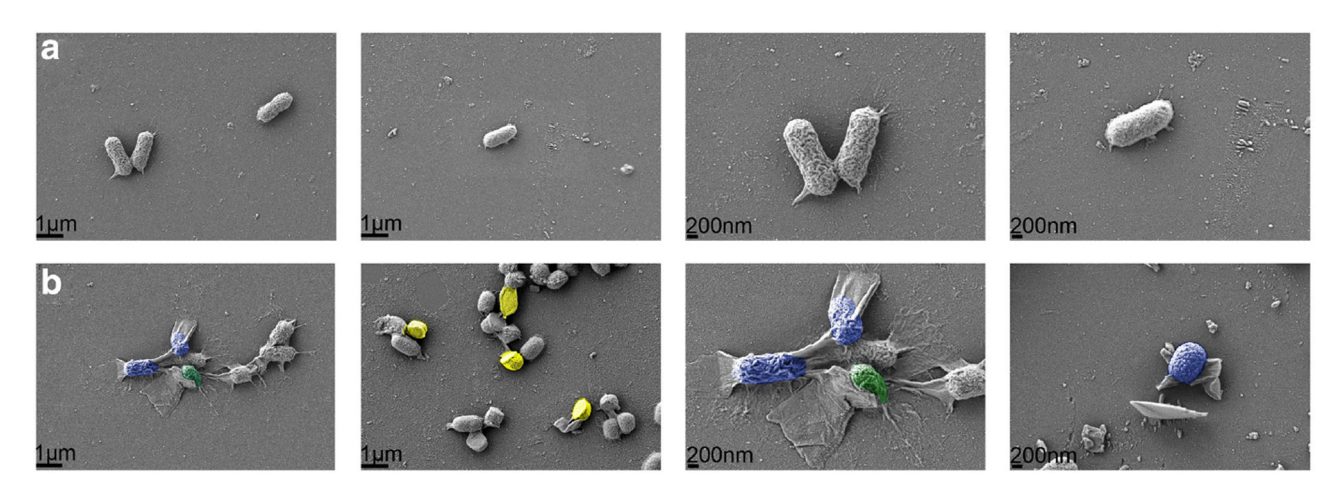


Figure 14: Scanning electron microscopy of *Escherichia coli* cell treated (a) without nanocomposite and (b) with GO suspensions. Reproduced with permission from references [192].

enhanced granulation tissue creation in treating wound infections and injuries and improving recovery. GO-QAS nanocomposite might undeniably be manufactured as an antimicrobial agent for wound treatment and antibacterial wound dressing [192]. In a further study, Valentini $et\ al.$ used functionalized G to research antibacterial and cytotoxicity factors. Functionalized G was used to create GO via the chemical and electrochemical (GO_(LiCl)) routes and the bacteria against Gram-positive $Staphylococcus\ aureus$, Gramnegative, and $E.\ coli$ microorganisms. They discovered that (GO_(LiCl)) has relatively high antimicrobial activity, suggesting that it could be used to develop anticancer drugs in the future [193]. Scanning electron microscopy of $Escherichia\ coli$ cells treated without nanocomposite and with GO suspensions is shown in Figure 14.

Figure 15 shows the application of G and its derivatives as oral bacteria inhibitors, such as *S. mutans* (*S.m*), *E. faecalis* (*E.f*), *P. gingivalis* (*P.g*), *A. actinomycetemcomitans* (*A.a*), *F. nucleatum* (*F.n*), and *P. intermedia* (*P.i*). He *et al.* reported that the number of bacterial cells decreased in GO-exposed groups compared to the control group [194]. They found that GO nanosheets caused cell membrane and cell wall integrity loss. The intracellular densities of *S.m*, *F.n*, and *P.g* decreased when surrounded by GONS, indicating that they lost some intracellular substance. They also compared the activity of *P.g*, *S.m*, and *F.n* treated with different concentrations of GO and found that bacterial activity decreased with the increase in GO concentration.

The antibacterial properties of GO and rGO sheets led researchers to suggest that these nanomaterials could have antiviral properties. According to a study by Ye *et al.*, GO and rGO exhibit comparable antiviral activity, indicating that the oxygen-containing group is not essential for antiviral activity. At a noncytotoxic concentration (6 g/mL),

they demonstrated that GO and rGO have broad-spectrum antiviral activity against both DNA viruses (PRV) and RNA viruses (Porcine epidemic diarrhea virus; PEDV). GO was found to have significant antiviral properties even at low concentrations (1.5 g/mL). It has been observed that GO can inactivate viruses even before they enter the cell due to physical disruption of the structure caused by direct contact with the sharp edge of the GO layers. The antiviral activity depended on concentration and incubation time and was effective against DNA and RNA viruses [195].

Furthermore, the antiviral activity of GO may also be attributed to the negative charge of GO, which promotes electrostatic interaction with positively charged viruses. The higher the interactions, the more the virus is destroyed and inactivated. Samethand et al. investigated the antiviral activity of GO layers and partially reduced sulfonated GO. The result showed that both the nanomaterials have a negative charge due to carbonyl and sulfonate surface groups and can block herpes simplex virus type 1 (HSV-1) infections [196]. Deokar et al. designed and synthesized sulfonated magnetic nanoparticles functionalized with rGO (SMRGO) to capture and photothermally kill HSV-1 [197]. The light absorbance of G can be utilized to eliminate virus particles once they have been captured. SMRGO were successfully used to capture and photothermally destroy HSV-1 using NIR light. These findings show that G composites could aid in treating viral diseases, including but not limited to HSV-1 [197].

The biomedical applications of G and its derivatives have enormous specific and unique characteristics. Through the compilation of Tables 3–7, we present a reader-friendly guide that highlights how G is potentially used in various biomedical fields. Each table offers a snapshot of G and its derivatives' contributions, making it easy to explore their role in enhancing biomedical applications.

4.2 GQDs for biomedical applications

4.2.1 Biosensing applications

GQDs have excellent PL performance with certain functional groups, allowing them to bond with target analytes via electrostatic interactions, $\pi-\pi$ conjugation, or electron transfer, resulting in GQD PL turn-on or turn-off [207]. Hai et~al. reported that GQDs could also be coated with additional compounds, resulting in moderate optical characteristics with specific recognition or dual emissions [207]. GQDs outperform organic dyes and semiconductor quantum dot probes for biosensing devices in terms of sensitivity, selectivity, stability, and security.

4.2.1.1 Ion sensing

In biological systems, ions need regulation and transportation at a cellular level, and their acute toxicity implies precise measurement with high sensitivity and selectivity [208,209]. Biosensors are developed based on the affinity of different functional groups on GQDs to detect a specific ion. A large number of studies have been presented for sensing different types of ions, such as Cu²⁺ [210], Pb²⁺ [211], Hg²⁺ [212], Ag⁺ [213], Fe³⁺ [135], and others [110,214]. One of the major studies used ethylenediamine-modified GQDs with a QY of 83% to detect Ni²⁺ with a detection limit of 30 nM. The PL of GQDs was substantially quenched upon the addition of Ni²⁺. *In vitro* sensing was demonstrated by treating rat adipocyte-derived stem cells with GQDs, and the PL was quenched upon adding Ni²⁺ to the cell [215].

In a recent study, biomass-derived GQDs, inherently functionalized with hydroxyl/carboxyl groups, were utilized as a photoluminescence detection probe for sensing ferric ions (Fe³⁺) [135]. The selectivity of the GQDs-based biosensor was assessed by evaluating the photoluminescence quenching efficiency of Fe³⁺ compared to numerous other metal ions. Moreover, the sensitivity was evaluated at a range of 1–50 μ m, and the detection limit was reported to be as low as 2.5 μ M, highlighting the practical

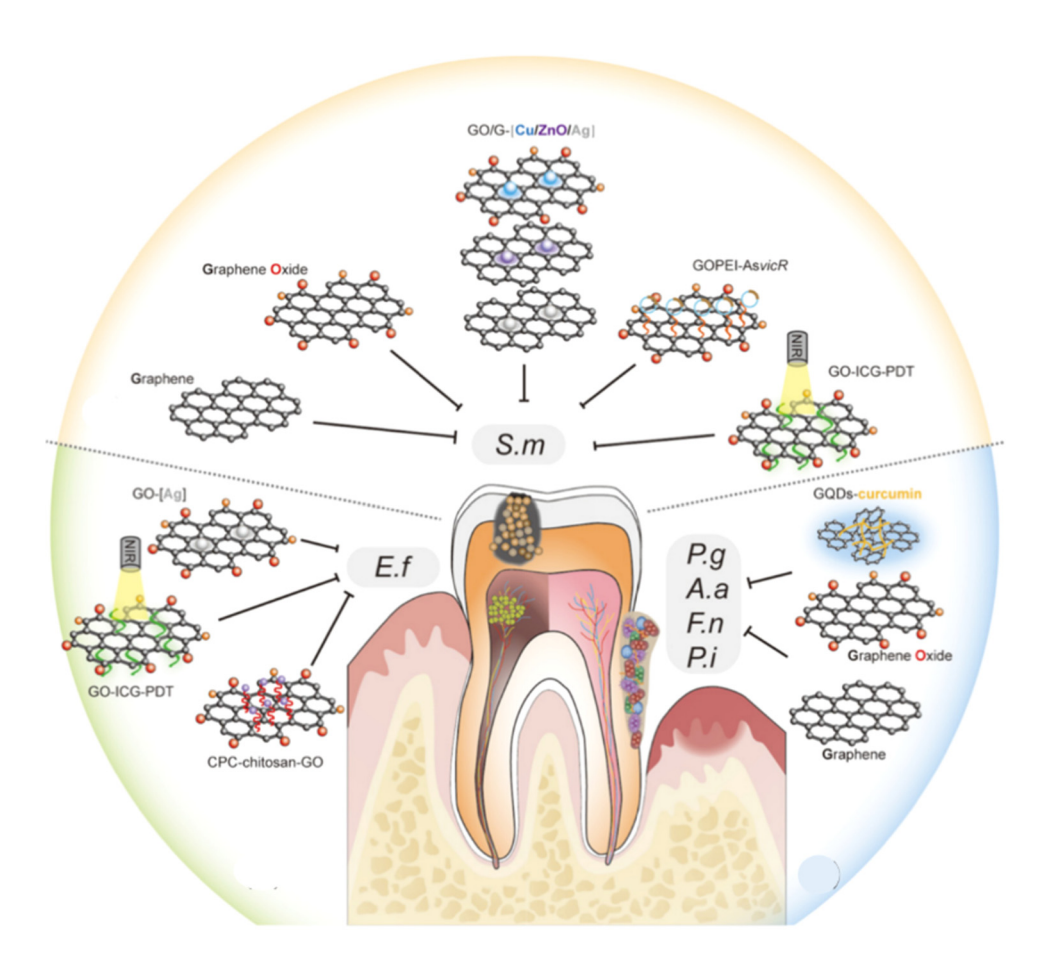


Figure 15: An illustration of the G-based materials as oral bacteria inhibitors. Graphene-based materials can inhibit the growth of cariogenic bacteria *S.m.*, control dental pulp infection by effectively reducing the biovolumes of *E.f.*, and suppress periodontal pathogens, such as *P.g.*, *A.a.*, *F.n.*, and *P.i.* Reproduced from Ref. [194].

Fable 3: Graphene material for biosensor

Precursor materials	Synthesis method of graphene materials Sensor type	Sensor type	Target molecules	ГОР	Ref.
GO-Ag-Fe ₃ O ₄ NiO/GO	Electrochemical oxidation Oxidation of graphite using Hummer's	Electrochemical impedance spectroscopy (EIS) Cyclic voltammetry (CV) and differential pulse	Ascorbic acid Ascorbic acid, dopamine, and	74 nM 0.14, 0.10, and 5.50 μM [145]	[22] [145]
N-rGO	Oxidation of graphite using Hummer's method	CV and DPV	Ascorbic acid, dopamine, and uric acid	9.6, 0.1, and 0.2 μM	[146]
Graphene wall/Cu ₂ O	CVD	EIS	Glucose	0.21 µM	[147]
MoS ₂ -G	CVD	Surface plasmon resonance)	Glucose	I	[148]
GO-Pep-FAM	Oxidation of graphite using Hummer's method	Fluorescence detection	HIV-1 protease	$1.18\mathrm{ng}\;\mathrm{mL}^{-1}$	[149]
GO-Au nanostar	Oxidation of graphite using Hummer's method	CV and EIS	SARS-CoV-2	$0.18 \times 10^{-19}\%$ V/V/	[23]
rGO-Au NPs	Oxidation of graphite using Hummer's method	CV, square wave voltammetry, and EIS	Hepatitis B	0.0014 fg/mL	[150]
rGO Chemical reduction GO-AuNPs Oxidation of graphite Thionine functionalized rGO Ultrasonication exfoliation	Chemical reduction Oxidation of graphite Ultrasonication exfoliation	FET based immunoassay Surface-enhanced Raman scattering CV and EIS	Inactivated Ebola virus DNA DNA	2.4 pg·mL ⁻¹ 10 fM 4.28 × 10 ⁻¹⁹ M	[151] [152] [153]

applicability of the sensor (Figure 16). The high selectivity and sensitivity of the sensor were attributed to the strong affinity of biomass-derived GQDs toward Fe³⁺.

4.2.1.2 In vitro sensing of small molecules

GQDs have been widely employed in biosensing based on their optical properties. Biosensors based on GQDs utilize the affinity of specific functional groups within GQDs toward analyte molecules. When the affinity of a functional group is higher toward an analyte molecule, binding between GQDs and analyte molecules occurs, resulting in different electronic states of GQDs. The GQD's electronic state variation changes photoluminescence and helps detect analytes [110,214]. GQDs have been used to detect DNA and other analytes [214]. In general, sensitivity, selectivity, and simplicity are the main requirements for an efficient sensor, and GQDs provide an excellent platform due to their good photostability and fast response.

GQDs-based sensors have also been developed for in vitro sensing of small molecules. For example, GODs functionalized with (2,4-dinitrophenyl) tyrosine (DNPTYR) were utilized to develop a turn-on sensor for indicating the H₂S attack. Different types of diseases, including cancer and Alzheimer's, are related to an unusual concentration of H₂S in the cells. The mechanism involved in this novel sensor is the photoinduced electron transfer between the DNPTYR functional group and GQDs. The photoluminescence of GQDs was quenched due to the covalent conjugation of DNPTYR. However, after adding H₂S, photoluminescence recovered due to the cleavage of the dinitrophenyl group by H₂S. Figure 17 demonstrates the schematic illustration of the H₂S biosensor. This novel biosensor could potentially detect the in vitro levels of H₂S. MCF-7 cells were incubated with GQDs-DNPTYR until the particles were interred in the cells. The photoluminescence of GQDs was enhanced by adding H₂S, as indicated by small specs of green in confocal microscope images (Figure 17b). Finally, phorbol myristate acetate (PMA) was added to the cells to reduce the H₂S concentration, which resulted in the photoluminescence quenching again. The detection limit of the biosensor was calculated to be 2 nM, signifying the system's viability [216]. The outstanding biocompatibility, good photostability and excellent water solubility are several obvious advantages of GQDs for biosensing over other systems, such as organic dyes and semiconductor QDs.

Most of the GQDs-based sensing systems are based on the interaction of the analyte with the molecules attached to GQDs, resulting in the recovery of photoluminescence through an irreversible process. While in other GQDsbased sensors, analyte interaction occurs directly with

Table 4: Graphene-based scaffold for tissue engineering

Materials	Preparation method	Type of tissue or cells	Improvement in mechanical and physical properties	Key result	Ref.
Pd/polypyrrole (PPy)/rGO	Oxidative polymerization	Bone tissue	rGO and PPy enhance mechanical properties of scaffolds	Pd/PPy/rGO has 91.90% of cell viability corresponding to 10 µg mL ⁻¹ of Pd/PPv/rGO NC for Saos-2 osteo cells	[161]
rGO/PPy/casein phosphopeptide (3D rGO/ PPY/CPD)	Electrostatic layer by layer assembly	Bone tissue	Hydrophilic and good water uptake performance	rGO/PPY/CPP facilitated the accelerated development of hydroxyapatite (HA) in a solution with a strength of 1.5 times more than that of simulated body fluid in an <i>in vitro</i> setting	[162]
HA/GO/Chitosan (CS) ternary composite hydrogel	3D molding	Bone tissue	Having compact microstructure and high mechanical strength	High porosity (84.37%) and large pores (average pore size of 122 m) provide benefits to osteoblast proliferation and differentiation	[163]
Ferric ion crosslinking-GO	3D printing and freeze- drying	Liver tissue	Having controllable porous structure	Low cytotoxicity, good viability, and good attachment behaviour (the immobilized cells were approximately 3.06 \times 10 6 cells/cm 3 in the scaffold)	[164]
PCL/gelatin/G nanofibrous	Electrospinning	Nerve tissue	Hydrophilic, G has preserved the structural integrity of the scaffold	Higher hydrophilicity is suitable for cell adhesion, attachment, and proliferation: no cytotoxicity detected	[165]
Polyvinylidene fluoride (PVDF)/GO	Non-solvent induced phase separation	Nerve tissue	Adding 3 wt% GO to PVDF scaffolds enhanced the tensile modulus and strength	On the first day of culture, the GO-PVDF scaffold (3 wt% GO) exhibited significantly greater cell viability owing to its increased hydrophilicity.	[166]
GO aerogel/gelatin	Thermal-induced phase separation	Nerve tissue	Mechanical strength was increased after addition of GO aerogels (22.6 MPa)	In vitro analysis revealed an increase in metabolic activity, which resulted in the differentiation of P19 cells on the scaffold surface	[167]

Table 5: Graphene material for drug delivery

Materials	Type of drugs	Experimental model for drug release	Key result	Ref.
CS/tripolyphosphate/GO hydrogel	Sumatriptan succinate	In vitro	The addition of GO increased the swelling degree (100–200%) and a decrease in drug release rates (20–45%)	[170]
Metronidazole (MTD)-Chi/GO bionanocomposite	MTD	In vitro	angles actions (2017-27.9) MTD-Chi/GO, particularly MCG12, demonstrated more effective drug release patterns than pure MTD drug (90.34% at pH 7.4 at 24h and 9.50% at pH 1.2 at 12 h)	[171]
Polyvinylpyrrolidone-functionalized GO (GO-PVP)	Quercetin and gefitinib	In vitro	GO-PVPs loaded with anticancer drugs showed higher cumulative release and cytotoxicity against PA-1 ovarian cancer cells	[172]
CS derivatives/rGO/alginate	Fluorescein sodium	In vitro	Quaternized carboxymethyl chitosan (QCMC)-rGO showed a optimum drug- loading rate of 82.8%. <i>In vitro</i> release rate of fluorescein sodium from QCMC-rGO/ alginate showed ~95% at pH 7.4 and 1.7	[173]
GO with 3-aminopropyltrimethoxysilane	Doxorubicin	In vitro	After 30 min, the values for DOX release at pH 5.4 and 7.4 were 87.1 and 11.3%, respectively. At pH 5.4, DOX release was defined as 99.3–100.0% after 6.0–7.0 h, but at pH 7.4. DOX release was 94.3% after 72.0 h.	[174]
Gold nanorods/GO@polydopamine	Doxorubicin	In vitro	Drug release at pH 4.5 was 49.84% with laser irradiation of 4 W cm ⁻² for 12 h. DOX release amount in PBS at pH 7.4 was 9.51%.	[175]
Polyethylenimine-PEG-rGO (mBPEI-PEG-rGO)	Doxorubicin	<i>In vitro</i> and <i>in vivo</i>	In low pH, the drug loading was 81%, and the release was greater than 50%. mBPEI-PEG-rGO increased the cell uptake efficiency and cytotoxicity of DOX in cancer cells in both <i>in vitro</i> and <i>in vito</i> and the sts	[176]
rGO encapsulated CS/alginate GO@CoFe ₂ O₄@Ag	Doxycycline Ciprofloxacin	In vitro In vitro	At pH 7.4, 90% of DXC was released after 8 h. Drug release efficiency of ciprofloxacin was higher at pH 4 with ~50% release	[177] [178]

Table 6: Graphene material for bioimaging

Materials	Type of imaging technique	PL emission	Key result	Ref.
GO-modified luminescent lanthanide (Ln³*- NCs@GO)	Fluorescence imaging	NCs emit luminescence at 540, 650, and 1,525 nm	NCs@GO demonstrated strong dispersibility in a variety of solvents, easy surface modification, improved cell uptake effectiveness and cytocompatibility, and multicolor imaging	[182]
Silver sulfide quantum dot@mesoporous silica/ GO/folic acid (QD@Si-D/GO-FA)	Fluorescence imaging dual-modal	~1,120 nm	Based on <i>in vivo</i> and <i>in vitro</i> investigations, the NCs demonstrated recognition of FA receptors present in tumor cells, therefore enabling chemo-photothermal treatment	[183]
rGO@AunS	Photothermal imaging dual-modal	I	FA crosslinking on the surface of rGO@AuNS-lipid allows binding when FA receptors on the surface of cancer cells are recognized. Through receptor-mediated endocytosis, this binding process improves the effectiveness of imaging diagnostics.	[184]
Graphene/folic acid-zinc oxide	Fluorescence imaging	High intensity peak at 485 and low intensity peak at 538 nm	Fast tumor tissue absorption was shown by a robust and distinct fluorescent signal in mice following nanocomposite injection	[185]
AgInZnS-GO (AIZS-GO)	Fluorescence imaging	530–680 nm under excitation of UV (365 nm)	The photoluminescence intensity of AIZS-GO does not diminish during irradiation, demonstrating strong biocompatibility and long-term fluorescent label imaging. NCs also exhibit multicolor bioimaging	[186]
GO nanoparticles (nGOs)	Fluorescence imaging	PL emission at 455 nm	nGOs showed bright blue-green emission in the range of 430–510 nm and had photostability in cells.	[187]
Triphenylamine-derivative (DNDT)-modified nanographene oxide	Fluorescence imaging	PL emission 364–410 nm	GO-KH550-DNDT showed blue emission in the range of 364–410 nm in the nucleus cells and stability.	[188]
Gadolinium-decorated rGO (Gd-rGO)	Magnetic resonance imaging	1	Gd-rGONSs have the potential to be a viable MRI T1 contrast agent for magnetically induced imaging. At 1.5 T magnetic field, Gd-rGONSs has a 4-fold relaxivity value (r1).	[189]

Table 7: Graphene material with antibacterial and antiviral properties

Materials	Synthesis method of graphene materials	Bacteria/virus	Mechanism	Inhibition	Ref.
GO nanoparticles	Oxidation of graphite using Hummer's method	Pseudomonas putida	Membrane damage	~90–100% for biofilm 48h	[198]
GO and rGO	Oxidation of graphite using Tour's method	Staphylococcus aureus and Pseudomonas aeruginosa	Membrane damage	GO = 48.6 and 93.7% rGO = 93.3 and 67.7%.	[199]
GO-AgNPs	Oxidation of graphite using Hummer's method	Escherichia coli and the Staphylococcus aureus	Disruption of membrane integrity and inhibition of cell division	Severe inhibition	[200]
rGO films	Chemical reduction	Staphylococcus aureus and Pseudomonas aeruginosa	Inhibition of cell division	81–84% and 50–62%	[201]
Magnetic GO–TiO ₂	Oxidation of graphite using Hummer's method	Escherichia coli	Membrane damage	100%	[202]
rGO-ZnO	Oxidation of graphite using Hummer's method	Escherichia coli and Staphylococcus aureus	Membrane damage by •OH radicals' generation	~100%	[203]
Dialdehyde cellulose (DAC)/GO/ Cysteine (Cys) and DAC/GO/Methionine (Meth)	Oxidation of graphite using Hummer's method	E. coli, P. aeruginosa, B. subtilis, S. aureus, C. albicans, and C. neoformans	Membrane damage by amino residue	DAC/GO/Cys = 19 ± 1.01 , 27 ± 0.95 , 17 ± 1.27 , 11 ± 0.69 , 23 ± 0.87 , and 32 ± 0.93 DAC/GO/Meth = 1 ± 1.00 , 13 ± 0.61 , 15 ± 0.32 , 12 ± 0.72 , and 18 ± 0.55 mm	[204]
GO-PVP β-cyclodextrin (CD) functionalized GO	Ultrasonication Ultrasonication	PEDV Respiratory syncytial virus	Inhibits virus entry into host cells Virus inactivation and viral attachment inhibition	~90% 5.00 g/mL materials could stop the virus from being able to spread	[205]

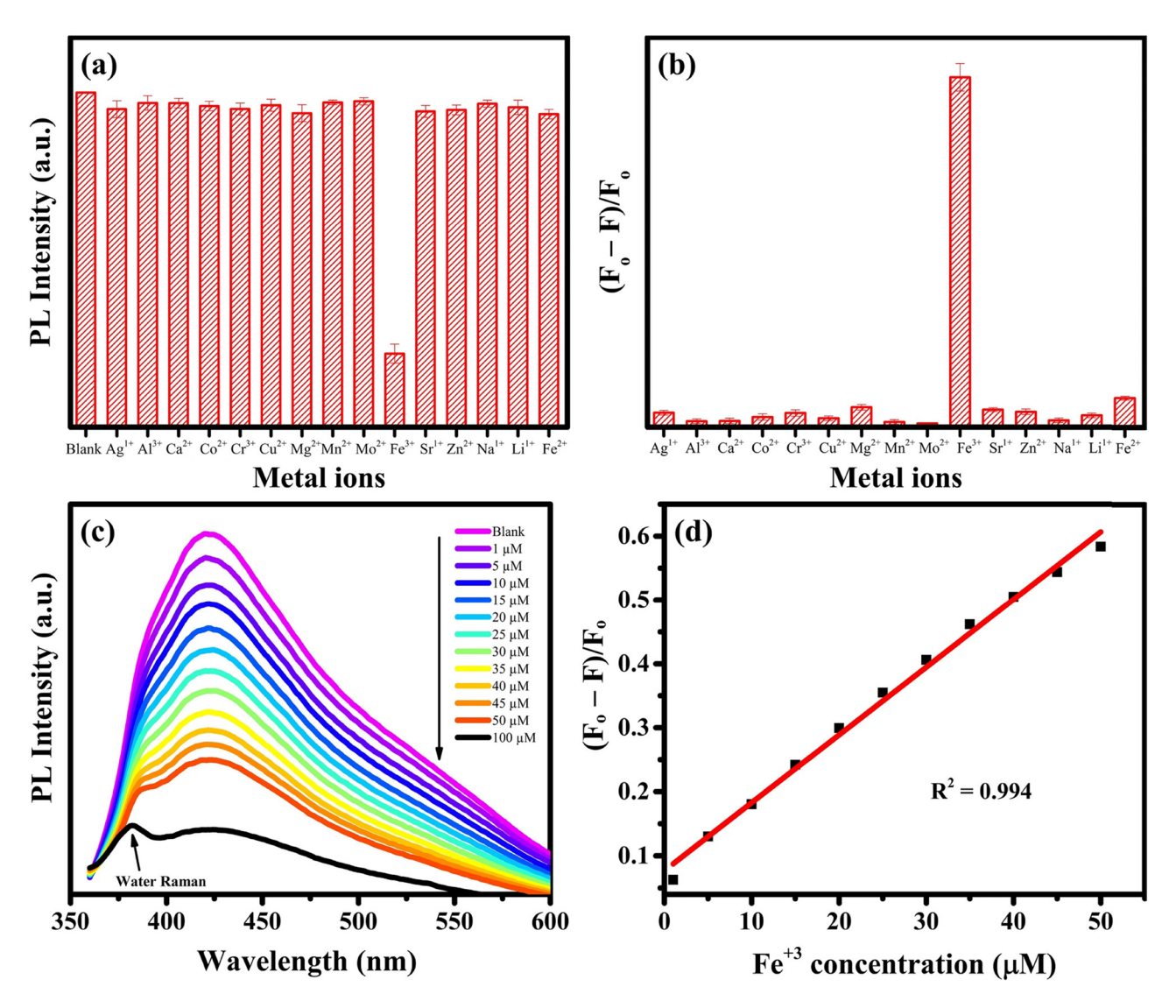


Figure 16: The biomass-derived GQDs-based sensor for selective and sensitive detection of ferric ions (Fe^{3+}). (a) Comparison of the photoluminescence intensities of GQDs solution in the presence of 100 μ M of different metal ions, (b) the assessment of the different metal ion's affinity toward GQD, (c) the photoluminescence spectra of GQDs at various concentrations of Fe^{3+} , and (d) equivalent liner regression plot [135].

GQDs, usually modified with specific functional groups. The affinity between the functional groups and analytes is vital in these biosensing probes. For example, aminefunctionalized N-GQDs were utilized to sense 2,4,6-trinitrophenol (TNP) [217]. To evaluate the selectivity of N-GQDs toward TNP, the level of photoluminescence quenching in the presence of TNP was compared to the presence of other aromatic compounds similar to TNP and various metal ions. The results indicated that considerable photoluminescence quenching only occurred in the presence of TNP. This selectivity was attributed to the overlap between the emission spectrum of N-GQDs and the absorbance spectrum of TNP, leading to effective resonance electron transfer.

4.2.1.3 In vitro sensing

In addition to *in vitro* investigations where GQDs are utilized to detect analytes in a cellular environment, *in vivo* sensing could bring the GQDs nearer to clinical research. Recent advancements in the GQDs field indicate that *in vivo* biosensing is also possible through GQDs. For example, GQDs with NIR-II windows for photoluminescence emission has been used for deeper tissue penetration. Although good biocompatibility and water solubility suggest that these GQDs can be potentially used for *in vivo* biosensing, only a few studies have been conducted on GQDs based on *in vivo* biosensing. CA and neutral red-derived carbon quantum dots, usually called CDs, were used for *in vivo* biosensing noble metal ions, such as Au³⁺, Pt²⁺, and Pd²⁺ in zebrafish [218]. CDs' optical and

26 — Murni Handayani et al. DE GRUYTER

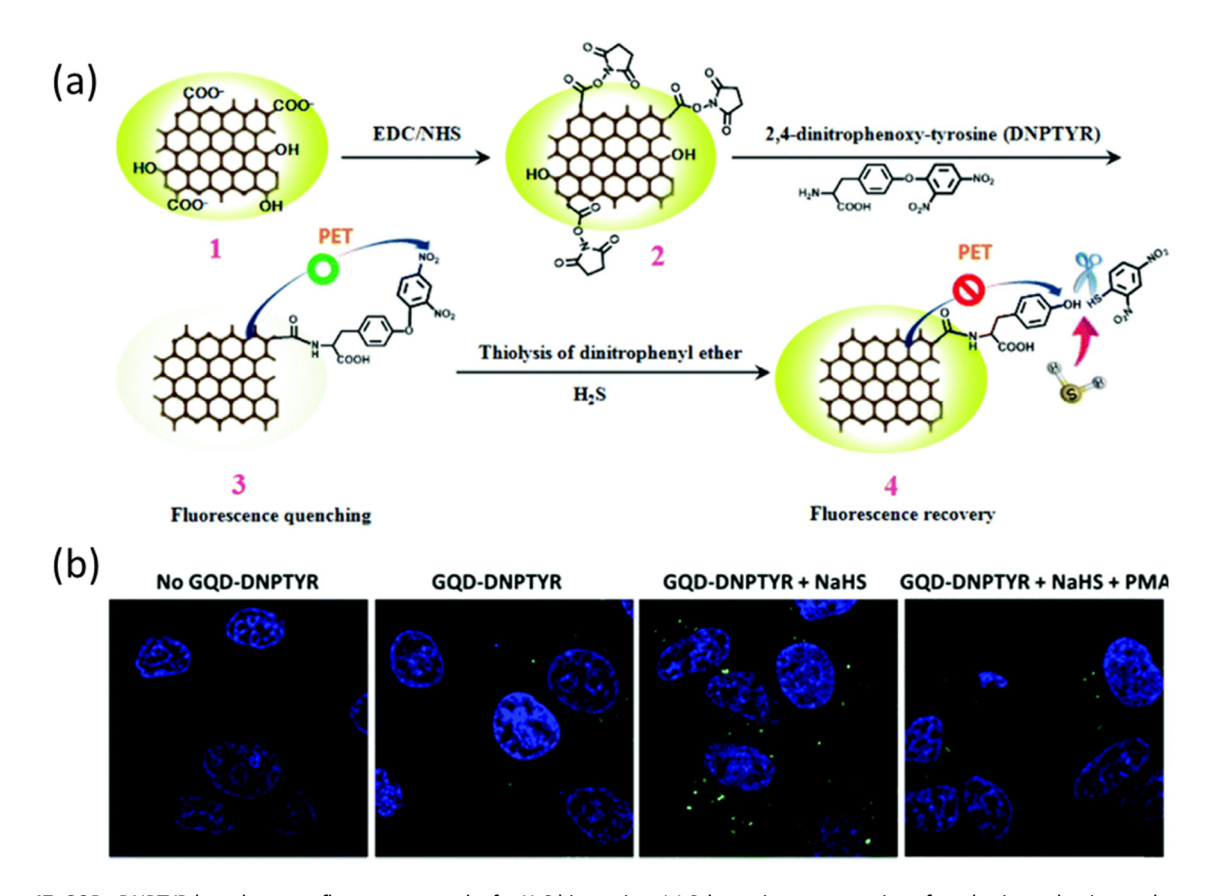


Figure 17: GQDs-DNPTYR-based turn-on fluorescence probe for H_2S biosensing. (a) Schematic representation of synthesis mechanism and quenching of GQDs by DNPTYR and (b) confocal microscope image of MCF-7 cells (first left), after 1h incubation with GQDs-DNPTYR (second left), 25 min after the addition of H_2S (third left) and in the presence of PMA and H_2S (rightmost) [216].

physicochemical properties were similar to those of GQDs, especially synthesized by the hydrothermal method, highlighting the potential of GQDs for *in vivo* sensing. In order to evaluate *in vivo* sensing ability of CDs, the zebrafish were placed in a CDs solution for 4 h after feeding with different concentrations of Pt²⁺. Subsequently, fluorescence imaging of the zebrafish was performed, and the photoluminescence intensity of CDs was measured against the Pt²⁺ concentration. The results indicated a good relationship between the CDs photoluminescence intensity and Pt²⁺ concentration [218]. Although several barriers exist for translation to mammalian models, such as high signal absorbance by the tissues and immunogenicity of GQDs, this study indicates that GQDs-based biosensors can be used in living systems.

4.2.1.4 Hydrogen peroxide (H₂O₂) sensing

 $\rm H_2O_2$ is an essential chemical widely used as an oxidant in industries. However, the toxic nature of $\rm H_2O_2$ implies that its precise measurement is substantially important [219]. Several methods have been developed for its detection and measurement, among which electrochemical sensing is

advantageous owing to its high accuracy, fast response, and ease of handling [220]. As an alternative to usually employed enzymatic sensing, GQDs have recently emerged as a nonenzymatic sensing platform for H₂O₂ [221]. Recently, GQDs and ZnO nanofiber composite platforms were developed for intracellularly sensing H₂O₂ after anticancer drug treatment [222]. Excellent response and catalytic activity were observed due to the high surface area and synergetic effect of GQDs and ZnO nanofibers. In another study, GQDs/MWCNTs composite on glassy carbon electrodes was utilized to sense H₂O₂ by reduction [223]. N-GQDs were used as a calorimetric indicator of glucose and H₂O₂ and as a catalyst for reducing H₂O₂. The kinetics of N-GQDs for reducing H₂O₂ were compared with different substrates. The results showed that the kinetics of N-GQDs were much higher than other substrates, showing a high affinity of N-GQDs toward aromatic compounds [224].

4.2.2 Tissue engineering (implant)

GQDs-based materials possess a highly beneficial physicochemical property that has been used in tissue engineering, from tissue scaffolds, high-strength hydrogels, wound healing agents, to bone regeneration agents. Oiu et al. investigated the effects of GQDs on MSCs osteogenic differentiation and evaluate the effect of GQDs exposure on MSC differentiation after incubating MSCs with different GODs concentrations for 7 and 14 days. The result showed that MSCs incubated with GQDs had higher alkaline phosphatase (ALP) activity than the control group, indicating that GODs enhance the osteogenic differentiation of MSCs. To further confirm the findings, they used quantitative polymerase chain reaction to measure the expression of phenotypically related genes associated with osteogenic differentiation at the mRNA level. The expression of bone extracellular matrix proteins such as osteopontin (OPN) and osteocalcin (OCN) was also investigated. The result after 14 days of incubation showed Runt-related transcription factor 2 (Runx2) mRNA expression in MSCs cultured with GQDs at a concentration of 50 µg/mL was up-regulated by 13.9-folds compared to control cells, indicating that Runx2 mRNA expression in MSCs cultured with GQDs significantly increased in a concentration- and time-dependent manner. The OPN expression was also increased in a concentrationand time-dependent manner up to 10 days of exposure, whereas OCN expression remained unchanged after 7 days of GQD exposure but increased in a concentration-dependent manner on days 10 and 14. These findings confirmed that GQDs could be potentially used in applying stem cell and musculoskeletal tissue engineering [196]. A more recent study investigated the effect of graphene oxide quantom dots (GOQDs) on the osteogenic differentiation of SHEDs, stem cells derived from human exfoliated deciduous teeth, which recently emerged as one of the most promising MSCs in bone tissue engineering. The resulting study showed that GOQDs promoted SHED proliferation significantly, and GOQDs performed better in promoting SHEDs osteogenesis than GO. Furthermore, GOODs were dispersed uniformly throughout the cytoplasm of SHEDs due to their photoluminescence characteristics [232]. These studies suggest that GQDs-based nanomaterials are promising for tissue engineering advancement.

4.2.3 Drug delivery

Drug loading, targeting, and efficacy have been improved with nanoparticle-based DDS [236]. Recent research shows that GQDs are less poisonous, more hydrophobic, and have stronger fluorescence than graphene [237]. Furthermore, GQDs have been proven to improve the chemotherapeutic efficacy of anticancer medications that are unsatisfactory due to drug resistance [20]. Several studies have used DFT or MD simulations to understand GQDs properties better,

for example, the 5-fluorouracil (FU) interaction with undoped/ doped GODs [238]. The findings suggest AlN and AlP-doped GQDs as FU drug carriers in nanomedicine. These nanoparticles have a low toxicity, a large surface/volume ratio, and a wide range of surface functionalization options compared to other nanoparticles. In addition, GQDs hold great biological prospects. Nitrogen-doped modified GQDs have also been shown to have drug-carrying potential. N-GQD has been reported to be employed as the DDS of methotrexate, an anticancer medication, and in vitro cytotoxicity studies showed that N-GQD is highly biocompatible [239]. The position of nitrogen doping on GODs has varied implications on its potential to be used as a drug carrier of gemcitabine as reported by Vantaparast et al. By using DFT calculations, they revealed that the binding energy values for each nitrogen doping location were negative, indicating that gemcitabine adsorption happened spontaneously on both GQDs and N-GQDS. However, the binding energy values of pure GQD and edge-NGQD were lower than those of the central N-GQD, indicating lower performance as a drug carrier [238].

4.2.4 Bioimaging

Along with small-molecule sensing, GQDs have been successfully implemented in bioimaging acute diseases such as cancer. The metabolic and nutritional environment of tumors is quite different from healthy tissues. Particularly, the pH in tumors is considerably low due to the anaerobic hydrolysis of ATP and the generation of lactic acid. Moreover, energy-deficient conditions are found in tumors [245]. Such an abnormal behavior of tumors has been used for efficient cancer diagnostics [246]. Numerous studies have demonstrated that the photoluminescence of GQDs varies with a change in the pH of the solution. Recently, nitrogen and sulfur co-doped GQDs (pRF-GQDs) demonstrated blue photoluminescence above pH 6.8 and transition to green photoluminescence below pH 6.8. In order to realize the practical application of the pH-based diagnostic system, pRF-GQDs were injected into mice bearing HeLa tumors, and fluorescence measurements were performed after 24 h. The results showed that green photoluminescence was observed in tumors.

Moreover, after imaging various tissues under identical conditions, a relatively high concentration of pRF-GQDs was found in tumor tissues due to enhanced penetration, permeation, and retention of GODs. The pRF-GODs system was demonstrated for fluorescence imaging of different tumors in mice, such as HepG2, PANC-1, U87MG, A549, and HeLa tumors [247]. The spatial resolution of tumors is relatively higher than the required value for early-stage 28 — Murni Handayani et al. DE GRUYTER

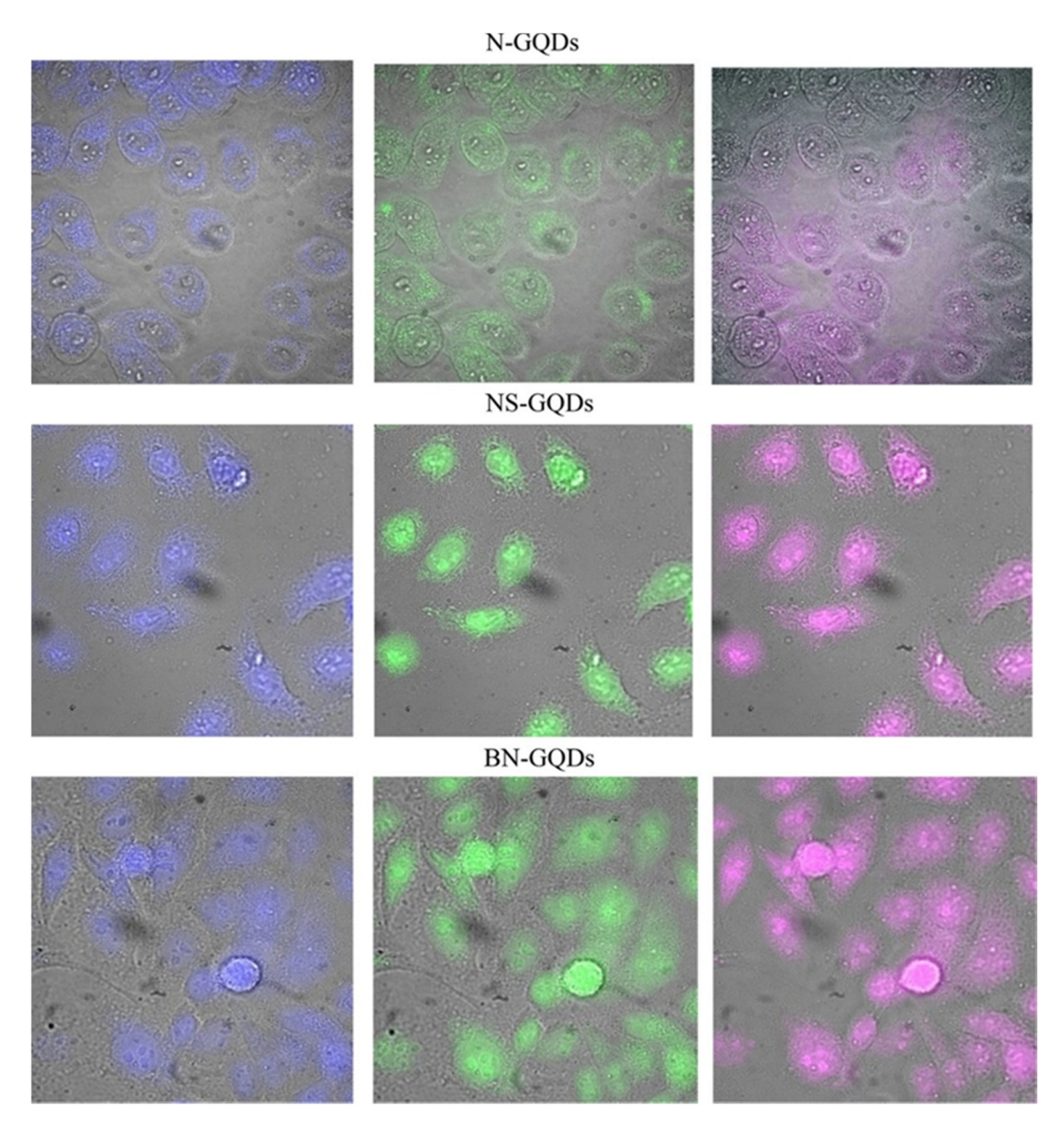


Figure 18: Multicolor imaging of N-GQDs, NS-GQDs, and BN-GQDs in blue, green, and near-IR. Reproduced with permission from Ref. [248].

cancer diagnostics. Thus, these results indicate the high potential of GQDs as an advanced platform for cancer diagnosis.

Intracellular multicolor imaging using N-GQDs, boron/ nitrogen (BN-GQDs), and nitrogen/sulfur-doped GQDs (NS-GQDs) as fully biocompatible multifunctional platforms for multicolor visible/near-IR imaging and cancer-sensing has been presented by Campbell *et al.* [248]. The GQDs were derived from a single biocompatible glucosamine precursor. The experiment shows high-yield intrinsic fluorescence emitted in blue/green color and NIR are applicable for multicolor *in vitro* imaging on their own or in combination with other fluorophores as seen in Figure 18. Furthermore,

the materials offer the capabilities for *in vivo* near-IR fluorescence tracking. Each type of quantum dot is imaged at various excitation and emission wavelengths and shows emission when internalized into a HeLa cell in blue (450 nm), green (535 nm), and NIR (750 nm).

4.2.5 Antibacterial and antiviral property

GQDs with biocompatible, photo-stable, enhanced surface grafting and superior thermal, electrical, and mechanical properties inherited from graphene are well suited for use in the biological field, including the antibacterial and antiviral fields. Sun *et al.* designed an antibacterial system by combining GQDs with a low dose of a standard medical reagent, H_2O_2 . Gram-positive bacteria *E. coli* and gramnegative bacteria *S. aureus* were used as models to investigate the antibacterial activities of the designed system. The results suggest that GQDs could act as a catalyst to enhance the antibacterial activity of H_2O_2 in this system. It is shown that the antibacterial ability of H_2O_2 has been significantly improved with the assistance of GQDs (100 g/mL). H_2O_2 significantly reduced the viability of both *E. coli* and *S. aureus* cells in a concentration-dependent manner. The enhanced antibacterial activity of H_2O_2 could also inhibit the growth of *E. coli* and *S. aureus* bacteria [255].

Furthermore, the GQD-Band-Aids, with the assistance of H₂O₂ at low doses, were prepared to examine the antibacterial efficacy of the designed system in actual wound disinfection. Kunming mice with a wound on their back were used as models to test the antibacterial efficacy of the designed system for wound disinfection in vivo. The wounds of mice were treated with H₂O₂+GQD/Band-Aid. The result showed that bacteria in the H₂O₂+GQD/Band-Aid treated group were nearly four orders lower than those in the saline-treated group, which implied that the combination of H₂O₂ and GQD/Band-Aid could kill bacteria during the wound treatment most effectively. These results indicate that GQD-Band-Aid has potential use for wound disinfection since GQD-Band-Aid showed an excellent antibacterial property in vivo with a low concentration of H₂O₂ [255].

Zeng et al. reported that GO quantum dots covalently functionalized poly (vinylidene fluoride) (GOQDs-PVDF) membrane exhibits significantly improved hydrophilic, antibacterial, and anti-biofouling properties while maintaining the permeation properties of the pristine PVDF membrane [256]. The presence of the GOQD coating layer effectively inhibits bacterial cell growth and prevents biofilm formation on the membrane surface, resulting in a higher bacterial inactivation efficiency. The GOQD loading on the membrane could be adjusted to obtain an optimal functionalized membrane with improved water permeability, antibacterial activity, and biofouling resistance. This finding shows the potential application of GOQDs-PVDF membrane as an antimicrobial agent and anti-biofouling membrane [256].

Chowdhury *et al.* studied the electrochemical detection of Hepatitis E virus (HEV) by a graphene-based nanocomposite NS-GQDs and gold-embedded polyaniline nanowires) [257]. The study found that gold nanoparticles loaded polyaniline nanowire improves electron transport and provides a large surface area for loading monoclonal antibody-conjugated GQDs. Whereas the latter may serve as active sites

for the target HEV. Compared to other traditional electrochemical sensors, introducing an external electrical pulse during the virus accumulation step boosts the sensitivity of the antiviral drug toward HEV. In addition, the external electrical pulse in this study could give insight into GQDs (with sizes of around 500 nm) to attach to the virus effectively [257].

Studies on the antiviral performance of GQDs based nanocomposites are still in small numbers compared to antibacterial performance. The significant differences in the size of the virus (2–300 nm) and bacteria (500–5,000 nm) make viral studies more challenging to conduct. Nevertheless, graphene and GQDs-based nanocomposites show promising applications in antiviral field for such nanomaterials.

Beyond graphene, another fascinating material is GQDs. These structures, with their remarkable properties, showcase diverse applications, ranging from biosensors to antibacterial and antiviral agents, as depicted in the data across Tables 8–12. These tables provide a comprehensive overview, ensuring that readers can effortlessly grasp the potential uses of GQDs in biomedical applications.

5 Challenge and its possible solution

In recent years, there has been significant interest in the utilization of graphene and GQDs in biomedical applications. However, their implementation in the biomedical application also poses notable challenges that require attention. In this study, we aim to identify the specific issues and challenges associated with the use of graphene and GQDs in biomedical applications, as well as explore potential directions for addressing these challenges.

5.1 Synthesis, cost-effectiveness, and waste management

Large-scale synthesis methodologies and cost-effectiveness remain significant concerns that demand serious attention and require resolution [263]. In order to overcome the limitations in large-scale and affordable synthesis methods, it is advisable to optimize existing techniques. This can be achieved by researching different parameters such as precursor materials, reaction conditions, and catalysts, which can effectively reduce production costs [264]. Furthermore, the exploration and development of alternative synthesis processes that can be feasibly scaled up at reasonable costs

Precursor materials	Synthesis method PL emission Sensor type	PL emission		Target molecules	ГОР	Ref.
B-doped GQDs	Hydrothermal	480 and 520 nm	480 and 520 nm Direct fluorescence Fe ³⁺	Fe ³⁺	31.2 nM	[225]
Layered double hydroxide GQD composite	Hydrothermal	350 nm	Fluorescence	Ascorbic acid	1.73 µmol L ⁻¹	[226]
GQDs/CoNiAl-layered double-hydroxide	Pyrolysis	380 nm	Amperometry	Glucose	6 µM	[227]
Aniline functionalized GQDs	Hydrothermal	470 nm	Fluorescence probe	Glucose	2.1 µM	[228]
Aunps/n-GQDs- <i>P</i> -MOF	Hydrothermal	ı	Amperometry	Glucose	0.7 µM	[229]
PEDOT:PSS/Ti3C2/GQD	Hydrothermal	ı	EIS and DPV	Glucose	65 µМ	[230]
GQDs and ionic liquid (IL) modified screen-printed carbon	Carbonization	460 nm	CV and EIS	Ascorbic acid, dopamine and uric acid 6.64, 0.06, and 0.03 µM	id 6.64, 0.06, and 0.03	
electrode						

Table 9: GQDs material for tissue engineering

Materials	Preparation	PL emission	Type of tissue or cells	Type of tissue Improvement in mechanical and physical Key result or cells properties	Key result	Ref.
GQD gelatin methacrylamide hydrogel	Lyophilization and UV irradiation	480, 540, and 520	Bone tissue	Good mechanical properties	In vitro and in vivo analysis showed that negatively charged GOD [—] may boost bone regeneration	[225]
GO quantum dots (GOQDs)	Electrospinning	570 nm	Nerve tissue	The addition of GOQD increased mechanical strength to 5.27 + 0.16 MPa	The application of GOQD in the scaffold promoted motor and sensory recovery	[233]
PCL/PVA-TCP-CD nanofibers Electrospinning	Electrospinning	463 ± 5 nm	Bone tissue	The material increased mechanical propertis	The material increased mechanical propertis national profile rated and differentiated	[234]
Oxidized alginate/gelatin- nitrogen-GQDs	Freeze drying	I	Cartilage tissue	Pore diameters are smaller (102 m), water absorption is lower (813%), and mechanical	osteogenicany The nanocomposite hydrogels tested in this study are [235] injectable, making them a promising candidate for use	[235]
•				strength are improved	in the treatment of degenerative cartilage	

Table 10: GQDs material for drug delivery

Materials	Type of drugs	Experimental model for drug release	Key result	Ref.
CS/GQDs/Cytarabine (Cyt) and GQDs/Cyt Cyt	Cyt	In vitro	The cumulative release of Cyt from CS/GQDs/Cyt and GQDs/Cyt at pH 5.8 were [240] 75.6 and 90.8%	[240]
GQDs@Bio-MOF(Cu)	Naproxen	In vitro	The drug release was 71.58% at pH 6.8 and pH 7.4.	[171]
Arginine-glycine-aspartic acid-conjugated GQDs	Doxorubicin	In vitro	Drug loading capacity was about 54.6%. Doxorubicin drug release is about 40.1% at pH 5.0 and 9.2% at pH 7.4	[241]
GQDs-CoFe ₂ O ₄ @SiO ₂ /Folic Acid	Doxorubicin	In vitro	. Doxorubicin drug release was 71% at pH	[242]
MiRGD-GQDs peptideticles	Doxorubicin and curcumin In vitro	In vitro	Drug release were 80 and 33.8% for Doxorubicin and Curcumin at acidic condition	[243]
Carboxymethyl cellulose-GQDs	Doxorubicin	In vitro	Drug release was ~60% at pH 4.5	[244]

Table 11: GQDs material for bioimaging

Materials	Type of imaging technique	PL emission	Key result	Ref.
N-GQDs	Fluorescence imaging	Yellow emission at 562 nm	After 24 h in N-GQDs solution at 37°C, fibroblast cell viability was not affected by [249] concentrations of N-GQDs up to 300 g/mL. This demonstrates the high biocompatibility and minimal cytotoxicity of N-GQDs <i>in vitro</i> .	[249]
NGQDs	Fluorescence imaging	Green and blue emission at 500–550 nm	NGQD-d can be served as fluorescent nanoagent for <i>in vivo</i> bioimaging in zebrafish	[250]
GQDs	Fluorescence imaging	Deep red at 610 nm	GQDs can penetrate to the cells through endocytosis process and the PL stable for 48 h.	[251]
GQDs	Fluorescence imaging	Red emission at 650 and 750 nm	GQDs showed emission in the range of 650–750 nm (NIR region). Cells containing [252] mGQDs showed NIR emission at 561 and 637 nm	[252]
Nitrogen-sulfur doped GQDs (NS-GQDs)	Fluorescence imaging	Blue emission at 480 nm	The addition of Cu ²⁺ in the cells containingd NS-GQDs did not interfere the fluorescence imaging, showing the stability of NS-GQDs	[253]
Boron-doped GQDs (B-GQDs) and phosphorus- Fluorescence imaging doped GQDs (P-GQDs)	Fluorescence imaging	Blue and yellow emission at 460 and 630 nm	The cells viability was not decreased after addition of both B-GQDS and P-GQDs [254] showing high biocompatibility of the materials	[254]

 Fable 12:
 GQDs material with antibacterial and antiviral property

Materials	Synthesis method of GQDs Bacteria/virus materials	Bacteria/virus	Mechanism	Inhibition	Ref.
N-doped GQDs	Microwave-assisted synthesis	Methicillin-resistant Staphylococus aureus	Generation of hyperthermia by N-GQDs plus a NIR-II laser	I	[198]
Crystalline GQDs GQDs/SnO2	Hydrothermal Hydrothermal	Pseudomonas aeruginosa Pseudomonas aeruginosa	Membrane damage Membrane disruption and leakage	Crystalline GQDs could inhibit the growth of bacteria GQDs/SnO, nanocomposite had larger zone of inhibition	[258]
TiO ₂ /Sb ₂ S ₃ /GQDs Hydrothermal	Hydrothermal	E. coli and Staphylococcus	Membrane damage caused by strong	means good antibacterial properties MIC value for <i>E. coli</i> and <i>Staphylococcus aureus</i> were 0.03	[260]
Cotton/Ag/GQDs Hydrothermal	Hydrothermal	aureus E. coli and Staphylococcus	electrostatic interactions Membrane damage by reactive oxidative species	and 0.1, showing high antibacterial activity MIC value for <i>E. coli</i> and <i>Staphylococcus aureus</i> were 0.01	[261]
GQDs@AgNPs	Hydrothermal	dureus E. coli and Staphylococcus aureus	Change the membrane permeability; DNA damage; decrease dehydrogenase activity	MIC value for <i>E. coli</i> and $Staphylococcus$ activity and 25 ± 0.2 , showing high antibacterial activity	[262]

are highly encouraged. In addition to the aforementioned synthesis and production cost issues, there are other challenges arising from the synthesis process. The waste generated from the use of graphene and GQDs can contaminate water sources. Nano-sized particles from these materials can be released into the environment, posing a potential threat to aquatic ecosystems and the organisms within them. We suggest to develop environmentally friendly synthesis methods that generate less waste. This can be achieved by using more environmentally friendly materials, such as renewable precursors and environmentally friendly solvents [265]. By implementing these strategies, the synthesis process can effectively reduce its environmental impact. Moreover, it is also advisable to implement an effective waste management system to prevent the generated waste from contaminating water sources [266]. Thus, appropriate and efficient waste treatment procedures are required to achieve this.

5.2 Biocompatibility and toxicity

Graphene and GQDs are appealing for biomedical applications due to their unique features. However, in addition to their potential, the compatibility of these materials with living tissues and organisms needs to be considered. Graphene and GQDs can undergo degradation or agglomeration over time [267], which may affect their biocompatibility and performance in biomedical applications. Additionally, biocompatibility and toxicity remain key concerns for these applications. Investigations of the biocompatibility and the toxicity of graphene and its derivatives have been reported through in vivo animal tests and in vitro cell cultures. In vivo biodistribution of graphene functionalized with PEG in mice has been investigated [268]. The result indicates that PEGylated graphene (PEG-GO) does not cause appreciable toxicity at a tested dose of 20 mg/kg for 3 months. PEG-GO was mainly accumulated in the liver and spleen, and it was removed from these organs by renal and fecal excretion [268].

Chang *et al.* have reported *in vitro* toxicity of GO on A 549 cells by examining the effect of size and dose on biocompatibility of GO exposed to A549 cells [269]. The investigation shows that GO does not enter A549 cell and has no obvious cytotoxicity. However, GO arouses oxidative stress, and induces the slight decrease in the cell viability at high GO dose. Therefore, the effect of GO on A549 cells is dose and size related. GOs with sizes of 780 \pm 410 nm (l-GO), 430 \pm 300 nm (m-GO), and 160 \pm 90 nm (s-GO) were used in their work. The cells maintained a high level of viability (over 80%), even at high GO concentration of 200 µg/mL.

However, viability loss was observed for s-GO at 200 µg/mL. At this dosage, cell viability was 67% for 24 h incubation [269].

Wang et al. studied the effect of GO on human fibroblast cells and mice to investigate the biocompatibility of GO. The GO was synthesized by the Hummer method. The result exhibits that GOs with dose less than 20 µg/mL does not show toxicity to human fibroblast cells, and the dose of more than 50 µg/mL shows obvious cytotoxicity such as decreasing cell adhesion, inducing cell apoptosis, entering into lysosomes, mitochondrion, endoplasm, and cell nucleus. For the investigation on 30 mice, GOs under low dose (0.1 mg) and middle dose (0.25 mg) do not show obvious toxicity to mice, but under high dose (0.4 mg) shows chronic toxicity, such as 4/9 mice death and lung granuloma formation, mainly located in lung, liver, spleen, and kidney, almost could not be cleaned by kidney [270].

A study on the exposure of 1 and 10 mg/L GO on eastern oysters (Crassostrea virginica) showed an elevated lipid peroxidation and a reduction in total protein levels in tissues of the digestive glands [271]. Another study showed a negative regenerative effect of GO concentration at 0.01, 0.10, and 1.00 mg/L on Diopatra neapolitana [272]. The effect of oxidative stress when GO and carboxyl graphene were introduced to the fish cell at different concentrations also has been reported in the literature [273].

Hu et al. reported highly biocompatible GQDs (HGQDs) with narrow size distribution range from 1.2 to 3.2 nm which have been successfully synthesized only by glucose in aqueous solution via one-step hydrothermal method. Importantly, no acute toxicity or morphological changes were noted from in vitro cytotoxicity and fluorescence imaging studies of the prepared HGQDs as determined by CCK-8 assay, flow cytometric analysis and confocal microscopy imaging. The more interesting results are that the cancer cells, normal cells, and gram-negative bacteria can be imaged without being destroyed. It is proved that the biocompatibility of HGQDs is better than that of conventional GQDs. The ex vivo fluorescence imaging of isolated organs demonstrated that the HGQDs accumulated in the liver, kidney, and brain at 24 h after intravenous injection of HGQDs. No inflammation was observed in the heart, liver, spleen, lung, and kidney at 20 days after the administration of the prepared HGQDs [274].

Therefore, to enhance their compatibility, research efforts focusing on surface functionalization, such as attaching functional groups or coatings, can modify their surface properties and improve biocompatibility [275]. Coating the materials with a biocompatible layer, such as biomolecules or polymers or encapsulating them within nanocarriers which can improve their stability, preventing unwanted interactions

and maintaining their properties over an extended period [276]. Thus, systematic research on surface modification and coating techniques to enhance biocompatibility should be systematically conducted. In the development of biomedical technology, G and GODs have demonstrated tremendous potential as new materials for numerous biomedical applications. However, the effect of G and GQD concentrations on toxicity must be carefully studied [277]. Thus, it is crucial to systematically research on the challenges and issues associated with the toxicity of G and GQDs at various concentration levels in a thorough and systematic manner. This approach is necessary to minimize the potential risks of toxicity.

6 Conclusion and future prospects

There are various approaches for synthesizing G and GQDs-based nanocomposites and preparing G nanocomposite material concerning its biomedical engineering applications. Numerous studies in the synthesis of graphene and GQDs-based nanocomposites research are being undertaken to explore graphene for its biomedical application. G/GO is continually discussed. More research is needed on G's ecotoxicity and non-recyclability. Graphene's interaction with the environment is still being studied. Dualproperty G could produce a new realm with exceptional qualities that exceed G's and are governed by its nanomaterial. Graphene derivatives are continuously being studied for environmental sensing applications. This research will be useful when synthesizing G and GQDs and developing improved methodologies for innovative functional G and GQD nanomaterials for further biomedical applications. However, it is difficult to find the application of Gin biomedicine, especially in implants and antivirals, due to the level of G and GQDs toxicity that can be tolerated and achieved by the human body or deck cells. Thus, in the future, scientists should be able to minimize the toxicity of graphene to make it safe for human use.

The synthesis of graphene and GQDs for biomedical engineering applications is an active research area in which studies are being conducted to investigate graphene's potential in various biomedical applications. However, important issues such as large-scale synthesis, cost-effectiveness, waste management, biocompatibility, and toxicity must be addressed in order to use G and GQDs for biomedical applications. Thus, it is advisable to optimize existing procedures, investigate alternative synthesis methods, implement ecofriendly approaches, adopt effective waste management systems, improve biocompatibility properties, and address

toxicity concerns. We can unlock the promise of G and GQDs for new and safe biomedical applications by overcoming these hurdles.

Acknowledgments: The authors acknowledge School of Electrical Engineering and Informatics, Bandung Institute of Technology for the support. The authors also acknowledge the support of the National Research and Innovation Agency (BRIN) through characterization facilities of the E-Layanan Sains (ELSA).

Funding information: The authors acknowledge research funding from Bandung Institute of Technology through Program Riset Internasional LPPM ITB 2022 [Grant number 4949/IT1.B07.1/TA.00/2022]. Murni Handayani acknowledges the Indonesia Toray Science Foundation (ITSF), Science and Technology Research Grant 2022, No. 1210/XII/ITSF/SEK/2022.

Author contributions: All authors have accepted responsibility for the entire content of this manuscript and approved its submission.

Conflict of interest: The authors state no conflict of interest.

References

- [1] Iannazzo D, Celesti C, Espro C. Recent advances on graphene quantum dots as multifunctional nanoplatforms for cancer treatment. Biotechnol J. 2021;16:1900422.
- [2] Goenka S, Sant V, Sant S. Graphene-based nanomaterials for drug delivery and tissue engineering. J Controlled Release. 2014;173:75-88.
- [3] Haque E, Kim J, Malgras V, Reddy KR, Ward AC, You J, et al. Recent advances in graphene quantum dots: synthesis, properties, and applications, Small Methods, 2018;2:1800050.
- [4] Younis MR, He G, Lin J, Huang P. Recent advances on graphene quantum dots for bioimaging applications. Front Chem. 2020;8:424.
- [5] Novoselov KS, Geim AK, Morozov SV, Jiang D, Zhang Y, Dubonos SV, et al. Electric field effect in atomically thin carbon films. Science. 2004;306:666-9.
- [6] Kalita H, Palaparthy VS, Baghini MS, Aslam M. Electrochemical synthesis of graphene quantum dots from graphene oxide at room temperature and its soil moisture sensing properties. Carbon N Y. 2020;165:9-17.
- [7] Late DJ, Rout CS, Chakravarty D, Ratha S. Emerging energy applications of two-dimensional layered materials. Can Chem Trans. 2015;3:118-57.
- Luong DX, Bets KV, Algozeeb WA, Stanford MG, Kittrell C, Chen W, [8] et al. Gram-scale bottom-up flash graphene synthesis. Nature. 2020;577:647-51.
- [9] Luo J, Chen S, Li Q, Liu C, Gao S, Zhang J, et al. Influence of graphene oxide on the mechanical properties, fracture

- toughness, and microhardness of recycled concrete. Nanomaterials 9:325. Epub ahead of print 2019. doi: 10.3390/ nano9030325.
- [10] Seo DH, Pineda S, Fang J, Gozukara Y, Yick S, Bendavid A, et al. Single-step ambient-air synthesis of graphene from renewable precursors as electrochemical genosensor. Nat Commun.
- [11] Wan LF, Cho ES, Marangoni T, Shea P, Kang S, Rogers C, et al. Edge-functionalized graphene nanoribbon encapsulation to enhance stability and control kinetics of hydrogen storage materials. Chem Mater. 2019;31:2960-70.
- [12] Yu ZG, Zhang YW. Band gap engineering of graphene with interlayer embedded BN: From first principles calculations. Diam Relat Mater. 2015:54:103-8.
- [13] Yang Y, Yang HX, Wu YQ, Pu H, Meng WJ, Gao RZ, et al. Graphene caging core-shell Si@Cu nanoparticles anchored on graphene sheets for lithium-ion battery anode with enhanced reversible capacity and cyclic performance. Electrochim Acta. 2020;341:136037.
- [14] Bediako DK, Rezaee M, Yoo H, Larson DT, Zhao SYF, Taniguchi T, et al. Heterointerface effects in the electrointercalation of van der Waals heterostructures. Nature. 2018;558:425-9.
- [15] Liu J, Ma Q, Huang Z, Liu G, Zhang H. Recent progress in graphene-based noble-metal nanocomposites for electrocatalytic applications. Adv Mater. 2019;31:1-20.
- [16] Zholnin AG, Klyatskina EA, Grigoryev EG, Salvador MD, Misochenko AA, Dobrokhotov PL, et al. Spark-plasma sintering of Al₂O₃-graphene nanocomposite. Inorg Mater: Appl Res. 2018:9:498-503.
- [17] Khan M, Tahir MN, Adil SF, Khan HU, Siddiqui MRH, Alwarthan AA, et al. Graphene based metal and metal oxide nanocomposites: synthesis, properties and their applications. J Mater Chem A Mater. 2015;3:18753-808.
- [18] Anwar AW, Majeed A, Igbal N, Ullah W, Shuaib A, Ilyas U, et al. Specific capacitance and cyclic stability of graphene based metal/ metal oxide nanocomposites: A review. J Mater Sci Technol. 2015:31:699-707.
- [19] Xue F, Shu R, Xie Y. Controlling synthesis and gas-sensing properties of ordered mesoporous In₂O₃-reduced graphene oxide (rGO) nanocomposite. Sci Bull (Beijing). 2015;60:1348-54.
- [20] Wang C, Zhang L, Huang H, Xi R, Jiang DP, Zhang SH, et al. A nanocomposite consisting of ZnO decorated graphene oxide nanoribbons for resistive sensing of NO2 gas at room temperature. Microchim Acta 186:554. Epub ahead of print 2019. doi: 10. 1007/s00604-019-3628-x.
- [21] Noamani S, Niroomand S, Rastgar M, Sadrzadeh M. Carbonbased polymer nanocomposite membranes for oily wastewater treatment. NPJ Clean Water. 2019;2:1-14.
- [22] Hashemi SA, Mousavi SM, Bahrani S, Ramakrishna S, Babapoor A, Chiang WH. Coupled graphene oxide with hybrid metallic nanoparticles as potential electrochemical biosensors for precise detection of ascorbic acid within blood. Anal Chim Acta. 2020:1107:183-92.
- [23] Alireza Hashemi S, Bahrani S, Mojtaba Mousavi S, Omidifar N, Ghaleh Golab Behbahan N, Arjmand M, et al. Ultra-precise labelfree nanosensor based on integrated graphene with Au nanostars toward direct detection of IgG antibodies of SARS-CoV-2 in blood. J Electroanal Chem. 2021;894:115341.
- [24] Geng D, Yang HY. Recent advances in growth of novel 2D materials: beyond graphene and transition metal dichalcogenides. Adv Mater. 2018;30:1800865.

- [25] Derakhshi M, Daemi S, Shahini P, Habibzadeh A, Mostafavi E, Ashkarran AA. Two-dimensional nanomaterials beyond graphene for biomedical applications. J Funct Biomater. 2022;13:27.
- [26] Mir SH, Yadav VK, Singh JK. Recent advances in the carrier mobility of two-dimensional materials: a theoretical perspective. ACS Omega. 2020;5:14203-11.
- Shi L-B, Cao S, Yang M. Strain behavior and carrier mobility for novel two-dimensional semiconductor of GeP: First principles calculations. Phys E Low Dimens Syst Nanostruct. 2019;107:124-30.
- [28] Pan D, Zhang J, Li Z, Wu M. Hydrothermal route for cutting graphene sheets into blue-luminescent graphene quantum dots. Adv Mater. 2010;22:734-8.
- [29] Kadian S. Manik G. Ashish K. Singh M. Chauhan RP. Effect of sulfur doping on fluorescence and quantum yield of graphene quantum dots: an experimental and theoretical investigation. Nanotechnology. 2019;30:435704.
- [30] Chatterjee M, Nath P, Kadian S, Kumar A, Kumar V, Roy P, et al. Highly sensitive and selective detection of dopamine with boron and sulfur co-doped graphene quantum dots. Sci Rep. 2022;12:9061.
- [31] Liao L, Peng H, Liu Z. Chemistry makes graphene beyond graphene. J Am Chem Soc. 2014;136:12194-200.
- [32] Mohanta Z, Gaonkar SK, Kumar M, Saini J, Tiwari V, Srivastava C, et al. Graphene research and their outputs: Status and prospect. J Sci: Adv Mater Devices. 2020;5:10-29.
- [33] Geim AK, Novoselov KS. The rise of graphene. Nat Mater. 2007;6:183-91.
- [34] Hashemi SA, Bahrani S, Mousavi SM, Omidifar N, Behbahan N, Arjmand M, et al. Graphene-based femtogram-level sensitive molecularly imprinted polymer of SARS-CoV-2. Adv Mater Interfaces. 2021;8:2101466.
- [35] Sunnardianto GK, Maruyama I, Kusakabe K. Systematic study of the effect of H adsorption on the electron-transfer rate in graphene. J Comput Theor Nanosci. 2016;13:4883-7.
- Morishita N, Sunnardianto GK, Miyao S, Kusakabe K. Theoretical [36] analysis of pseudodegenerate zero-energy modes in vacancycentered hexagonal armchair nanographene. J Phys Soc Jpn. 2016;85:084703.
- [37] Suvarnaphaet P. Pechprasarn S. Graphene-based materials for biosensors: A review. Sensors. 2017;17:2161.
- [38] Zhu Y, Murali S, Cai W, Li X, Suk JW, Potts JR, et al. Graphene and graphene oxide: Synthesis, properties, and applications. Adv Mater. 2010;22:3906-24.
- Wang X, Zhao Y, Tian E, Li J, Ren Y. Graphene oxide-based polymeric membranes for water treatment. Adv Mater Interfaces. 2018:5:1701427.
- [40] Febriana E, Handayani M, Susilo DNA, Yahya MS, Ganta M, Sunnardianto GK. A simple approach of synthesis of graphene oxide from pure graphite: Time stirring duration variation. In AIP Conference Proceedings. AIP Publishing; 2021.
- [41] Handayani M, Ganta M, Susilo DNA, Yahya S, Sunnardianto GK, Darsono N. Synthesis of graphene oxide from used electrode graphite with controlled oxidation process. In IOP Conference Series: Materials Science and Engineering. IOP Publishing; 2019. p. 012032.
- [42] Hashemi SA, Bahrani S, Mousavi SM, Omidifar N, Arjmand M, Behbahan NGG, et al. Ultrasensitive biomolecule-less nanosensor based on β-cyclodextrin/quinoline decorated graphene oxide

- toward prompt and differentiable detection of corona and influenza viruses. Adv Mater Technol. 2021;6:2100341.
- [43] Delbari SA, Ghadimi LS, Hadi R, Farhoudian S, Nedaei M, Babapoor A, et al. Transition metal oxide-based electrode materials for flexible supercapacitors: A review. J Alloy Compd. 2021;857:158281.
- [44] Agarwal V, Zetterlund PB. Strategies for reduction of graphene oxide-A comprehensive review. Chem Eng J. 2021;405:127018.
- [45] Handayani M, Mulyaningsih Y, Aulia Anggoro M, Abbas A, Setiawan I, Triawan F, et al. One-pot synthesis of reduced graphene oxide/chitosan/zinc oxide ternary nanocomposites for supercapacitor electrodes with enhanced electrochemical properties. Mater Lett. 2022;314:131846.
- [46] Ponomarenko LA, Schedin F, Katsnelson MI, Yang R, Hill EW, Novoselov KS, et al. Chaotic Dirac billiard in graphene quantum dots. Science (1979). 2008;320:356-8.
- [47] Zhang F, Liu F, Wang C, Xin X, Liu J, Guo S, et al. Effect of lateral size of graphene quantum dots on their properties and application. ACS Appl Mater Interfaces. 2016;8:2104-10.
- [48] Mohanty N, Moore D, Xu Z, Sreeprasad TS, Nagaraja A, Rodriguez AA, et al. Nanotomy-based production of transferable and dispersible graphene nanostructures of controlled shape and size. Nat Commun. 2012;3:844.
- [49] Yan J, Pan G, Lin W, Tang Z, Zhang J, Li J, et al. Multi-responsive graphene quantum dots hybrid self-healing structural color hydrogel for information encoding and encryption. Chem Eng J. 2023;451:138922.
- [50] Hu Y, Neumann C, Scholtz L, Turchanin A, Resch-Genger U, Eigler S. Polarity, intramolecular charge transfer, and hydrogen bond co-mediated solvent effects on the optical properties of graphene quantum dots. Nano Res. 2023;16:45-52.
- Liu K, Li H, Wang F, Su Y. Recent advancement in graphene quantum dots based fluorescent sensor: Design, construction and bio-medical applications. Coord Chem Rev. 2023;478:214966.
- [52] Abbas A, Rubab S, Rehman A, Irfan S, Sharif HMA, Liang Q, et al. One-step green synthesis of biomass-derived graphene quantum dots as a highly selective optical sensing probe. Mater Today Chem. 2023:30:101555.
- [53] Abbas A, Liang Q, Abbas S, Liagat M, Rubab S, Tabish TA. Ecofriendly sustainable synthesis of graphene quantum dots from biowaste as a highly selective sensor. Nanomaterials. 2022;12:3696.
- [54] Zhu S, Song Y, Wang J, Wan H, Zhang Y, Ning Y, et al. Photoluminescence mechanism in graphene quantum dots: Quantum confinement effect and surface/edge state. Nano Today. 2017;13:10-4.
- [55] Rajender G, Goswami U, Giri PK. Solvent dependent synthesis of edge-controlled graphene quantum dots with high photoluminescence quantum yield and their application in confocal imaging of cancer cells. J Colloid Interface Sci. 2019;541:387-98.
- Kumar R, Kumar J, Kadian S, Srivastava P, Manik G, Bag M. [56] Tunable ionic conductivity and photoluminescence in guasi-2D CH₃NH₃PbBr₃ thin films incorporating sulphur doped graphene quantum dots. Phys Chem Chem Phys. 2021;23:22733-42.
- [57] Ye R, Peng Z, Metzger A, Lin J, Mann JA, Huang K, et al. Bandgap engineering of coal-derived graphene quantum dots. ACS Appl Mater Interfaces. 2015;7:7041-8.
- [58] Yan Y, Chen J, Li N, Tian J, Li K, Jiang J, et al. Systematic bandgap engineering of graphene quantum dots and applications for

- photocatalytic water splitting and CO₂ reduction. ACS Nano. 2018:12:3523-32.
- [59] Choi S-H. Unique properties of graphene quantum dots and their applications in photonic/electronic devices. J Phys D Appl Phys. 2017;50:103002.
- Wu J, Lin H, Moss DJ, Loh KP, Jia B. Graphene oxide for photonics, electronics and optoelectronics. Nat Rev Chem. 2023;7:1-22.
- Ghosh D. Sarkar K. Devi P. Kim KH. Kumar P. Current and future [61] perspectives of carbon and graphene quantum dots: From synthesis to strategy for building optoelectronic and energy devices. Renew Sustain Energy Rev. 2021;135:110391.
- [62] Hasan MT, Gonzalez-Rodriguez R, Ryan C, Faerber N, Coffer JL, Naumov AV. Photo-and electroluminescence from nitrogendoped and nitrogen-sulfur codoped graphene quantum dots. Adv Funct Mater. 2018;28:1804337.
- [63] Zhao J, Tang L, Xiang J, Ji R, Hu Y, Yuan J, et al. Fabrication and properties of a high-performance chlorine doped graphene quantum dot based photovoltaic detector. RSC Adv. 2015:5:29222-9.
- [64] Wang X, Sun G, Routh P, Kim DH, Huang W, Chen P. Heteroatomdoped graphene materials: syntheses, properties and applications. Chem Soc Rev. 2014;43:7067-98.
- [65] Rani P, Dalal R, Srivastava S. Effect of surface modification on optical and electronic properties of graphene quantum dots. Appl Surf Sci. 2023;609:155379.
- [66] Georgakilas V, Tiwari JN, Kemp KC, Perman JA, Bourlinos AB, Kim KS, et al. Noncovalent functionalization of graphene and graphene oxide for energy materials, biosensing, catalytic, and biomedical applications. Chem Rev. 2016;116:5464-519.
- Miao X, Qu D, Yang D, Nie B, Zhao Y, Fan H, et al. Synthesis [67] of carbon dots with multiple color emission by controlled graphitization and surface functionalization. Adv Mater. 2018;30:1704740.
- Tabish TA, Scotton CJ, Ferguson DCJ, Lin L, der Veen AV, Lowry S, et al. Biocompatibility and toxicity of graphene quantum dots for potential application in photodynamic therapy. Nanomedicine. 2018;13:1923-37.
- Geng B, Hu J, Li Y, Feng S, Pan D, Feng L, et al. Near-infrared phosphorescent carbon dots for sonodynamic precision tumor therapy. Nat Commun. 2022:13:5735.
- [70] Kalkal A, Kadian S, Pradhan R, Manik G, Packirisamy G. Recent advances in graphene quantum dot-based optical and electrochemical (bio) analytical sensors. Mater Adv. 2021:2:5513-41.
- Ni P, Li Q, Xu C, Lai H, Bai Y, Chen T. Optical properties of nitrogen and sulfur co-doped carbon dots and their applicability as fluorescent probes for living cell imaging. Appl Surf Sci. 2019:494:377-83.
- [72] Mondal MK, Mukherjee S, Joardar N, Roy D, Chowdhury P, Sinha Babu SP. Synthesis of smart graphene quantum dots: A benign biomaterial for prominent intracellular imaging and improvement of drug efficacy. Appl Surf Sci. 2019;495:143562.
- Xu X, He G, Wang L, Wang W, Jiang S, Fang Z. Optimization of [73] electrical performance and stability of fully solution-driven α -InGaZnO thin-film transistors by graphene quantum dots. J Mater Sci Technol. 2023;141:100-9.
- [74] Du F-P, Zhang H, Yao J-A, Chen SY, Xiao JK, Fu P, et al. Enhanced thermoelectric performance by constructing PEDOT: PSS/graphene quantum dots/single-walled carbon nanotube multilaver films. J Alloy Compd. 2022;911:164998.

- [75] Mousavi SM, Hashemi SA, Kalashgrani MY, Omidifar N, Bahrani S, Vijayakameswara Rao N, et al. Bioactive graphene quantum dots based polymer composite for biomedical applications. Polym (Basel). 2022;14:617.
- [76] Wilczewska P, Breczko J, Bobrowska DM, Wysocka-Żołopa M, Goclon J, Basa A, et al. Enhancement of polypyrrole electrochemical performance with graphene quantum dots in polypyrrole nanoparticle/graphene quantum dot composites. J Electroanal Chem. 2022;923:116767.
- [77] Zhu H, Li L, Shi M, Xiao P, Liu Y, Yan X. Coupling of graphene quantum dots with MnO2 nanosheets for boosting capacitive storage in ionic liquid electrolyte. Chem Eng J. 2022;437:135301.
- [78] Kumar P, Dhand C, Dwivedi N, Singh S, Khan R, Verma S, et al. Graphene quantum dots: A contemporary perspective on scope, opportunities, and sustainability. Renew Sustain Energy Rev. 2022;157:111993.
- [79] Bhuyan MSA, Uddin MN, Islam MM, Bipasha FA, Hossain SS. Synthesis of graphene. Int Nano Lett. 2016;6:65-83.
- [80] Eissa S, N'diaye J, Brisebois P, Izquierdo R, Tavares AC, Siaj M. Probing the influence of graphene oxide sheets size on the performance of label-free electrochemical biosensors. Sci Rep. 2020:10:13612.
- [81] Krishnan SK, Singh E, Singh P, Meyyappan M, Nalwa HS. A review on graphene-based nanocomposites for electrochemical and fluorescent biosensors. RSC Adv. 2019;9:8778-881.
- [82] Tian W, Li W, Yu W, Liu X. A review on lattice defects in graphene: types, generation, effects and regulation. Micromachines (Basel). 2017:8:163.
- [83] Alhourani A, Førde J-L, Eichacker LA, Herfindal L, Hagland HR. Improved pH-responsive release of phenformin from low-defect graphene compared to graphene oxide. ACS Omega.
- [84] Najafi rad Z, Farzad F, Razavi L. Surface functionalization of graphene nanosheet with poly (I-histidine) and its application in drug delivery: Covalent vs non-covalent approaches. Sci Rep. 2022;12:19046.
- [85] Lakshmanakumar M, Nesakumar N, Sethuraman S, Rajan KS, Krishnan UM, Rayappan J. Functionalized graphene quantum dot interfaced electrochemical detection of cardiac troponin I: an antibody free approach. Sci Rep. 2019;9:17348.
- [86] Esfahani S. Akbari I. Soleimani-Amiri S. Mirzaei M. Ghasemi Gol A. Assessing the drug delivery of ibuprofen by the assistance of metal-doped graphenes: insights from density functional theory. Diam Relat Mater. 2023;135:109893.
- [87] Deng S, Gao E, Wang Y, Sen S, Sreenivasan ST, Behura S, et al. Confined, oriented, and electrically anisotropic graphene wrinkles on bacteria. ACS Nano. 2016;10:8403-12.
- [88] Hu KM, Liu YQ, Zhou LW, Xue ZY, Peng B, Yan H, et al. Delamination-Free Functional Graphene Surface by Multiscale, Conformal Wrinkling. Adv Funct Mater. 2020;30:2003273.
- [89] Geim A, Novoselov K. Graphene calling. Nat Mater. 2007;6:169.
- [90] Novoselov KS, Geim AK, Morozov SV, Jiang D, Zhang Y, Dubonos SV, et al. Electric field effect in atomically thin carbon films. Science (1979). 2004;306:666-9.
- [91] Zhu H, Cao Y, Zhang J, Zhang W, Xu Y, Guo J, et al. One-step preparation of graphene nanosheets via ball milling of graphite and the application in lithium-ion batteries. | Mater Sci.
- Papageorgiou DG, Kinloch IA, Young RJ. Mechanical properties of [92] graphene and graphene-based nanocomposites. Prog Mater Sci. 2017;90:75-127.

- [93] Emtsev KV, Bostwick A, Horn K, Jobst J, Kellogg GL, Ley L, et al. Towards wafer-size graphene layers by atmospheric pressure graphitization of silicon carbide. Nat Mater. 2009;8:203-7.
- [94] Paton KR, Varrla E, Backes C, Smith RJ, Khan U, O'Neill A, et al. Scalable production of large quantities of defect-free few-layer graphene by shear exfoliation in liquids. Nat Mater. 2014;13:624-30.
- [95] Dimiev AM, Ceriotti G, Metzger A, Kim ND, Tour JM. Chemical mass production of graphene nanoplatelets in ~100% yield. ACS Nano. 2016;10:274-9.
- [96] Raccichini R, Varzi A, Passerini S, Scrosati B. The role of graphene for electrochemical energy storage. Nat Mater. 2015;14:271-9.
- [97] Abdelkader AM, Cooper AJ, Dryfe RA, Kinloch IA. How to get between the sheets: A review of recent works on the electrochemical exfoliation of graphene materials from bulk graphite. Nanoscale. 2015;7:6944-56.
- [98] Parvez K, Li R, Puniredd SR, Hernandez Y, Hinkel F, Wang S, et al. Electrochemically exfoliated graphene as solution-processable, highly conductive electrodes for organic electronics. ACS Nano. 2013;7:3598-606.
- [99] Shih CJ, Vijayaraghavan A, Krishnan R, Sharma R, Han JH, Ham MH, et al. Bi- and trilayer graphene solutions. Nat Nanotechnol. 2011;6:439-45.
- [100] Ohta T, Bostwick A, McChesney JL, Seyller T, Horn K, Rotenberg E. Interlayer interaction and electronic screening in multilayer graphene. 2006;2:2-5.
- [101] Han D, Wang X, Zhao Y, Chen Y, Tang M, Zhao Z. High-quality graphene synthesis on amorphous SiC through a rapid thermal treatment. Carbon. 2017;124:105-10.
- [102] Morozov SV, Novoselov KS, Katsnelson MI, Schedin F, Ponomarenko LA, Jiang D, et al. Strong suppression of weak localization in graphene. Phys Rev Lett. 2006;97(1):016801.
- [103] Giusca CE, Spencer SJ, Shard AG, Yakimova R, Kazakova O. Exploring graphene formation on the C-terminated face of SiC by structural. chemical and electrical methods. Carbon N Y. 2014;69:221-9.
- [104] Saeed M, Alshammari Y, Majeed SA, Al-Nasrallah E. Chemical vapour deposition of graphene synthesis, characterisation, and application: A review. Molecules. 2020;25:2-62.
- [105] Morton JA, Kaur A, Khavari M, Tyurnina AV, Priyadarshi A, Eskin DG, et al. An eco-friendly solution for liquid phase exfoliation of graphite under optimised ultrasonication conditions. Carbon N Y. 2023;204:434-46.
- [106] Lee H, Choi JI, Park J, Jang SS, Lee SW. Role of anions on electrochemical exfoliation of graphite into graphene in aqueous acids. Carbon N Y. 2020;167:816-25.
- [107] Chen Y, Zhao Y, Han D, Fu D, Chen Y, Zhou D, et al. A graphite enclosure assisted synthesis of high-quality patterned graphene on 6H-SiC by ion implantation. Carbon N Y. 2021;172:353-9.
- [108] Tian P, Tang L, Teng KS, Lau SP. Graphene quantum dots from chemistry to applications. Mater Today Chem. 2018;10:221-58.
- [109] Singh I, Arora R, Dhiman H, Pahwa R. Carbon quantum dots: Synthesis, characterization and biomedical applications. Turk J Pharm Sci. 2018;15:219-30.
- [110] Li M, Chen T, Gooding JJ, Liu J. Review of carbon and graphene quantum dots for sensing. ACS Sens. 2019;4:1732-48.
- Li K, Liu W, Ni Y, Li D, Lin D, Su Z, et al. Technical synthesis and biomedical applications of graphene quantum dots. J Mater Chem B. 2017;5:4811-26.
- Yang F, Zhao M, Zheng B, Xiao D, Wu L, Guo Y. Influence of pH on the fluorescence properties of graphene quantum dots using

- ozonation pre-oxide hydrothermal synthesis. J Mater Chem. 2012:22:25471-9.
- [113] Tetsuka H, Asahi R, Nagoya A, Okamoto K, Tajima I, Ohta R, et al. Optically tunable amino-functionalized graphene quantum dots. Adv Mater. 2012;24:5333-8.
- Kumar Chaturvedi A, Pappu A, Kumar Srivastava A, Kumar Gupta M. Synthesis, dielectric and mechanical properties of paddy straw derived graphene quantum dots-stone waste nanocomposite. Mater Lett. 2021;301:130323.
- [115] Srivastava A, Badatya S, Chaturvedi AK, Kashyap DK, Srivastava AK, Gupta MK. Paddy-Straw-Derived graphene quantum dots reinforced vertical aligned zinc oxide nanosheetbased flexible triboelectric nanogenerator for self-powered UV sensors and tribotronics application. ACS Appl Mater Interfaces. 2023;15:24724-35.
- [116] Shen J, Zhu Y, Yang X, Zong J, Zhang J, Li C. One-pot hydrothermal synthesis of graphene quantum dots surface-passivated by polyethylene glycol and their photoelectric conversion under near-infrared light. N J Chem. 2012;36:97-101.
- [117] Dong Y, Chen C, Zheng X, Gao L, Cui Z, Yang H, et al. One-step and high yield simultaneous preparation of single- and multi-layer graphene quantum dots from CX-72 carbon black. J Mater Chem. 2012:22:8764-6.
- [118] Nguyen HY, Le XH, Dao NT, Pham NT, Vu THH, Nguyen NH, et al. Microwave-assisted synthesis of graphene quantum dots and nitrogen-doped graphene quantum dots: Raman characterization and their optical properties. Adv Nat Sci: Nanosci Nanotechnol. 2019;10:025005.
- [119] Luo Z, Qi G, Chen K, Zou M, Yuwen L, Zhang X, et al. Microwaveassisted preparation of white fluorescent graphene quantum dots as a novel phosphor for enhanced white-light-emitting diodes. Adv Funct Mater. 2016;26:2739-44.
- [120] Shinde DB, Pillai VK. Electrochemical preparation of luminescent graphene quantum dots from multiwalled carbon nanotubes. Chem - A Eur J. 2012;18:12522-8.
- [121] Kalita H, Harikrishnan V, Shinde DB, Pillai VK, Aslam M. Hysteresis and charge trapping in graphene quantum dots. Appl Phys Lett.
- [122] Lu J, Yang JX, Wang J, Lim A, Wang S, Loh KP. One-pot synthesis of fluorescent carbon nanoribbons, nanoparticles, and graphene by the exfoliation of graphite in ionic liquids. ACS Nano. 2009;3:2367-75.
- [123] Zhang M, Bai L, Shang W, Xie W, Ma H, Fu Y, et al. Facile synthesis of water-soluble, highly fluorescent graphene quantum dots as a robust biological label for stem cells. J Mater Chem. 2012;22:7461-7.
- Ananthanarayanan A, Wang X, Routh P, Sana B, Lim S, Kim DH, et al. Facile synthesis of graphene quantum dots from 3D graphene and their application for Fe³⁺ sensing. Adv Funct Mater. 2014:24:3021-6.
- Liu R, Wu D, Feng X, Müllen K. Bottom-up fabrication of photoluminescent graphene quantum dots with uniform morphology. J Am Chem Soc. 2011;133:15221-3.
- Dong Y, Shao J, Chen C, Li H, Wang R, Chi Y, et al. Blue luminescent [126] graphene quantum dots and graphene oxide prepared by tuning the carbonization degree of citric acid. Carbon N Y. 2012;50:4738-43.
- [127] Li R, Liu Y, Li Z, Shen J, Yang Y, Cui X, et al. Bottom-up fabrication of single-layered nitrogen-doped graphene quantum dots through intermolecular carbonization arrayed in a 2D plane. Chem - A Eur J. 2016;22:272-8.

- [128] Yan X, Cui X, Li LS. Synthesis of large, stable colloidal graphene quantum dots with tunable size. J Am Chem Soc. 2010;132:5944–5.
- [129] Zhao C, Song X, Liu Y, Fu Y, Ye L, Wang N, et al. Synthesis of graphene quantum dots and their applications in drug delivery. J Nanobiotechnol. 2020;18:142. Epub ahead of print 2020. doi: 10. 1186/s12951-020-00698-z.
- [130] Wang L, Li W, Wu B, Li Z, Pan D, Wu M. Room-temperature synthesis of graphene quantum dots via electron-beam irradiation and their application in cell imaging. Chem Eng J. 2017;309:374–80.
- [131] Facure MHM, Schneider R, Mercante LA, Correa DS. Rational hydrothermal synthesis of graphene quantum dots with optimized luminescent properties for sensing applications. Mater Today Chem. 2022;23:100755.
- [132] Dong Y, Chen C, Zheng X, Gao L, Cui Z, Yang H, et al. One-step and high yield simultaneous preparation of single- and multi-layer graphene quantum dots from CX-72 carbon black. J Mater Chem. 2012;22:8764–6.
- [133] Li W, Li M, Liu Y, Pan D, Li Z, Wang L, et al. Three minute ultrarapid microwave-assisted synthesis of bright fluorescent graphene quantum dots for live cell staining and white LEDs. ACS Appl Nano Mater. 2018;1:1623–30.
- [134] Ghaffarkhah A, Hosseini E, Kamkar M, Sehat AA, Dordanihaghighi S, Allahbakhsh A, et al. Synthesis, applications, and prospects of graphene quantum dots: A comprehensive review. Small. 2022;18:2102683.
- [135] Abbas A, Tabish TA, Bull SJ, Lim TM, Phan AN. High yield synthesis of graphene quantum dots from biomass waste as a highly selective probe for Fe³⁺ sensing. Sci Rep. 2020;10:1–16.
- [136] Pumera M. Graphene in biosensing. Mater Today. 2011;14:308–15.
- [137] Seo G, Lee G, Kim MJ, Baek SH, Choi M, Ku KB, et al. Rapid detection of COVID-19 causative virus (SARS-CoV-2) in human nasopharyngeal swab specimens using field-effect transistor-based biosensor. ACS Nano. 2020;14:5135–42.
- [138] Morozov SV, Novoselov KS, Katsnelson MI, Schedin F, Ponomarenko LA, Jiang D, et al. Strong suppression of weak localization in graphene. Phys Rev Lett. 2006;97:7–10.
- [139] Peña-Bahamonde J, Nguyen HN, Fanourakis SK, Rodrigues DF. Recent advances in graphene-based biosensor technology with applications in life sciences. J Nanobiotechnology. 2018;16:1–17.
- [140] Wu X, Xing Y, Zeng K, Huber K, Zhao JX. Study of fluorescence quenching ability of graphene oxide with a layer of rigid and tunable silica spacer. Langmuir. 2018;34:603–11.
- [141] Li H, Huang X, Mehedi Hassan M, Zuo M, Wu X, Chen Y, et al. Dual-channel biosensor for Hg²⁺ sensing in food using Au@ Ag/graphene-upconversion nanohybrids as metal-enhanced fluorescence and SERS indicators. Microchem J. 2020;154:104563.
- [142] Wong XY, Quesada-González D, Manickam S, New SY, Muthoosamy K, Merkoçi A. Integrating gold nanoclusters, folic acid and reduced graphene oxide for nanosensing of glutathione based on "turn-off" fluorescence. Sci Rep. 2021;11:2375.
- [143] Kadadou D, Tizani L, Wadi VS, Banat F, Alsafar H, Yousef AF, et al. Detection of SARS-CoV-2 in clinical and environmental samples using highly sensitive reduced graphene oxide (rGO)-based biosensor. Chem Eng J. 2023;453:139750.
- [144] Fan J, Yuan L, Liu Q, Tong C, Wang W, Xiao F, et al. An ultrasensitive and simple assay for the Hepatitis C virus using a reduced graphene oxide-assisted hybridization chain reaction. Analyst. 2019;144:3972–9.

- [145] Gao J, He P, Yang T, Zhou L, Wang X, Chen S, et al. Electrodeposited NiO/graphene oxide nanocomposite: an enhanced voltammetric sensing platform for highly sensitive detection of uric acid, dopamine and ascorbic acid. J Electroanal Chem. 2019;852:113516.
- [146] Zhang H, Liu S. Electrochemical sensors based on nitrogen-doped reduced graphene oxide for the simultaneous detection of ascorbic acid, dopamine and uric acid. J Alloy Compd. 2020;842:155873.
- [147] Yang H, Bao J, Qi Y, Zhao J, Hu Y, Wu W, et al. A disposable and sensitive non-enzymatic glucose sensor based on 3D graphene/ Cu₂O modified carbon paper electrode. Anal Chim Acta. 2020:1135:12–9.
- [148] Yu H, Chong Y, Zhang P, Ma J, Li D. A D-shaped fiber SPR sensor with a composite nanostructure of MoS₂-graphene for glucose detection. Talanta. 2020;219:121324.
- [149] Zhang Y, Chen X, Roozbahani GM, Guan X. Graphene oxide-based biosensing platform for rapid and sensitive detection of HIV-1 protease. Anal Bioanal Chem. 2018;410:6177–85.
- [150] Mohsin DH, Mashkour MS, Fatemi F. Design of aptamer-based sensing platform using gold nanoparticles functionalized reduced graphene oxide for ultrasensitive detection of Hepatitis B virus. Chem Pap. 2021;75:279–95.
- [151] Jin X, Zhang H, Li Y-T, Xiao MM, Zhang ZL, Pang DW, et al. A field effect transistor modified with reduced graphene oxide for immunodetection of Ebola virus. Microchim Acta. 2019;186:1–9.
- [152] Khalil I, Yehye WA, Julkapli NM, Rahmati S, Sina AA, Basirun WJ, et al. Graphene oxide and gold nanoparticle based dual platform with short DNA probe for the PCR free DNA biosensing using surface-enhanced Raman scattering. Biosens Bioelectron. 2019;131:214–23.
- [153] Ye Y, Xie J, Ye Y, Cao X, Zheng H, Xu X, et al. A label-free electrochemical DNA biosensor based on thionine functionalized reduced graphene oxide. Carbon N Y. 2018;129:730–7.
- [154] Nayak TR, Andersen H, Makam VS, Khaw C, Bae S, Xu X, et al. Graphene for controlled and accelerated osteogenic differentiation of human mesenchymal stem cells. ACS Nano. 2011;5:4670–8.
- [155] Shadjou N, Hasanzadeh M, Khalilzadeh B. Graphene based scaffolds on bone tissue engineering. Bioengineered. 2018;9:38–47.
- [156] Mohammadi S, Shafiei SS, Asadi-Eydivand M, Ardeshir M, Solati-Hashjin M. Graphene oxide-enriched poly (\varepsilon-caprolactone) electrospun nanocomposite scaffold for bone tissue engineering applications. J Bioact Compat Polym. 2017;32:325–42.
- [157] Mohammadi S, Shafiei SS, Asadi-Eydivand M, Ardeshir M, Solati-Hashjin M. Graphene oxide-enriched poly(ε-caprolactone) electrospun nanocomposite scaffold for bone tissue engineering applications. J Bioact Compat Polym. 2017;32:325–42.
- [158] Kalbacova M, Broz A, Kong J, Kalbac M. Graphene substrates promote adherence of human osteoblasts and mesenchymal stromal cells. Carbon N Y. 2010;48:4323–9.
- [159] Li N, Zhang X, Song Q, Su R, Zhang Q, Kong T, et al. The promotion of neurite sprouting and outgrowth of mouse hippocampal cells in culture by graphene substrates. Biomaterials. 2011;32:9374–82.
- [160] Ahmed MK, Menazea AA, Mansour SF, Al-Wafi R. Differentiation between cellulose acetate and polyvinyl alcohol nanofibrous scaffolds containing magnetite nanoparticles/graphene oxide via pulsed laser ablation technique for tissue engineering applications. I Mater Res Technol. 2020;9:11629–40.
- [161] Murugesan B, Pandiyan N, Arumugam M, Sonamuthu J, Samayanan S, Yurong C, et al. Fabrication of palladium

- nanoparticles anchored polypyrrole functionalized reduced graphene oxide nanocomposite for antibiofilm associated orthopedic tissue engineering. Appl Surf Sci. 2020;510:145403.
- [162] Jie W, Song F, Li X, Li W, Wang R, Jiang Y, et al. Enhancing the proliferation of MC3T3-E1 cells on casein phosphopeptide-biofunctionalized 3D reduced-graphene oxide/polypyrrole scaffolds. RSC Adv. 2017;7:34415-24.
- [163] Yu P, Bao R-Y, Shi X-J, Yang W, Yang MB. Self-assembled highstrength hydroxyapatite/graphene oxide/chitosan composite hydrogel for bone tissue engineering. Carbohydr Polym. 2017;155:507-15.
- [164] Lu R, Zhang W, He Y, Zhang S, Fu Q, Pang Y, et al. Ferric ion crosslinking-based 3D printing of a graphene oxide hydrogel and its evaluation as a bio-scaffold in tissue engineering. Biotechnol Bioeng. 2021;118:1006-12.
- [165] Heidari M, Bahrami SH, Ranjbar-Mohammadi M, Milan PB. Smart electrospun nanofibers containing PCL/gelatin/graphene oxide for application in nerve tissue engineering. Mater Sci Eng: C. 2019;103:109768.
- [166] Abzan N, Kharaziha M, Labbaf S. Development of three-dimensional piezoelectric polyvinylidene fluoride-graphene oxide scaffold by non-solvent induced phase separation method for nerve tissue engineering. Mater Des. 2019;167:107636.
- [167] Zeinali K, Khorasani MT, Rashidi A, Daliri Joupari M. Preparation and characterization of graphene oxide aerogel/gelatin as a hybrid scaffold for application in nerve tissue engineering. Int J Polym Mater Polym Biomater. 2021;70:674-83.
- [168] Dasari Shareena TP, McShan D, Dasmahapatra AK, Tchounwou PB. A Review on Graphene-Based Nanomaterials in Biomedical Applications and Risks in Environment and Health. Nanomicro Lett. 2018;10:1-34.
- [169] Lage T, Rodrigues RO, Catarino S, Gallo J, Bañobre-López M, Minas G. Graphene-based magnetic nanoparticles for theranostics: An overview for their potential in clinical application. Nanomaterials. 2021;11(5):1073. doi: 10.3390/nano11051073.
- [170] Jafari Z, Rad AS, Baharfar R, Asghari S, Esfahani MR. Synthesis and application of chitosan/tripolyphosphate/graphene oxide hydrogel as a new drug delivery system for Sumatriptan Succinate. | Mol Lig. 2020;315:113835.
- Kumar G, Chaudhary K, Mogha NK, Kant A, Masram DT. Extended release of metronidazole drug using chitosan/graphene oxide bionanocomposite beads as the drug carrier. ACS Omega. 2021;6:20433-44.
- [172] Tiwari H, Karki N, Pal M, Basak S, Verma RK, Bal R, et al. Functionalized graphene oxide as a nanocarrier for dual drug delivery applications: The synergistic effect of quercetin and gefitinib against ovarian cancer cells. Colloids Surf B Biointerfaces. 2019;178:452-9.
- [173] Chen K, Ling Y, Cao C, Li X, Chen X, Wang X. Chitosan derivatives/ reduced graphene oxide/alginate beads for small-molecule drug delivery. Mater Sci Eng: C. 2016;69:1222-8.
- Mahmoud ME, Attia AA, Helmy MW, Hemdan IH, Abouelanwar ME. Doxorubicin drug release behavior from amino-silanated graphene oxide nanocarrier. Diam Relat Mater. 2023;131:109569.
- [175] Qi Z, Shi J, Zhu B, Li J, Cao S. Gold nanorods/graphene oxide nanosheets immobilized by polydopamine for efficient remotely triggered drug delivery. J Mater Sci. 2020;55:14530-43.
- Tong C, Zhang X, Fan J, Li B, Liu B, Daniyal M, et al. PEGylated mBPEI-rGO nanocomposites facilitate hepotocarcinoma

- treatment combining photothermal therapy and chemotherapy. Sci Bull (Beijing). 2018;63:935-46.
- [177] Singh G, Nenavathu BP. Development of rGO encapsulated polymeric beads as drug delivery system for improved loading and controlled release of doxycycline drug. Drug Dev Ind Pharm. 2020;46:462-70.
- Kooti M, Sedeh AN, Motamedi H, Rezatofighi SE. Magnetic graphene oxide inlaid with silver nanoparticles as antibacterial and drug delivery composite. Appl Microbiol Biotechnol. 2018;102:3607-21.
- Horgan CC, Bergholt MS, Nagelkerke A, Thin MZ, Pence IJ, [179] Kauscher U, et al. Integrated photodynamic Raman theranostic system for cancer diagnosis, treatment, and post-treatment molecular monitoring. Theranostics. 2021;11:2006-19.
- [180] Lin J, Chen X, Huang P. Graphene-based nanomaterials for bioimaging. Adv Drug Deliv Rev. 2016;105:242-54.
- [181] Ferrer-Ugalde A, Sandoval S, Pulagam KR, Muñoz-Juan A, Laromaine A, Llop J, et al. Radiolabeled Cobaltabis (dicarbollide) Anion-Graphene Oxide Nanocomposites for In Vivo Bioimaging and Boron Delivery. ACS Appl Nano Mater. 2021:4:1613-25.
- [182] Song X, Li S, Guo H, You W, Shang X, Li R, et al. Grapheneoxide-modified lanthanide nanoprobes for tumor-targeted visible/ NIR-II luminescence imaging. Angew Chem Int Ed. 2019;58:18981-6.
- [183] Song Y-Y, Li C, Yang X-Q, An J, Cheng K, Xuan Y, et al. Graphene oxide coating core-shell silver sulfide@ mesoporous silica for active targeted dual-mode imaging and chemo-photothermal synergistic therapy against tumors. J Mater Chem B. 2018;6:4808-20.
- [184] Jia X, Xu W, Ye Z, Wang Y, Dong Q, Wang E, et al. Functionalized graphene@ gold nanostar/lipid for pancreatic cancer gene and photothermal synergistic therapy under photoacoustic/photothermal imaging dual-modal guidance. Small. 2020;16:2003707.
- Wanas W, Abd El-Kaream SA, Ebrahim S, Soliman M, Karim M. Cancer bioimaging using dual mode luminescence of graphene/ FA-ZnO nanocomposite based on novel green technique. Sci Rep. 2023;13:27.
- Zang Z, Zeng X, Wang M, Hu W, Liu C, Tang X. Tunable photoluminescence of water-soluble AgInZnS-graphene oxide (GO) nanocomposites and their application in-vivo bioimaging. Sens Actuators B Chem. 2017;252:1179-86.
- [187] Yogesh GK, Shuaib EP, Roopmani P, Gumpu MB, Krishnan UM, Sastikumar D. Synthesis, characterization and bioimaging application of laser-ablated graphene-oxide nanoparticles (nGOs). Diam Relat Mater. 2020;104:107733.
- Lei L, Ma H, Yang M, Qin Y, Ma Y, Wang T, et al. Fluorophorefunctionalized graphene oxide with application in cell imaging. N J Chem. 2017;41:12375-9.
- [189] Chawda N, Basu M, Majumdar D, Poddar R, Mahapatra SK, Banerjee I. Engineering of gadolinium-decorated graphene oxide nanosheets for multimodal bioimaging and drug delivery. ACS Omega. 2019;4:12470-9.
- [190] Akhavan O, Ghaderi E. Toxicity of graphene and graphene oxide nanowalls against bacteria. ACS Nano. 2010;4:5731-6.
- [191] Liu S, Zeng TH, Hofmann M, Burcombe E, Wei J, Jiang R, et al. Antibacterial Activity of Graphite, Graphite Oxide, Graphene Oxide, and Reduced Graphene Oxide: Membrane and Oxidative Stress. ACS Nano. 2011;5:6971-80.
- Liu T, Liu Y, Liu M, Wang Y, He W, Shi G, et al. Synthesis of graphene oxide-quaternary ammonium nanocomposite with

- synergistic antibacterial activity to promote infected wound healing. Burn Trauma. 2018;6:1–23.
- [193] Valentini F, Calcaterra A, Ruggiero V, Pichichero E, Martino A, Iosi F, et al. Functionalized graphene derivatives: Antibacterial properties and cytotoxicity. J Nanomater. 2019;2019:1–14. doi: 10.1155/2019/2752539.
- [194] He J, Zhu X, Qi Z, Wang C, Mao X, Zhu C, et al. Killing dental pathogens using antibacterial graphene oxide. ACS Appl Mater Interfaces. 2015;7:5605–11.
- [195] Ye S, Shao K, Li Z, Guo N, Zuo Y, Li Q, et al. Antiviral activity of graphene oxide: How sharp edged structure and charge matter. ACS Appl Mater Interfaces. 2015;7:21578–9.
- [196] Sametband M, Kalt I, Gedanken A, Sarid R. Herpes simplex virus type-1 attachment inhibition by functionalized graphene oxide. ACS Appl Mater Interfaces. 2014;6:1228–35.
- [197] Deokar AR, Nagvenkar AP, Kalt I, Shani L, Yeshurun Y, Gedanken A, et al. Graphene-based 'hot Plate' for the capture and destruction of the herpes simplex virus type 1. Bioconjugate Chem. 2017;28:1115–22.
- [198] Fallatah H, Elhaneid M, Ali-Boucetta H, Overton TW, El Kadri H, Gkatzionis K. Antibacterial effect of graphene oxide (GO) nanoparticles against Pseudomonas putida biofilm of variable age. Environ Sci Pollut Res. 2019;26:25057–70.
- [199] Sengupta I, Bhattacharya P, Talukdar M, Neogi S, Pal SK, Chakraborty S. Bactericidal effect of graphene oxide and reduced graphene oxide: Influence of shape of bacteria. Colloid Interface Sci Commun. 2019;28:60–8.
- [200] Tang J, Chen Q, Xu L, Zhang S, Feng L, Cheng L, et al. Graphene oxide–silver nanocomposite as a highly effective antibacterial agent with species-specific mechanisms. ACS Appl Mater Interfaces. 2013;5:3867–74.
- [201] Ali NH, Amin MCIM, Ng S-F. Sodium carboxymethyl cellulose hydrogels containing reduced graphene oxide (rGO) as a functional antibiofilm wound dressing. J Biomater Sci Polym Ed. 2019:30:629–45.
- [202] Chang Y-N, Ou X-M, Zeng G-M, Gong JL, Deng CH, Jiang Y, et al. Synthesis of magnetic graphene oxide–TiO₂ and their antibacterial properties under solar irradiation. Appl Surf Sci. 2015;343:1–10.
- [203] Dhandapani P, AlSalhi MS, Karthick R, Chen F, Devanesan S, Kim W, et al. Biological mediated synthesis of RGO-ZnO composites with enhanced photocatalytic and antibacterial activity. J Hazard Mater. 2021;409:124661.
- [204] Hashem AH, Hasanin M, Kamel S, Dacrory S. A new approach for antimicrobial and antiviral activities of biocompatible nanocomposite based on cellulose, amino acid and graphene oxide. Colloids Surf B Biointerfaces. 2022;209:112172.
- [205] Du T, Lu J, Liu L, Dong N, Fang L, Xiao S, et al. Antiviral activity of graphene oxide–silver nanocomposites by preventing viral entry and activation of the antiviral innate immune response. ACS Appl Bio Mater. 2018;1:1286–93.
- [206] Yang XX, Li CM, Li YF, Wang J, Huang CZ. Synergistic antiviral effect of curcumin functionalized graphene oxide against respiratory syncytial virus infection. Nanoscale. 2017;9:16086–92.
- [207] Hai X, Feng J, Chen X, Wang J. Tuning the optical properties of graphene quantum dots for biosensing and bioimaging. J Mater Chem B. 2018;6:3219–34.
- [208] Xu JJ, Zhao WW, Song S, Fan C, Chen HY. Functional nanoprobes for ultrasensitive detection of biomolecules: An update. Chem Soc Rev. 2014;43:1601–11.

- [209] Zhang J, Cheng F, Li J, Zhu JJ, Lu Y. Fluorescent nanoprobes for sensing and imaging of metal ions: Recent advances and future perspectives. Nano Today. 2016;11:309–29.
- [210] Wang F, Gu Z, Lei W, Wang W, Xia X, Hao Q. Graphene quantum dots as a fluorescent sensing platform for highly efficient detection of copper(II) ions. Sens Actuators B Chem. 2014;190:516–22.
- [211] Niu X, Zhong Y, Chen R, Wang F, Liu Y, Luo D. A "turn-on" fluorescence sensor for Pb²⁺ detection based on graphene quantum dots and gold nanoparticles. Sens Actuators B Chem. 2018;255:1577–81.
- [212] Anh NTN, Chowdhury AD, Doong RA. Highly sensitive and selective detection of mercury ions using N, S-codoped graphene quantum dots and its paper strip based sensing application in wastewater. Sens Actuators B Chem. 2017:252:1169–78.
- [213] Ran X, Sun H, Pu F, Ren J, Qu X. Ag nanoparticle-decorated graphene quantum dots for label-free, rapid and sensitive detection of Ag⁺ and biothiols. Chem Commun. 2013;49:1079–81.
- [214] Chung S, Revia RA, Zhang M. Graphene quantum dots and their applications in bioimaging, biosensing, and therapy. Adv Mater. 2021;33:1–26.
- [215] Xu A, He P, Huang T, Li J, Hu X, Xiang P, et al. Selective supramolecular interaction of ethylenediamine functionalized graphene quantum dots: Ultra-sensitive photoluminescence detection for nickel ion in vitro. Synth Met. 2018;244:106–12.
- [216] Li N, Than A, Chen J, Xi F, Liu J, Chen P. Graphene quantum dots based fluorescence turn-on nanoprobe for highly sensitive and selective imaging of hydrogen sulfide in living cells. Biomater Sci. 2018;6:779–84.
- [217] Lin L, Rong M, Lu S, Song X, Zhong Y, Yan J, et al. A facile synthesis of highly luminescent nitrogen-doped graphene quantum dots for the detection of 2, 4, 6-trinitrophenol in aqueous solution. Nanoscale. 2015;7:1872–8.
- [218] Gao W, Song H, Wang X, Liu X, Pang X, Zhou Y, et al. Carbon dots with red emission for sensing of Pt²⁺, Au³⁺, and Pd²⁺ and their bioapplications in vitro and in vivo. ACS Appl Mater Interfaces. 2018;10:1147–54.
- [219] Su Y, Zhou X, Long Y, Li W. Immobilization of horseradish peroxidase on amino-functionalized carbon dots for the sensitive detection of hydrogen peroxide. Microchim Acta. 2018;185:1–8.
- [220] Hassanvand Z, Jalali F, Nazari M, Parnianchi F, Santoro C. Carbon nanodots in electrochemical sensors and biosensors: A review. ChemElectroChem. 2021;8:15–35.
- [221] Mollarasouli F, Asadpour-Zeynali K, Campuzano S, Yáñez-Sedeño P, Pingarrón JM. Non-enzymatic hydrogen peroxide sensor based on graphene quantum dots-chitosan/methylene blue hybrid nanostructures. Electrochim Acta. 2017;246:303–14.
- [222] Yang C, Hu LW, Zhu HY, Ling Y, Tao JH, Xu CX. RGO quantum dots/ ZnO hybrid nanofibers fabricated using electrospun polymer templates and applications in drug screening involving an intracellular $\rm H_2O_2$ sensor. J Mater Chem B. 2015;3:2651–9.
- [223] Bai J, Sun C, Jiang X. Carbon dots-decorated multiwalled carbon nanotubes nanocomposites as a high-performance electrochemical sensor for detection of $\rm H_2O_2$ in living cells. Anal Bioanal Chem. 2016;408:4705–14.
- [224] Lin L, Song X, Chen Y, Rong M, Zhao T, Wang Y, et al. Intrinsic peroxidase-like catalytic activity of nitrogen-doped graphene quantum dots and their application in the colorimetric detection of $\rm H_2O_2$ and glucose. Anal Chim Acta. 2015;869:89–95.

- [225] Ge S, He J, Ma C, Liu J, Xi F, Dong X. One-step synthesis of boron-doped graphene quantum dots for fluorescent sensors and biosensor. Talanta. 2019;199:581–9.
- [226] Shi H, Chen L, Niu N. An off-on fluorescent probe based on graphene quantum dots intercalated hydrotalcite for determination of ascorbic acid and phytase. Sens Actuators B Chem. 2021;345:130353.
- [227] Samuei S, Fakkar J, Rezvani Z, Shomali A, Habibi B. Synthesis and characterization of graphene quantum dots/CoNiAl-layered double-hydroxide nanocomposite: Application as a glucose sensor. Anal Biochem. 2017;521:31–9.
- [228] Tam TV, Hur SH, Chung JS, Choi WM. Novel paper- and fiber opticbased fluorescent sensor for glucose detection using anilinefunctionalized graphene quantum dots. Sens Actuators B Chem. 2021;329:129250.
- [229] Zhang Y, Wei X, Gu Q, Zhang J, Ding Y, Xue L, et al. Cascade amplification based on PEI-functionalized metal–organic framework supported gold nanoparticles/nitrogen–doped graphene quantum dots for amperometric biosensing applications. Electrochim Acta. 2022;405:139803.
- [230] Nashruddin SNA, Abdullah J, Mohammad Haniff MAS, Mat Zaid MH, Choon OP, Mohd Razip Wee MF. Label free glucose electrochemical biosensor based on poly (3, 4-ethylenedioxy thiophene): Polystyrene sulfonate/titanium carbide/graphene quantum dots. Biosensors (Basel). 2021;11:267.
- [231] Kunpatee K, Traipop S, Chailapakul O, Chuanuwatanakul S. Simultaneous determination of ascorbic acid, dopamine, and uric acid using graphene quantum dots/ionic liquid modified screenprinted carbon electrode. Sens Actuators B Chem. 2020;314:128059.
- [232] Qiu J, Li D, Mou X, Li J, Guo W, Wang S, et al. Effects of graphene quantum dots on the self-renewal and differentiation of mesenchymal stem cells. Adv Healthc Mater. 2016;5:702–10.
- [233] Yan Z, Ye T, Yang L, Jiang H, Chen C, Chen S, et al. Nanobiology dependent therapeutic convergence between biocompatibility and bioeffectiveness of graphene oxide quantum dot scaffold for immuno-inductive angiogenesis and nerve regeneration. Adv Funct Mater. 2023;33:2211709.
- [234] Shafiei S, Omidi M, Nasehi F, Golzar H, Mohammadrezaei D, Rezai Rad M, et al. Egg shell-derived calcium phosphate/ carbon dot nanofibrous scaffolds for bone tissue engineering: Fabrication and characterization. Mater Sci Eng: C. 2019;100:564–75.
- [235] Ghanbari M, Salavati-Niasari M, Mohandes F. Thermosensitive alginate-gelatin-nitrogen-doped carbon dots scaffolds as potential injectable hydrogels for cartilage tissue engineering applications. RSC Adv. 2021;11:18423-31.
- [236] Liu D, Yang F, Xiong F, Gu N. The smart drug delivery system and its clinical potential. Theranostics. 2016;6:1306–23.
- [237] Zhu S, Meng Q, Wang L, Zhang J, Song Y, Jin H, et al. Highly photoluminescent carbon dots for multicolor patterning, sensors, and bioimaging. Angew Chem - Int Ed. 2013;52:3953–7.
- [238] Vatanparast M, Shariatinia Z. AlN and AlP doped graphene quantum dots as novel drug delivery systems for 5-fluorouracil drug: Theoretical studies. J Fluor Chem. 2018;211:81–93.
- [239] Khodadadei F, Safarian S, Ghanbari N. Methotrexate-loaded nitrogen-doped graphene quantum dots nanocarriers as an efficient anticancer drug delivery system. Mater Sci Eng: C. 2017;79:280–5.

- [240] Sheng Y, Dai W, Gao J, Li H, Tan W, Wang J, et al. pH-sensitive drug delivery based on chitosan wrapped graphene quantum dots with enhanced fluorescent stability. Mater Sci Eng: C. 2020;112:110888.
- [241] Dong J, Wang K, Sun L, Sun B, Yang M, Chen H, et al. Application of graphene quantum dots for simultaneous fluorescence imaging and tumor-targeted drug delivery. Sens Actuators B Chem. 2018;256:616–23.
- [242] Teng Y, Yuan S, Shi J, Pong PWT. A multifunctional nanoplatform based on graphene quantum dots-cobalt ferrite for monitoring of drug delivery and fluorescence/magnetic resonance bimodal cellular imaging. Adv Nanobiomed Res. 2022;2:2200044.
- [243] Moasses Ghafary S, Rahimjazi E, Hamzehil H, Modarres Mousavi SM, Nikkhah M, Hosseinkhani S. Design and preparation of a theranostic peptideticle for targeted cancer therapy: Peptidebased codelivery of doxorubicin/curcumin and graphene quantum dots. Nanomedicine. 2022;42:102544.
- [244] Javanbakht S, Namazi H. Doxorubicin loaded carboxymethyl cellulose/ graphene quantum dot nanocomposite hydrogel films as a potential anticancer drug delivery system. Mater Sci Eng: C. 2018;87:50–9.
- [245] Gerweck LE, Seetharaman K. Cellular pH gradient in tumor versus normal tissue: Potential exploitation for the treatment of cancer. Cancer Res. 1996;56:1194–8.
- [246] Tannock IF, Rotin D. Acid pH in tumors and its potential for therapeutic exploitation. Cancer Res. 1989;49:4373–84.
- [247] Fan Z, Zhou S, Garcia C, Fan L, Zhou J. PH-Responsive fluorescent graphene quantum dots for fluorescence-guided cancer surgery and diagnosis. Nanoscale. 2017;9:4928–33.
- [248] Campbell E, Hasan MT, Gonzalez Rodriguez R, Akkaraju GR, Naumov AV. Doped graphene quantum dots for intracellular multicolor imaging and cancer detection. ACS Biomater Sci Eng. 2019;5:4671–82.
- [249] Zhao N, Li B, Chen D, Ahmad R, Zhu Y, Li G, et al. Yellow emissive nitrogen-doped graphene quantum dots as a label-free fluorescent probe for Fe³⁺ sensing and bioimaging. Diam Relat Mater. 2020:104:107749.
- [250] Shah H, Xie W, Wang Y, Jia X, Nawaz A, Xin Q, et al. Preparation of blue-and green-emissive nitrogen-doped graphene quantum dots from graphite and their application in bioimaging. Mater Sci Eng: C. 2021;119:111642.
- [251] Narasimhan AK, Lakshmi B S, Santra TS, Rao MSR, Krishnamurthi G. Oxygenated graphene quantum dots (GQDs) synthesized using laser ablation for long-term real-time tracking and imaging. RSC Adv. 2017;7:53822–9.
- [252] Kumawat MK, Thakur M, Gurung RB, Srivastava R. Graphene quantum dots from mangifera indica: application in near-infrared bioimaging and intracellular nanothermometry. ACS Sustain Chem Eng. 2017;5:1382–91.
- [253] Schroer ZS, Wu Y, Xing Y, Wu X, Liu X, Wang X, et al. Nitrogen–sulfur-doped graphene quantum dots with metal ionresistance for bioimaging. ACS Appl Nano Mater. 2019;2:6858–65.
- [254] Wang G, He P, Xu A, Guo Q, Li J, Wang Z, et al. Promising fast energy transfer system between graphene quantum dots and the application in fluorescent bioimaging. Langmuir. 2018;35:760–6.
- [255] Sun H, Gao N, Dong K, Ren J, Qu X. Graphene quantum dots-bandaids used for wound disinfection. ACS Nano. 2014;8:6202–10.
- [256] Zeng Z, Yu D, He Z, Liu J, Xiao FX, Zhang Y, et al. Graphene oxide quantum dots covalently functionalized PVDF membrane with significantly-enhanced bactericidal and antibiofouling performances. Sci Rep. 2016;6:20142.

- [257] Chowdhury AD, Takemura K, Li T-C, Suzuki T, Park EY. Electrical pulse-induced electrochemical biosensor for hepatitis E virus detection. Nat Commun. 2019;10:3737.
- [258] Raju L, Jacob MS, Rajkumar E. Don't dust off the dust!-A facile synthesis of graphene quantum dots derived from indoor dust towards their cytotoxicity and antibacterial activity. N J Chem. 2022;46:14859-66.
- Mohan AN, Manoi B. Biowaste derived graphene quantum dots [259] interlaced with SnO 2 nanoparticles-a dynamic disinfection agent against Pseudomonas aeruginosa. N J Chem. 2019;43:13681-9.
- [260] Teymourinia H, Salavati-Niasari M, Amiri O, Yazdian F. Application of green synthesized TiO2/Sb2S3/GQDs nanocomposite as high efficient antibacterial agent against E. coli and Staphylococcus aureus. Mater Sci Eng: C. 2019:99:296-303.
- [261] Teymourinia H, Amiri O, Salavati-Niasari M. Synthesis and characterization of cotton-silver-graphene quantum dots (cotton/Ag/ GQDs) nanocomposite as a new antibacterial nanopad. Chemosphere. 2021;267:129293.
- [262] Zhang L, Liu L, Wang J, Niu M, Zhang C, Yu S, et al. Functionalized silver nanoparticles with graphene quantum dots shell layer for effective antibacterial action. | Nanopart Res. 2020;22:1-12.
- [263] Choi SH, Yun SJ, Won YS, Oh CS, Kim SM, Kim KK, et al. Large-scale synthesis of graphene and other 2D materials towards industrialization. Nat Commun. 2022;13:1484.
- Munuera J, Britnell L, Santoro C, Cuéllar-Franca R, Casiraghi C. A review on sustainable production of graphene and related life cycle assessment. 2d Mater. 2021;9:012002.
- [265] Torres FG, Troncoso OP, Rodriguez L, De-la-Torre GE. Sustainable synthesis, reduction and applications of graphene obtained from renewable resources. Sustain Mater Technol. 2021;29:e00310.
- [266] Lü M, Li J, Yang X, Zhang C, Yang J, Hu H, et al. Applications of graphene-based materials in environmental protection and detection. Chin Sci Bull. 2013;58:2698-710.
- Kuo W-S, Tai N-H, Chang T-W. Deformation and fracture in graphene nanosheets. Compos Part A Appl Sci Manuf. 2013:51:56-61.

- [268] Yang K, Wan J, Zhang S, Zhang Y, Lee ST, Liu Z. In vivo pharmacokinetics, long-term biodistribution, and toxicology of PEGylated graphene in mice. ACS Nano. 2011;5:516-22.
- [269] Chang Y, Yang S-T, Liu J-H, Dong E, Wang Y, Cao A, et al. In vitro toxicity evaluation of graphene oxide on A549 cells. Toxicol Lett. 2011;200:201-10.
- Wang K, Ruan J, Song H, Zhang J, Wo Y, Guo S, et al. Biocompatibility of graphene oxide. Nanoscale Res Lett. 2011:6:1-8
- [271] Khan B, Adeleye AS, Burgess RM, Smolowitz R, Russo SM, Ho KT. A 72-h exposure study with eastern oysters (Crassostrea virginica) and the nanomaterial graphene oxide. Environ Toxicol Chem. 2019:38:820-30.
- [272] De Marchi L. Neto V. Pretti C. Figueira E. Brambilla L. Rodriguez-Douton MJ, et al. Physiological and biochemical impacts of graphene oxide in polychaetes: The case of Diopatra neapolitana. Comp Biochem Physiol Part C: Toxicol Pharmacol. 2017;193:50-60.
- [273] Lammel T, Boisseaux P, Navas JM. Potentiating effect of graphene nanomaterials on aromatic environmental pollutantinduced cytochrome P450 1A expression in the topminnow fish hepatoma cell line PLHC-1. Environ Toxicol. 2015:30:1192-204.
- [274] Yan C, Hu X, Guan P, Hou T, Chen P, Wan D, et al. Highly biocompatible graphene quantum dots: green synthesis, toxicity comparison and fluorescence imaging. J Mater Sci. 2020;55:1198-215.
- [275] Guo Z, Chakraborty S, Monikh FA, Varsou DD, Chetwynd AJ, Afantitis A, et al. Surface functionalization of graphene-based materials: Biological behavior, toxicology, and safe-by-design aspects. Adv Biol. 2021;5:2100637.
- [276] Shi S, Chen F, Ehlerding EB, Cai W. Surface engineering of graphene-based nanomaterials for biomedical applications. Bioconjugate Chem. 2014;25:1609-19.
- Chiticaru EA, Ioniță M. Graphene toxicity and future perspectives in healthcare and biomedicine. FlatChem. 2022;35:100417.